National Library of Canada
Canadian Theses Service
Ottawa, Canada
K1A 0N4

Bibliothèque nationale du Canada
Services des thèses canadiennes

CANADIAN THESES

THÈSES CANADIENNES

NOTICE

The quality of this microfiche is heavily dependent upon the quality of the original thesis submitted for microfilming. Every effort has been made to ensure the highest quality of reproduction possible.

If pages are missing, contact the university which granted the degree.

Some pages may have indistinct print especially if the original pages were typed with a poor typewriter ribbon or if the university sent us an inferior photocopy.

Previously copyrighted materials (journal articles, published tests, etc.) are not filmed.

Reproduction in full or in part of this film is governed by the Canadian Copyright Act, R.S.C. 1970, c. C-30.

AVIS

La qualité de cette microfiche dépend grandement de la qualité de la thèse soumise au microfilmage. Nous avons tout fait pour assurer une qualité supérieure de reproduction.

S'il manque des pages, veuillez communiquer avec l'université qui a conféré le grade.

La qualité d'impression de certaines pages peut laisser à désirer, surtout si les pages originales ont été dactylographiées à l'aide d'un ruban usé ou si l'université nous a fait parvenir une photocopie de qualité inférieure.

Les documents qui font déjà l'objet d'un droit d'auteur (articles de revue, examens publiés, etc.) ne sont pas microfilmés.

La reproduction, même partielle, de ce microfilm est soumise à la Loi canadienne sur le droit d'auteur, SRC 1970, c. C-30.

THIS DISSERTATION
HAS BEEN MICROFILMED
EXACTLY AS RECEIVED

LA THÈSE A ÉTÉ
MICROFILMÉE TELLE QUE
NOUS L'AVONS REÇUE

Canada

NL-339 (r.86/06)

THE UNIVERSITY OF ALBERTA

POLYAMINO AROMATIC COMPOUNDS AND THEIR DICATION SALTS AS ELECTRON DONOR-ACCEPTOR SYSTEMS

BY

NAM H. NGUYEN

A THESIS

SUBMITTED TO THE FACULTY OF GRADUATE STUDIES AND RESEARCH

IN PARTIAL FULFILLMENT OF THE REQUIREMENTS FOR THE DEGREE

OF MASTER OF SCIENCE

DEPARTMENT OF CHEMISTRY

EDMONTON, ALBERTA

SPRING, 1986

Permission has been granted to the National Library of Canada to microfilm this thesis and to lend or sell copies of the film.

The author (copyright owner) has reserved other publication rights, and neither the thesis nor extensive extracts from it may be printed or otherwise reproduced without his/her written permission.

L'autorisation a été accordée à la Bibliothèque nationale du Canada de microfilmer cette thèse et de prêter ou de vendre des exemplaires du film.

L'auteur (titulaire du droit d'auteur) se réserve les autres droits de publication; ni la thèse ni de longs extraits de celle-ci ne doivent être imprimés ou autrement reproduits sans son autorisation écrite.

ISBN 0-315-30159-7

THE UNIVERSITY OF ALBERTA

RELEASE FORM

NAME OF AUTHOR: NAM H. NGUYEN

TITLE OF THESIS: POLYAMINO AROMATIC COMPOUNDS AND THEIR DICATION SALTS AS ELECTRON DONOR-ACCEPTOR SYSTEMS

DEGREE FOR WHICH THESIS WAS PRESENTED: M.Sc.

YEAR THIS DEGREE GRANTED: 1986

Permission is hereby granted to THE UNIVERSITY OF ALBERTA LIBRARY to reproduce single copies of this thesis and to lend or sell such copies for private, scholarly or scientific research purposes only.

The author reserves other publication rights, and neither the thesis nor extensive extracts from it may be printed or otherwise reproduced without the author's written permission.

(Signed) .....

PERMANENT ADDRESS:

6421 Silver Ridge Circle

Alexandria, VA 22310

USA

DATED March 27, 1986

THE UNIVERSITY OF ALBERTA

FACULTY OF GRADUATE STUDIES AND RESEARCH

The undersigned certify that they have read, and recommend to the Faculty of Graduate Studies and Research, for acceptance, a thesis entitled

POLYAMINO AROMATIC COMPOUNDS AND THEIR DICATION SALTS AS ELECTRON DONOR-ACCEPTOR SYSTEMS

submitted by NAM H. NGUYEN in partial fulfillment of the requirements for the degree of Master of Science in Chemistry.

Dennis D. Tanner
.....
Supervisor

.....

.....

.....

Date March 27, 1986

La connaissance est la clef de la vie ;

et la compréhension, celle du bonheur .

ABSTRACT

The identity of the observed paramagnetic species generated upon electrolysis of a methylene chloride solution of TMPE (Tetrakis(*p*-N,N-dimethylaminophenyl)ethylene) and upon mixing of solutions of TMPE and $TMPE^{2+}(X^-)_2$ (X = I, Cl, Br, NO_3, BF_4) was identified as the $TMPE^{+\bullet}$ cation radical. Its thermodynamic stability (K_{SEM}) in solvents of different polarity, namely acetonitrile and methylene chloride, was determined using the EPR continuous variation method and was found to follow the trend of behaviour which has been suggested previously. In low polarity solvents, e.g., methylene chloride, higher concentrations of the $TMPE^{+\bullet}$ cation radical was found in comparison to that in solvents of higher polarity, e.g., acetonitrile. The success in the application of the method in defining K_{SEM} was attested to by verifying the K_{SEM} of the TMPE/$TMPE^{2+}$ system in acetonitrile using a UV absorption method. However, the application of the continuous variation method to the TMPD/$TMPD^{2+}(ClO_4^-)_2$ system (N,N,N',N'-Tetramethyl-1,4-phenylenediamine) yielded K_{SEM} which is significantly in disagreement with those previously reported. In addition, the epr study of the 50:50 mixture of TMPD/$TMPD^{2+}$ in acetonitrile (total concentration 10^{-3} *M*) revealed that the paramagnetism decayed slowly with time and remained at a constant level after 7-8 days. An application of the continuous variation method to the TMPD/$TMPD^{2+}$ system at lower concentration (total concentration 10^{-4} *M*) revealed that the stoichiometry of the combination process has changed. The explanation for the decay of the paramagnetism was assigned to an irreversible radical dimerization process while an explanation for the change in stoichiometry at lower concentration remains unknown.

The reaction of the $TMPD^{2+}(ClO_4^-)_2$ salt with 2,6-di-*tert*-butylphenol in acetonitrile yielded, beside products of oxidative coupling, mainly di- and tri-phenolic products which have one more carbon newly incorporated. The experiments with labelled solvents were carried out and the results obtained ruled out the participation of the solvent in this reaction. The source of the incorporated carbon was suggested as arising from a methyl group of the $TMPE^{2+}(ClO_4^-)_2$ dication salt.

ACKNOWLEDGEMENTS

I would like to thank my research director, Professor D. D. Tanner, for his guidance and supervision during the course of this work. I would also like to thank Professor R. B. Sandin for his helpful suggestions at the beginning of this project and for stimulating our interest in this area. We are also indebted to Professor Jed Harrison for his help in carrying out the electrochemical work on TMPE.

The author is indebted to Darwin Reed and Dr. Peter Setiloane for help in preparing and analyzing several of the TMPE salts.

My thanks are due to the staff members of the Department of Chemistry, especially Messrs. Glen Bigam and Tom Brisbane (both of the high field nmr laboratory), John Olekszyk and Don Morgan (both of the mass spectrometry laboratory).

I wish to thank my colleagues for their invaluable comments and many suggestions during the preparation of this manuscript. To Ms. Lu Ziola for her dedicated typing of the thesis, I am grateful.

Many thanks to the Chemistry Department and the University of Alberta for financial support during the course of this work.

TABLE OF CONTENTS

Chapter		Page
ABSTRACT		v
ACKNOWLEDGEMENTS		vi
LIST OF TABLES		viii
LIST OF FIGURES		ix
LIST OF STRUCTURES AND ABBREVIATIONS		xi
INTRODUCTION		1
I.1	Background	1
I.2	Proposal	16
RESULTS		17
II.1	Electron Spin Resonance, Electrochemical and UV Absorption Studies of the TMPE/$TMPE^{2+}$ System	17
II.2	Electron Spin Resonance Study of the TMPD/$TMPD^{2+}(ClO_4^-)_2$ System	18
II.3	The Reactivity of $TMPD^{2+}(ClO_4^-)_2$ Towards 2,6-di-*tert*-Butylphenol	20
DISCUSSION		57
III.1	On the Behaviour of the TMPE/$TMPE^{2+}$ System	57
III.2	On the Behaviour of the TMPD/$TMPD^{2+}$ System	61
III.3	Oxidation of Phenols Using the Dication Salts	65
III.4	Conclusions	76
EXPERIMENTAL		77
IV.1	Materials	77
IV.2	Instrumentation	83
IV.3	Analytical Procedures	84
REFERENCES		92
Appendix Ia		100
Appendix Ib		101
Appendix Ic		104

LIST OF TABLES

Page

I. Proportionality Constants at Different Percentage of [TMPE]/[TMPE]+ [$TMPE^{2+}$] in Methylene Chloride 21

II. Summary of Data and Results of the TMPE/$TMPE^{2+}(Cl^-)_2$ System in Methylene Chloride 22

III. Proportionality Constants at Different Percentage of [TMPE]/[TMPE] + [$TMPE^{2+}$] in Acetonitrile 23

IV. Summary of Data and Results of the TMPE/$TMPE^{2+}(Cl^-)_2$ System in Acetonitrile 24

V. Proportionality Constants at Different Equivalences of Coulometric Electrolysis of TMPE in Methylene Chloride 25

VI. Summary of Data and Results of the TMPE Electrolysis in Methylene Chloride 26

VII. Proportionality Constants of Different Percentage of [TMPD]/[TMPD] + [$TMPD^{2+}$] in Acetonitrile 27

VIII. Summary of Data and Results of the TMPD/$TMPD^{2+}(ClO_4^-)_2$ System in Acetonitrile 28

IX. Equilibrium Constants of Different RED/OX Systems 29

X. Products Formed in the Reaction Between $TMPD^{2+}(ClO_4^-)_2$ and 2,6-di-*tert*-butylphenol (Part I) 30

XI. Products Formed in the Reaction Between $TMPD^{2+}(ClO_4^-)_2$ and 2,6-di-*tert*-butylphenol (Part II) 31

XII. Data of exact mass measurement of products formed in the reaction of $TMPD^{2+}(ClO_4^-)_2$ and 2,6-di-*tert*-butylphenol (Part I) 32

XIII. Data of exact mass measurement of products formed in the reaction of $TMPD^{2+}(ClO_4^-)_2$ and 2,6-di-*tert*-butylphenol (Part II) 35

XIV. Distribution of products in the reaction of $TMPD^{2+}(ClO_4^-)_2$ and 2,6-di-*tert*-butylphenol in different solvent systems 37

LIST OF FIGURES

Page

1. Plot of Relative Intensity of Epr Signal vs % of [TMPE]/[TMPE] + [$TMPE^{2+}$] in Methylene Chloride 38
2. Plot of Relative Intensity of Epr Signal vs. % of [TMPE]/[TMPE] + [$TMPE^{2+}$] in Acetonitrile 39
3. Plot of Relative Intensity of Epr Signal vs. Time of Electrolysis of TMPE in Methylene Chloride 40
4. Plot of % [SEM]/[RED] + [OX] versus % Oxidation 41
5. Plot of Relative Intensity of Epr Signal vs. % of [TMPD]/[TMPD] + [$TMPD^{2+}$] in Acetonitrile 42
6. Overmodulated Epr Signal at the 50:50 Mixture of TMPE/$TMPE^{2+}$ System in Methylene Chloride 43
7. Resolved Epr Spectrum of the 50:50 Mixture of TMPE/$TMPE^{2+}(Cl^-)_2$ System in Methylene Chloride 44
8. Resolved Epr Spectrum of the 50:50 Mixture of TMPE/$TMPE^{2+}(BF_4^-)_2$ System in Methylene Chloride 45
9. Overmodulated Epr Signal of the 50:50 Mixture of TMPD/$TMPD^{2+}(ClO_4^-)_2$ System in Acetonitrile 46
10. Resolved Epr Spectrum of the 50:50 Mixture of TMPD/$TMPD^{2+}(ClO_4^-)_2$ in Acetonitrile 47
11. Gc-ms Chromatogram of the Reaction Mixture of $TMPD^{2+}(ClO_4^-)_2$ and 2,6-di-*tert*-butylphenol (Part I) 48
12. Gc-ms Chromatogram of the Reaction Mixture of $TMPD^{2+}(ClO_4^-)_2$ and 2,6-di-*tert*-butylphenol (Part II) 49
13. Electrolytic Cell Employed for the Epr Study of TMPE 50

14. Plot of Relative Intensity of Epr Signal vs. Time of the 50:50 Mixture of TMPD/$TMPD^{2+}(ClO_4^-)_2$ System in Acetonitrile 51

15. Plot of the Dimeric Product Concentration vs. Time of the 50:50 Mixture of TMPD/$TMPD^{2+}(ClO_4^-)_2$ in Acetonitrile 52

16. UV Absorption Spectra of the TMPE/$TMPE^{2+}(Cl^-)_2$ System in Acetonitrile 53

17. UV Absorption Spectrum of the $TMPE^{+\cdot}$ Radical Cation of the TMPE/$TMPE^{2+}(Cl^-)_2$ System at Equilibrium 54

18. ^{13}C-nmr Chemical Shift Assignment for Compound (X) (See Table X) 55

19. Plot of Relative Intensity of Epr Signal vs. % [TMPD]/[TMPD] + [$TMPD^{2+}$] in Acetonitrile 56

LIST OF STRUCTURES AND ABBREVIATIONS

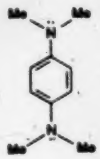

TMPD

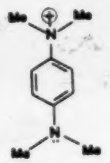

$TMPD^{+\bullet}$

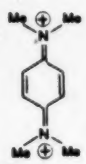

$TMPD^{2+}$

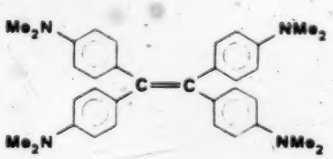

TMPE

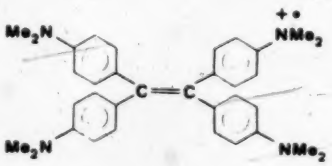

$TMPE^{+\bullet}$

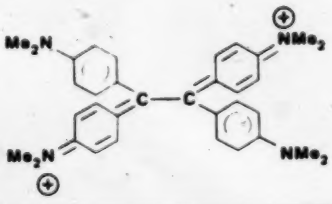

$TMPE^{2+}$

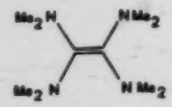

TDAE

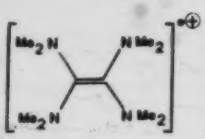

$TDAE^{\oplus\bullet}$

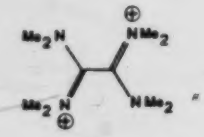

$TDAE^{2\oplus}$

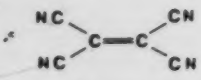

TCNE

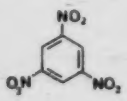

TNB

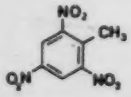

TNT

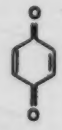

PBQ

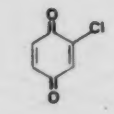

CBQ

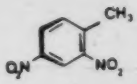

DNT

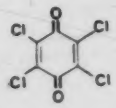

Chloranil

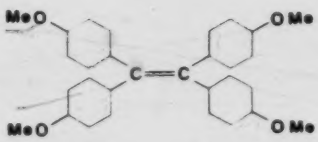

TAE

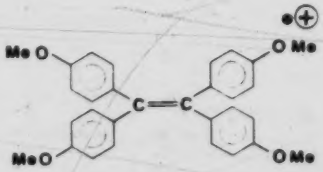

$TAE^{+\bullet}$

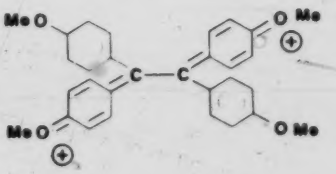

TAE^{2+}

INTRODUCTION

I.1 BACKGROUND

A large number of organic compounds have been recognized as being electron rich and capable of donating one or two electrons, in other words, serving as reducing agents. By contrast, their cation salts are often able to serve as oxidants. Of these compounds, the most widely studied groups are the aromatic amines and the conjugated open-chain amines, for example, N-substituted diaminobenzenes, N-substituted tetraaminophenylethylenes, N-substituted tetraaminoethylenes, etc.

These materials are representative of a wide variety of reducing agents of different strengths and are drawing increasing attention from chemists in recent years.[1-5] Organic compounds capable of undergoing one-electron transfer redox processes are comparatively rare and were, in fact, not known until the thirties.[6] The two-stage one-electron redox systems leading to stable radical ions were used, unrecognized, for almost fifty years in the dye industry.[7-9] The colored salt discovered by Wurster in 1879 was only recognized in 1925 by Weitz[10,11] of having the structure of a radical cation (see equation 1).

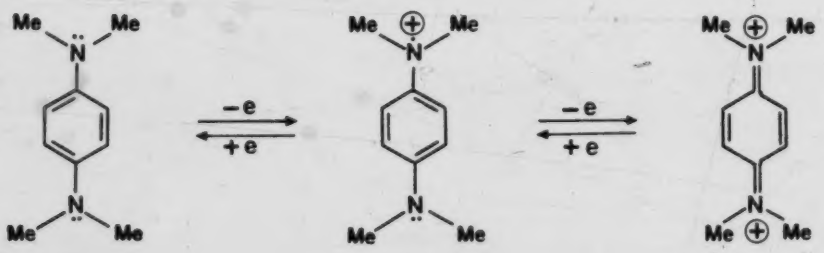

(1)

colorless blue colorless

The radical formed in the first one-electron transfer stage owes its stability to the delocalization of the single electron over the entire monocation fragment.[10,12]

Hünig and coworkers[1,14] first attempted to introduce a general classification of various structurally different redox systems into three main categories: (a) open-chain vinylogous redox system, (b) Wurster Type Redox System, and (c) Weitz Type Redox system.

Category (a): e.g., Compounds (1) and (2)

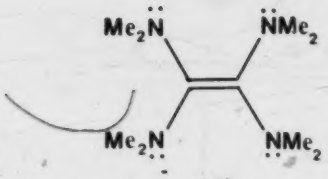

(1)

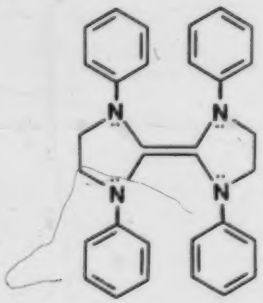

(2)

Category (b): e.g., Compounds (3) and (4)

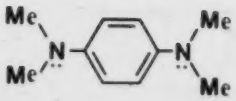

(3)

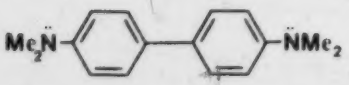

(4)

Category (c): e.g., Compounds (5) and (6)

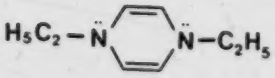

(5)

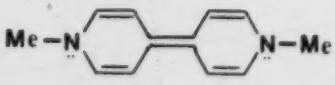

(6)

In principle, compounds of the general formula (A) can exist in three oxidation states that are related by two one-electron transfer processes.[1,13-15]

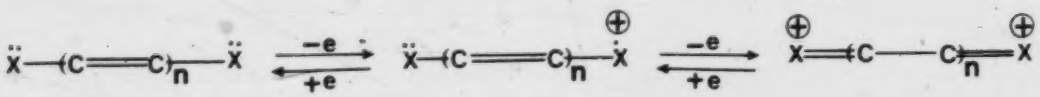

A_{RED} A_{SEM} A_{OX}

X may be NR_2, SR or OR; n = 0, 1, 2 ...

Whether the radical ion A_{SEM} can be detected or isolated depends both on its thermodynamic stability, which is expressed by the semiquinone formation constant K,[6,13] and on the reactivity of each of the three components towards the medium.

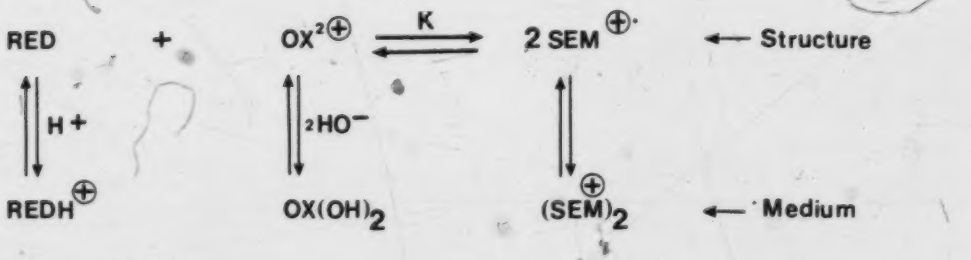

$$K = [SEM]^2/[RED][OX]$$

The greater value of K, the higher is the equilibrium concentration of radical cation. Some values of K are given in Table I.

The reactivity of the olefinic double bond can be strongly influenced by substituents. For example, the four electron-attracting cyano groups in tetracyanoethylene withdraw electrons so effectively from the central double bond that this compound is strongly

Table I. Semiquinone formation constants for the two-step oxidation of electron-rich olefins.

Compound	K
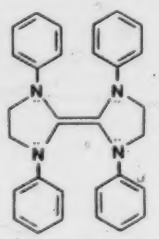	$25^{(23)}$
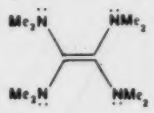	$230^{(24)}$
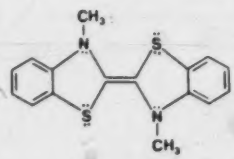	$1000^{(25)}$
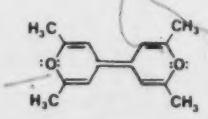	$6\times10^{4\,(25)}$
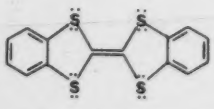	$10^{8\,(25)}$

electrophilic.[16] The opposite situation is found in the "electron-rich olefins",[17] in which four electron-donating substituents are attached to the carbons of the central double bond; examples of such compounds are tetraaminoethylenes, particularly tetrakis(dimethylamino)ethylene, TDAE, **(1)**[18] and 1,1',3,3'-tetraphenyl-2,2'-biimidazoleidinylidene **(2)**.[9,20]

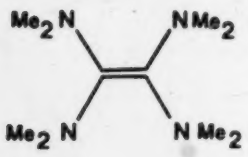

(1)

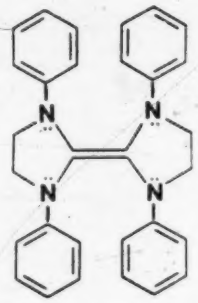

(2)

Depending on the strength of the interaction between the electron donor and the electron acceptor, Wiberg,[18] Briegleb[21] and Hoffman[22] classified the interaction into two categories:

a. Interaction by which complete electron transfer has occurred and salt-like product(s) are formed.

b. Interaction by which no net electron transfer has occurred and an electron donor-acceptor complex is formed.

It was also demonstrated that there exists a subtle borderline interaction between the two types of processes. An examination of the interaction of tetrakis(dimethylamino)ethylene (TDAE) with organic molecules having a lower oxidation potential than the electron acceptor, tetracyanoethylene (TCNE),[16] reveals that electron transfer from the donor TDAE to the organic acceptor is incomplete, resulting in the formation of electron donor-acceptor complexes.[21] The TDAE $(TCNE)_2$ complex is believed to be on the borderline between a salt and an electron donor-acceptor complex. An esr spectral study of increasingly concentrated acetonitrile solutions of TDAE $(TCNE)_2$ shows that the structure of the compound changes. At low concentration (10^{-3}–10^{-4} *M*), the spectra show a nonet having line widths of 0.1 and

0.2 G respectively and at high concentration (10^{-1} *M*) a singlet having a line width of 5 G.[26] Wiberg, however, pointed out that TDAE $(TCNE)_2$ also has a salt-like structure.[27,28] By analogy to the results found upon examination of the tetramethyl-*p*-phenylenediamine tetracyanoethylene, (TMPD) (TCNE) complex,[29] these results indicate that the ionization of TDAE $(TCNE)_2$ is reversible in solution (formation of an ion pair and electron donor-acceptor complex) and that TDAE $(TCNE)_2$ probably exists in the solid state as an electron donor-acceptor complex of the ions $TDAE^{2+}$ and $TCNE^-$, i.e., as a complex in which a more ionic limiting structure is involved in the ground state than in the excited state ("inverse" electron donor-acceptor complex[29]). A better example of the formation of an electron donor-acceptor complex is the interaction between TDAE and trinitrobenzene (TNB) which yields a diamagnetic[30] TDAE $(TNB)_2$ complex in acetonitrile.[31] Spectroscopic studies characterize it as an electron donor-acceptor complex, which is compatible with a sandwich arrangement of the molecules.

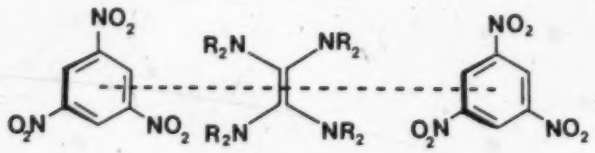

$TDAE(TNB)_2$, R = CH_3

Stronger electron acceptors such as oxygen or halogen can displace the weaker electron acceptor TNB from the complex and thus complete the oxidation of TDAE,[31] e.g.:

$$TDAE(TNB)_2 + Br_2 \rightarrow TDAE^{2+}(Br^-)_2 + 2TNB$$

The difference in the electronic structure of $[TDAE^{2+}][TCNE^-]_2$ (salt) and TDAE $(TNB)_2$ (electron donor-acceptor complex) is clear from the IR, ^{1}H-NMR, and UV spectra[27,31] (see

Table II).

The phenomenon of complete electron transfer in solution can be exemplified with the now classic example of the TMPD-chloranil reaction.[32-34] This pair forms a charge transfer complex in solvents of low dielectric constant (e.g., dioxane, benzene, 1,2-dichloroethane) without complete electron transfer, whereas in acetonitrile the detectable, first formed complex gives way to the separate cation and anion radicals, each of which is detectable by absorption and esr spectroscopy. Foster[38,39] points out that factors involved in determining the interaction between electron donor - electron acceptor are: the strength of the electron donor and acceptor ability, and the nature of the medium in which the interaction takes place. The ground state Ψ_N of the complex resulting from the interaction can be described in Mulliken's terminology[40-42] as:

$$\Psi_N = a\,\Psi(A,D) + b\Psi\,(A^-D^+)$$

where $\Psi(A,D)$ is the state function of the complex in which no bonding takes place, $\Psi(A^-D^+)$ is the state function of the complex in which one electron has been donated from D to A. The scalars a and b indicate the relative proportion of contribution of each of these states to the Ψ_N state. The Ψ_N function can be extended further if two electrons have been donated from D to A to give a third component of Ψ_N: $\Psi(A^{2-}D^{2+})$. One typical example for the complete transfer of one electron from D to A is the case of Tetramethyl-*p*-phenylenediamine (TMPD) and 1,3,5-trinitrobenzene (TNB) in methanolic solution.[39] The ground state of the resulted complex is the ionic form. For the case in which no complete transfer of an electron takes place, the complex formed between TMPD and 2,4,6-trinitrotoluene (TNT) in acetonitrile can be taken as a good example.[39] There are many typical cases in which the interaction is of the borderline type and results in the detection of paramagnetic species simultaneously with the observation of the formation of a new charge-transfer band. The complex formed between the acetonitrile solution of TMPD with each of the following acceptors: *p*-benzoquinone (PBQ), chloro-*p*-benzoquinone (CBQ), 2,5-dichloro-*p*-benzoquinone[39] are examples of this behavior. Interaction of tetrakis(*p*-dimethylaminophenyl)ethylene (TMPE) with acceptors such as 2,4-dinitrotoluene

Table II. Comparison of the spectra $[TDAE^{2+}][TCNE^{-}]_2$ and TDAE $(TNB)_2$

Spectrum	$[TDAE^{2+}][TCNE^{-}]_2$	$[TDAE][TNB]_2$
IR (Nujol)	$TDAE^{2+}$ and $TCNE^{-}$ bands	No $TDAE^{2+}$ bands
^1H-NMR (CH_3CN)	$TDAE^{2+}$ signals[a]	TDAE signal[b]
UV (CH_3CN)[c]	$TCNE^{-}$ absorption[35]	2 new CT bands[d]

[a] Considerably broadened and displaced to higher field strengths because of the paramagnetism of $TCNE^{-}$.

[b] Another signal is due to trinitrobenzene.

[c] Dilute solution.

[d] Charge-transfer bands at 545 (ϵ 210) and 442 nm (ϵ = 300).

-(DNT); 2,4,6-trinitrotoluene (TNT); 1,3,5-trinitrobenzene (TNB) in methanol results in a double electron transfer to form a diamagnetic dication.[39] The medium in which the interaction takes place also plays a critical role in determining whether the electron-transfer process occurs. In non-ionizing solvent, cyclohexane, the interaction between electron donor: TMPD, and electron acceptors : DNT, TMB and TNT all resulted in the formation of intermolecular charge-transfer complexes.[38,43-45] However, in aqueous solution only those systems dissolve which, because of the high electron affinity of the electron acceptor, can form the radical ion pair $A^{\bullet-}TMPD^{+\bullet}$. The cation is sufficiently stable in water to be detected experimentally, whereas most other radical anions react too rapidly with the water for their absorption spectra to be recorded.

Kuwata and Geske[24] obtained the radical cation $TDAE^{+\bullet}$ by the comproportionation reaction (2).

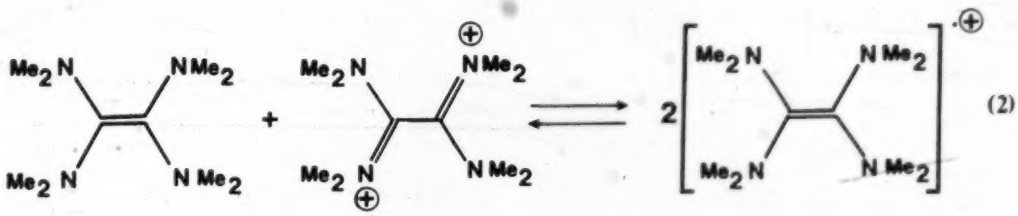

(2)

TDAE $\quad$ $TDAE^{2\oplus}$ $\quad$ $TDAE^{\oplus\cdot}$

The orange solution of the cation $TDAE^{+\bullet}$ ($\lambda_{max}^{CH_3CN}$ = 385 nm) obtained from TDAE $(ClO_4)_2$ and TDAE in dimethylformamide gives an ESR spectrum consisting of 300 observable lines. The equilibrium constant K for reaction (2) is 230, i.e., 89% of $TDAE^{+\bullet}$ exists in equilibrium with 5.5% of TDAE and 5.5% of $TDAE^{2+}$.[46]

The halfwave potentials, E_1, E_2 are:[24]

$$TDAE \rightleftarrows TDAE^{+} + e^{-} \qquad E_1 = -0.75 \text{ V}$$

$$TDAE^{+\bullet} \rightleftarrows TDAE^{2+} + e^{-} \qquad E_2 = -0.61 \text{ V}$$

The electrochemistry has been done on this system allowing the calculation of the radical formation constant K for the reversible processes. The distinctly negative potential of TDAE (which roughly corresponds to the standard potential of zinc: $Zn \rightarrow Zn^{2+} + 2e^{-}$; E_0 = –0.76 V) is a quantitative indication of the electron-donor character of the tetraaminoethylene system. The surprisingly low appearance potential of TDAE in comparison with those of other tetrasubstituted ethylenes also confirms that the atomic grouping $(\succ N)_2C{=}C(N\prec)_2$ is an "electron-rich" system. The appearance potentials of ethylene, tetramethylethylene, and TDAE are 10.5, 8.4 and < 6.5 eV respectively.[18] For this structural type the only compound that has been studied in any detail is tetrakis(dimethylamino)ethylene. The foregoing discussion shows that TDAE is a strong electron donor. This is substantiated by simple HMO calculations.[47]

The HMO scheme permits the comparison of the electron donor TDAE with other donors of similar structures. As the size of a carbon π-system increases, the energy of the

first anti-bonding orbital decreases, and the electron donor ability should decrease. Compounds derived from TDAE by insertion of organic groups which extend conjugation (e.g. **2,3,7**)[18] will be poorer reductants.

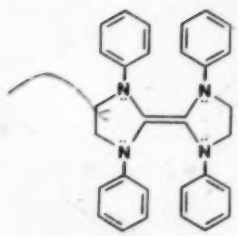

(2)

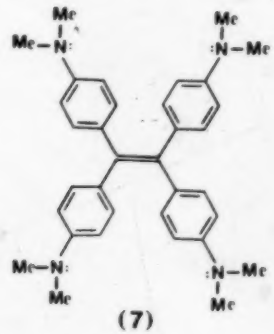

(7)

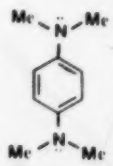

(3)

Sandin *et al.* pointed out that the insertion of the four p-phenylene groups into the structure of the electron rich N,N,N',N'-octamethyltetraaminoethylene (TDAE) gives rise to a structure, compound (**7**), which has a lowered electron donor strength ($E_{1/2}$ = +0.160 V vs. SCE),[48] attested to by its ability to be reversibly oxidized by iodine in non-aqueous solvents.[49-51] This interpretation, however, will be elaborated further in the discussion. Compound (**7**) also exhibits a certain acceptor character, and reacts with two equivalents of sodium to yield a dianion.[52,53] (TDAE does not react with lithium in diethylamine.[26]) The monoiodide of (**2**) can in fact be reduced even with silver[54] (Zn is required for TDAE); the half-wave potential of (**2**) is only –0.3 V[24] (TDAE: –0.75 V). The lowered electron donor ability is also evident in the readily reversible electron transfer process observed for the complex formed between TMPD and TCNE[29,55] ($TMPD^{+\bullet}$ $TCNE^{-}$ → TMPD + TCNE).

Foster *et al.*[38] commented that the medium can significantly affect the electron donor ability of TMPD and TMPE and that their effective order can be reversed by changing from one solvent to another. In cyclohexane TMPD is the stronger electron donor while the reverse holds true in both methanol and acetonitrile. Bard *et al.*[56] reported the equilibrium constants

of 55 and 1.6 for TAE in methylene chloride and acetonitrile, respectively, for the comproportionation reaction (3):

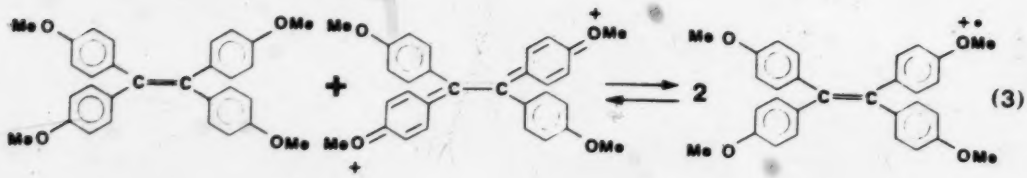

(3)

and suggested that the dication is more solvated in acetonitrile than in methylene chloride, thus shifting the equilibrium to the left, leaving a lower concentration of radical cation to be detected by esr. The reaction of type (4) is usually detected

$$\text{RED} + \text{OX} \overset{K}{\rightleftarrows} 2\,\text{SEM} \qquad (4)$$

spectroscopically, or by electrochemical techniques. Not many examples are known outside the violenes. These have been explored mostly in Hünig's laboratory.[14] The violenes are often made by oxidation of M by M^{2+} and the comproportionation constants K have been obtained for a number of compounds from the one- and two-electron oxidation potentials, E_1 and E_2, obtained electrochemically, eq. (5).[14,57,58]

$$\log K = (E_2 - E_1)/0.06 \qquad (V, 25°C) \qquad (5)$$

In a large number of cases, the constants are quite large, indicating that the violene radicals are the predominant species. The comproportionation constants have also been employed in combination with other physical techniques to obtain the forward and reverse rate constants of compound (**8**)[59] and (**9**).[60] Not all violene systems exist so far over on the radical cation side. Thus K_{comp} for compound (**10**) is 16 in acetonitrile solution[48,57] indicating that the equilibrium mixture contains 80% of the cation radical. In contrast, K_{comp} for (**11**) could not be obtained entirely by electrochemical methods and was estimated to be about 10^{14} (the value E_1 is not clearly defined).[62-64]

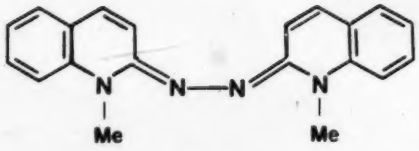

$K_{comp} = 2.14 \times 10^5$

(8)

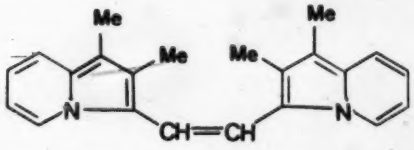

$K_{comp} = 8 \times 10^2$

(9)

Using optically transparent electrodes and rapid scan spectrophotometer Gruver and Kuwana[65] obtained $K = 3 \times 10^{12}$ for dimethyldihydrophenazin **(12)** and $K = 6 \times 10^6$ for the methylviologen (**6**). Nizuma *et al* [66] reported system **(13)** in ethanol lies far to the left, thus disproportionation of the biacrideninium cation radical is extensive. The inherent structure of the parent molecule can also play a decisive role in governing K, E_1 and E_2. Hünig[15,62] reported that elongation of the vinylene chain as in **(14)** rapidly reduces K_{comp}, but the vinylene bridges in **(15)** and **(16)** have hardly any influence. The general structural principle[1] presented in systems A to C (Scheme I) would thus generally be accessible to systems that differ strongly in respect of the position of the redox potentials E_1 and E_2, the thermodynamic and kinetic stabilities of the RED, SEM and OX partners, the sensitivity to acids and bases,[67] and the solubility in different solvents. Further, taking into account that the SEM form always shows absorption at by far the longest wavelength and that electron-transfer is diffusion-controlled,[67,68] then these redox systems can be considered for utilization as redox indicators,[69] as electron donors and acceptors,[70-72] as catalysts for electron transfer,[73-75] as light-sensitive systems,[76-77] and as electronic conductors.[78-84] Of these possible applications some have already acquired industrial importance and others seem highly promising.

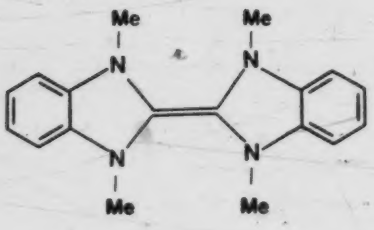

$K_{comp} = 16$

(10)

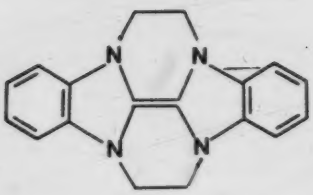

$K_{comp} = 10^{14}$

(11)

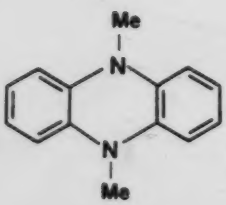

$K_{comp} = 3 \times 10^{12}$

(12)

$K_{comp} = 6 \times 10^{6}$

(6)

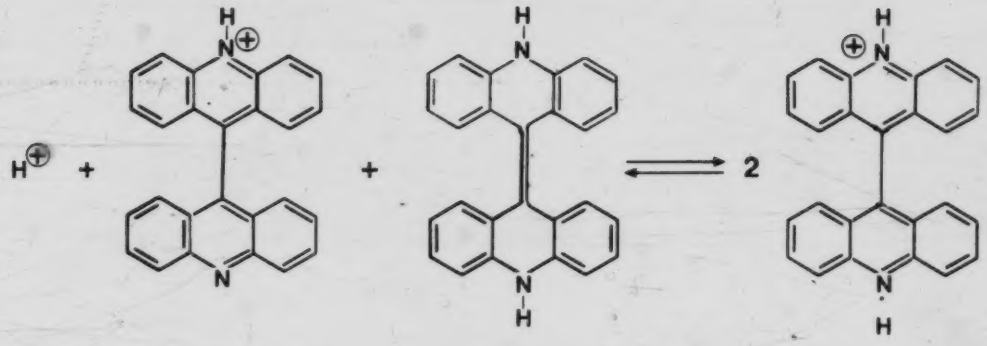

(13)

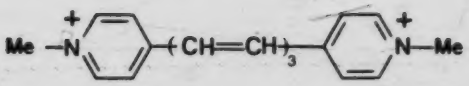

(14)

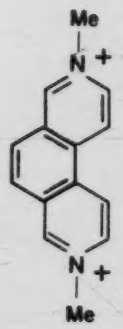

(15)

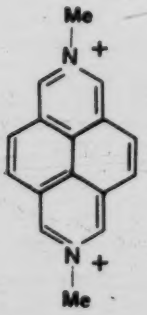

(16)

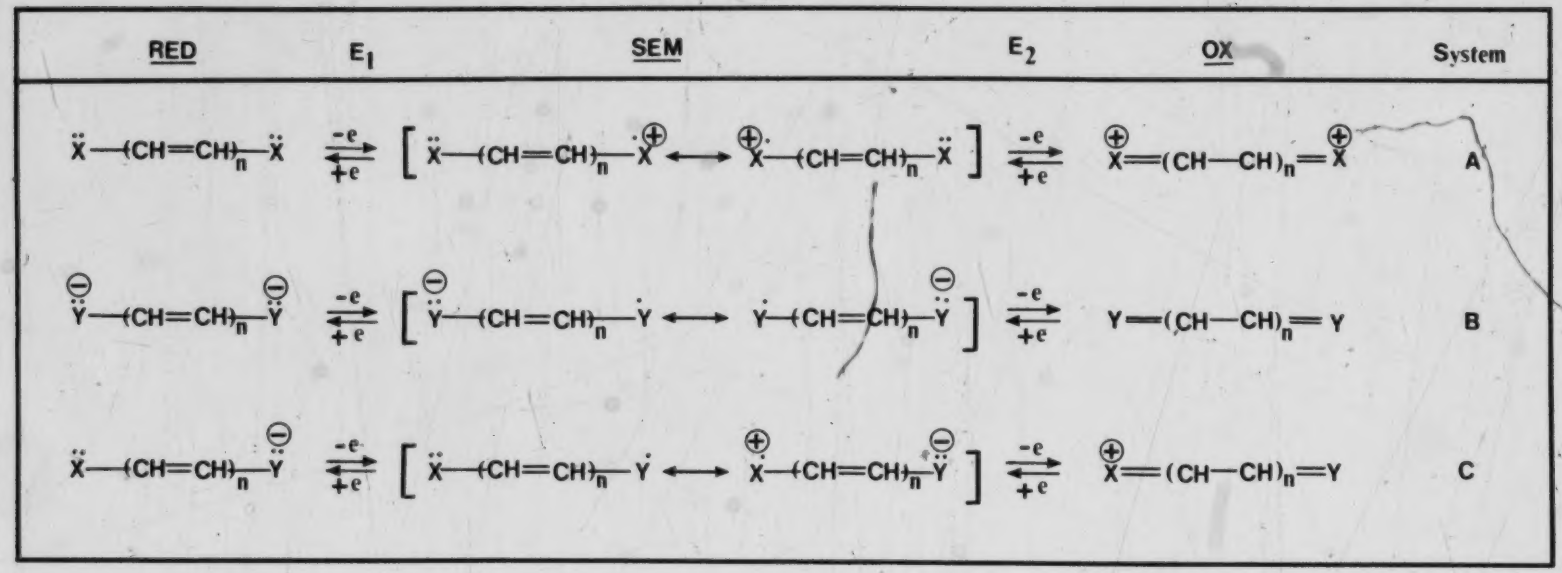

Scheme I

I.2 PROPOSAL

Sandin *et al.* attempted to rationalize the epr activity of the diiodide salt of TMPE in solution.[49,50] The observed featureless epr signal was suggested to originate from a reversible electron transfer process between the iodide anion and the $TMPE^{2+}$ dication fragment. Although Sandin[51] subsequently reported the existence of the $TMPE^{+\bullet}$ cation radical it remains unclear as to whether reversible electron transfer did occur between the counterions of the diiodide salt and whether disproportionation occurred between three molecules of the diiodide salt to give rise to two molecules of the TMPE ditriiodide salt and one molecule of TMPE. Furthermore, Bard *et al.*[56] observed a broad featureless epr signal upon partial oxidative electrolysis of an acetonitrile or methylene chloride solution of TMPE. An attempt to define the K_{SEM} of the generated $TMPE^{+\bullet}$ radical species led only to an estimate of the value. The identity of the paramagnetic species and the value of K_{SEM} still remained unsettled. The chemical reactivity of RED/OX systems such as $TMPE/TMPE^{2+}$ is also of fundamental interest, since very little chemistry of these systems has been reported.

RESULTS

II.1 ELECTRON SPIN RESONANCE, ELECTROCHEMICAL AND UV ABSORPTION STUDIES OF THE TMPE/$TMPE^{2+}$ SYSTEM

The resolved epr spectrum of the 50:50 mixture of TMPE/$TMPE^{2+}(Cl^-)_2$ system was obtained at 25°C in methylene chloride by mixing equal volumes of degassed (10^{-3} *M*) solutions of TMPE and $TMPE^{2+}(Cl^-)_2$. A moderately resolved spectrum consisting of at least 190 observable lines with the spacing between two adjacent groups of lines of approximately 0.71 Gauss was recorded, g 2.00328 (see Figure 7). The 50:50 mixtures of TMPE/$TMPE^{2+}(I^-)_2$; TMPE/$TMPE^{2+}(NO_3^-)_2$ in methylene chloride under degassed condition at 25°C, both gave resolved spectra identical to that of the TMPE/$TMPE^{2+}(Cl^-)_2$ system.

The 50:50 mixture of TMPE/$TMPE^{2+}(BF_4^-)_2$ in degassed methylene chloride at 25° gave an epr spectrum, which was not as well resolved (74 observable lines) with the spacing between two adjacent groups of lines of approximately 0.7 Gauss, g 2.00336 (see Figure 8). The intensity of the overmodulated epr signal (area under the curve) of the TMPE/$TMPE^{2+}(Cl^-)_2$ system in methlene chloride and acetonitrile was plotted against the variation of the absolute percentage of TMPE (ie. % of [TMPE]/[TMPE] + [$TMPE^{2+}$]). (see Figure 1 and 2). A series of proportionality constants were determined and an average value was calculated. The average proportionality constant was subsequently employed for the formation constant derivation (see Tables I, II, III and IV). The semiquinone formation constants found for TMPE/$TMPE^{2+}(Cl^-)_2$ system in methylene chloride and acetonitrile are 8.64 and 0.036 respectively (entries 2 and 1, Table IX).

The percentage of the $TMPE^{+\bullet}$ at equilibrium in methylene chloride and acetonitrile was found to be 60.75(total concentration 10^{-3} *M*) and 9.78(total concentration 2 x 10^{-3} *M*) respectively. Calibration against 2,2-diphenyl-1-picrylhydrazyl (DPPH) indicates that 13.9% of $TMPE^{+\bullet}$ exist at equilibrium in methylene chloride and 2.6% of $TMPE^{+\bullet}$ exist at equilibrium in acetonitrile (entry 1 and 2, Table IX).

The radical cation $TMPE^{+\bullet}$ was generated electrochemically at 25°C under degassed condition from the methylene chloride solution of TMPE (10^{-3} *M*) and Et_4NCl (0.11 *M*) (see Figure 13). The intensity of the overmodulated signal was plotted against time (see Table V, Figure 3). The length of time employed for the electrolysis was precalculated so that with a constant current of 136.4 μA passing through, an overall average of one electron per molecule is removed when the electrolysis time reaches 2 hours. The electrolysis was carried out for 4 hours, during which the cell was occasionally removed from the epr cavity, thoroughly mixed, and reinserted into the cavity. The intensity (area) of the overmodulated signal was plotted against time (see Figure 3). The unit on the abscissa of the plot was correspondingly converted into the absolute percentage of TMPE and a series of proportionality constants were obtained (see Table V). The average proportionality constant was subsequently employed for the calculation of the semiquinone equilibrium constant. The equilibrium constant found by this approach is 6.00 and the corresponding percentage of $TMPE^{+\bullet}$ at equilibrium in methylene chloride is 53.3% (see Table VI).

The identity of $TMPE^{+\bullet}$ was established by obtaining a resolved epr spectrum when the electrolysis reached one equivalent. The spectrum was found to be identical to that in Figure 7, g 2.00330. The UV absorption spectrum of the $TMPE^{+\bullet}$ was obtained by subtracting the spectra of TMPE and $TMPE^{2+}$ from the overall spectrum of the TMPE/$TMPE^{2+}$ system at equilibrium in acetonitrile (see Figure 16 and 17). The concentration of TMPE and $TMPE^{2+}$ at equilibrium was calculated from the equilibrium constant (K = 0.089) to be 2.41 x 10^{-4} *M* (the total initial concentration of TMPE and $TMPE^{2+}$ is 5 x 10^{-4} *M*).

II.2 ELECTRON SPIN RESONANCE STUDY OF THE TMPD/$TMPD^{2+}(ClO_4^-)_2$ SYSTEM

The resolved epr spectrum of the 50:50 mixture of the TMPD/$TMPD^{2+}(ClO_4^-)_2$ system in acetonitrile was obtained at 25°C by mixing equal volume of the degassed 10^{-3} *M* solutions of TMPD and $TMPD^{2+}(ClO_4^-)_2$. A resolved spectrum consisting of at least 78 observable lines with the spacing between two subsequent lines of approximately 2.0 Gauss was recorded, g 2.00395, see Figure 10. The identity of the paramagnetic species was

established by its comparison with the reported g factor and epr spectra of the $TMPD^{+\bullet}$ radical.

The intensity (area) of the overmodulated epr signal of the $TMPD/TMPD^{2+}(ClO_4^-)_2$ system in acetonitrile as plotted against the variation of the absolute percentage of TMPD (i.e. % [TMPD]/[TMPD] + $[TMPD^{2+}]$) (the total concentration is 10^{-3} *M*) (see Figure 5). A series of proportionality constants was obtained and their average value was subsequently employed to calculate the formation constant (see Table VII). The semiquinone formation constant found for $TMPD/TMPD^{2+}(ClO_4^-)_2$ system in acetonitrile is 34.28 which corresponds to an equilibrium concentration of 73.30 radical (see Table VIII) with respect to the total concentration of the TMPD and $TMPD^{2+}(ClO_4^-)_2$. Calibration against DPPH was in close agreement with the calculated value and indicates that the percentage of $TMPD^{+\bullet}$ is 85.9% at equilibrium.

When the intensity of the overmodulated epr signal of the $TMPD/TMPD^{2+}(ClO_4^-)_2$ system in acetonitrile was plotted against the variation of the absolute percentage of TMPD (the total concentration is 10^{-4} *M*) a skewed curve was obtained (see Figure 19) indicating the stoichiometry has changed. The UV absorptions of TMPD and $TMPD^{2+}(ClO_4^-)_2$ in acetonitrile solution (5.10^{-5} - 10^{-3} *M*) indicate the Beer-Lambert Law is obeyed up to 10^{-3} *M*.

The intensity of the epr signal decreased with time. The decreased intensity of the epr signal represented a comparatively slow decay (see Figure 14). After approximately 7-8 days the intensity of the epr signal remains unchanged. Assuming the decay of the intensity of the epr signal is due to a bimolecular process and a dimeric product is formed, the kinetics is found to be of second order with respect to the paramagnetic species and the half-life of the paramagnetic species is estimated to be 3 days (see Figure 15).

Mass spectrometric examination of the solid material, recovered after several half-lives, indicated the existence of the monomeric TMPD fragment (Chemical Ionization, MH^+ = 165). The Mass Spectrometry - Fast Atom Bombardment (MS-FAB, $M'H^+$ = 327 (M' is the molecular weight of the dimeric product), MH^+ = 165) indicated simultaneous existence of both the monomeric and the dimeric product of TMPD.

II.3 THE REACTIVITY OF $TMPD^{2+}(ClO_4^-)_2$ TOWARDS 2,6-DI-*TERT*-BUTYL-PHENOL

Preliminary studies of the reaction between $TMPD^{2+}(ClO_4^-)_2$ and 2,6-di-*tert*-butylphenol in acetonitrile showed that the reaction yielded a number of oxidative products. The products 2,6-di-*tert*-butyl-4-methylphenol (II), 2,6-di-*tert*-1,4-benzoquinone (III), 3,5-di-*tert*-butyl-4-hydroxy benzaldehyde (IV), 3,5,3',5'-tetra-*tert*-butyl-4,4'-diphenoquinone (VII), 4,4'-dihydroxy-3,5,3',5'-tetra-*tert*-butyldiphenyl (VIII), 4,4'-dihydroxy-3,5,3',5'-tetra-*tert*-butyldiphenylmethane (V), 2,6,3',5'-tetra-*tert*-butyl-4'-hydroxyphenyl-4-methylene-2,5-cyclohexadiene-1-one (VI), bis (3,5-di-tert-butyl-4-hydroxyphenyl)(3,5-di-*tert*-butyl-4-oxocyclohexa-2,5-dienylidene)methane (X) and tris(3,5-di-*tert*-butyl-4-hydroxyphenyl)methane (IX), are formed (see Tables X and XII).

Since several of the products formed contained one more carbon than either the dimeric or the trimeric phenol it was suspected that the solvent, acetonitrile was one of the reactants in their formation. When the reactions were run with either acetonitrile-1-^{13}C (6.3%) and acetonitrile-2-^{13}C (5.8%) the products were found to have been formed without ^{13}C enrichment. Furthermore, when the reaction was run in propionitrile as solvent the analysis of the reaction results showed the same pattern of products.

Compound (X) (see Table X) is chosen as a target molecule for the test due to its relative abundant yield and its ease to undergo flash chromatography separation.

The reaction of $TMPD^{2+}(ClO_4^-)_2$ and 2,6-di-*tert*-butylphenol in benzene at 90°C yields mainly 4,4'-dihydroxy-3,5,3',5'-tetra-*tert*-butyldiphenyl (VIII) (entry 4, Table XIV) with identifiable dealkylated products (compounds XI, XIII, XIV, Table XI). Prolongated reaction of the dication salt with the title phenol in propionitrile yielded more dealkylated products (compounds XI, XIV, XV and XVI, Table XI) as well as tlc non-eluted material.

Table I. Proportionality Constants at Different Percentage of [TMPE]/[TMPE] + [$TMPE^{2+}$] Equilibrium in Methylene Chloride

Point #	Relative Intensity x 10^4	% TMPE	Proportionality Constants C
1	11.5	5	
			.086
2	22.5	10	
			.091
3	34.0	15	
			.081
4	43.5	20	
			.082
5	52.0	25	
			.087
6	60.0	30	
			.089
7	67.0	35	
			.086
8	72.0	40	
			.085
9	75.0	45	
			.089
10	76.0	50	
			.076
11	75.0	55	
			.070
12	72.5	60	
			.069
13	68.5	65	
			.068
14	63.0	70	
			.069
15	56.0	75	
			.069
16	47.5	80	
			.074
17	37.0	85	
			.069
18	26.0	90	
			.071
19	13.5	95	

Table II. Summary of data and results obtained from the TMPE/$TMPE^{2+}(Cl^-)_2$ system in methylene chloride

$C_{average}$	=	0.08 ± 0.008
$[TMPE]_0 = [TMPE^{2+}]_0$	=	5.01×10^{-4} *M*
Rel. $Int._{at\ 50\%}$	=	7.6×10^{-3}
K	=	11.03 ± 5.19
% Radical	=	60.75 ± 6.05

Table III. Proportionality Constants at Different Percentage of [TMPE]/[TMPE] + [$TMPE^{2+}$] Equilibrium in Acetonitrile

Point #	Relative Intensity x 10^5	% TMPE	Proportionality Constants C
1	3.5	5	
			.745
2	5.1	10	
			1.396
3	6.4	15	
			.243
4	7.2	20	.068
5	7.8	25	
			1.846
6	8.4	30	
			1.136
7	8.8	35	
			1.689
8	9.1	40	
			3.476
9	9.2	45	
			4.605
10	9.3	50	
			4.605
11	9.2	55	
			3.476
12	9.1	60	
			4.262
13	9.0	65	
			3.899
14	8.7	70	
			3.21
15	8.2	75	
			1.817
16	7.7	80	
			.216
17	6.9	85	
			.015
18	5.8	90	
			.042
19	4.2	95	

Table IV. Summary of data and results obtained from the TMPE/$TMPE^{2+}(Cl^-)_2$ system in acetonitrile

$C_{average}$	=	2.04 ± 1.65
$[TMPE]_0 = [TMPE^{2+}]_0$	=	0.99×10^{-3} *M*
Rel. Int. $_{at\ 50\%}$	=	9.3×10^{-5}
K	=	0.089 ± 0.087
% Radical	=	9.78 ± 7.59

Table V. Proportionality Constants at Different Equivalences of Coulometric Electrolysis of TMPE in Methylene Chloride

Point #	Relative Intensity x 10^4	No. of Equivalence	% TMPE	Proportionality Constant C
1	3.8	.10	5	
				3.864
2	5.5	.20	10	
				4.144
3	6.7	.30	15	
				7.310
4	7.7	.4	20	
				8.463
5	8.5	.5	25	
				1.274
6	9.2	.6	30	
				1.128
7	9.7	.7	35	
				5.787
8	10	.8	40	
				2.303
9	10.3	.9	45	
				3.928
10	10.6	1.00	50	
				3.488
11	10.4	1.1	55	
				2.790
12	10.3	1.2	60	
				4.384
13	10	1.3	65	
				8.750
14	9.6	1.4	70	
				1.400
15	9.2	1.5	75	
				8.185
16	8.6	1.6	80	
				1.169
17	7.9	1.7	85	
				1.267
18	7.0	1.8	90	
				2.173
19	6.0	1.9	95	

Table VI. Summary of data and results obtained from the TMPE electrolysis in methylene chloride.

$C_{average}$	=	3.99 ± 2.58
$[TMPE]_0 = [TMPE^{2+}]_0$	=	5.05×10^{-4} *M*
Rel. Int. $_{at\ 50\%}$	=	10.6
K	=	6.00 ± 2.48
% Radical	=	53.3 ± 5.40

Table VII. Proportionality Constants at Different Percentage of [TMPD]/[TMPD] + [$TMPD^{2+}$] Equilibrium in Acetonitrile

Point #	Relative Intensity x 10^4	% TMPD	Proportionality Constants C
1	3.6	5	
			.242
2	6.4	10	
			.313
3	9.6	15	
			.292
4	12.4	20	
			.297
5	15.0	25	
			.316
6	17.6	30	
			.296
7	19.6	35	
			.282
8	21.0	40	
			.304
9	22.0	45	
			.200
10	22.2	50	
			.394
11	21.4	55	
			.380
12	19.8	60	
			.356
13	18.0	65	
			.376
14	15.6	70	
			.345
15	13.4	75	
			.385
16	10.6	80	
			.371
17	8.0	85	
			.364
18	5.4	90	
			.395
19	2.6	95	

Table VIII. Summary of data and results obtained from the TMPD/$TMPD^{2+}(ClO_4^-)_2$ system in acetonitrile

$C_{average}$	=	0.33 ± 0.02
$[TMPD]_0 = [TMPD^{2+}]_0$	=	5.01×10^{-4} *M*
Rel. Int. $_{at\ 50\%}$	=	22.2×10^{-4}
K	=	34.28 ± 14.80
% Radical	=	73.30 ± 4.50

Table IX. Equilibrium Constants of Different RED/OX Systems

Entry No.	Type of System	Solvent	K_{eq}	Calculated[d] % Radical	Calibrated[e] % Radical	Reference
1	TMPE/$TMPE^{2+}$ [a]	MeCN	0.089 ± 0.087	9.78 ± 7.59	2.6	This work
2	TMPE/$TMPE^{2+}$ [a]	CH_2Cl_2	11.03 ± 5.19	60.75 ± 6.05	13.9	This work
3	TMPE/$TMPE^{2+}$ [f]	CH_2Cl_2	6.00 ± 2.48	53.3 ± 5.40	None	This work
4	TMPD/$TMPD^{2+}$ [b]	MeCN	34.28 ± 14.80	73.30 ± 4.50	85.9	This work
5	TMPD/$TMPD^{2+}$ [c]	MeCN	9.3×10^{10}	>99.9	None	Ref. 3
6	TMPD/$TMPD^{2+}$ [c]	MeCN	6.7×10^{19}	>99.9	None	Ref. 95
7	TMPD/$TMPD^{2+}$ [c]	MeCN	4.5×10^{19}	>99.9	None	Ref. 96

a. Counter anion is chloride
b. Coutner anion is perchlorate
c. Dication is generated electrochemically.
d. Those from entry 1-4 were obtained from the epr curve. Those from entry 5-7 were obtained from equation $(E_2-E_1) = 0.059 \log K$.
e. Calibration was done using DPPH (2,2-diphenyl-1-picrylhydrazyl) free radical 95% purity.
f. The dication was generated electrochemically and the epr plot constructed.

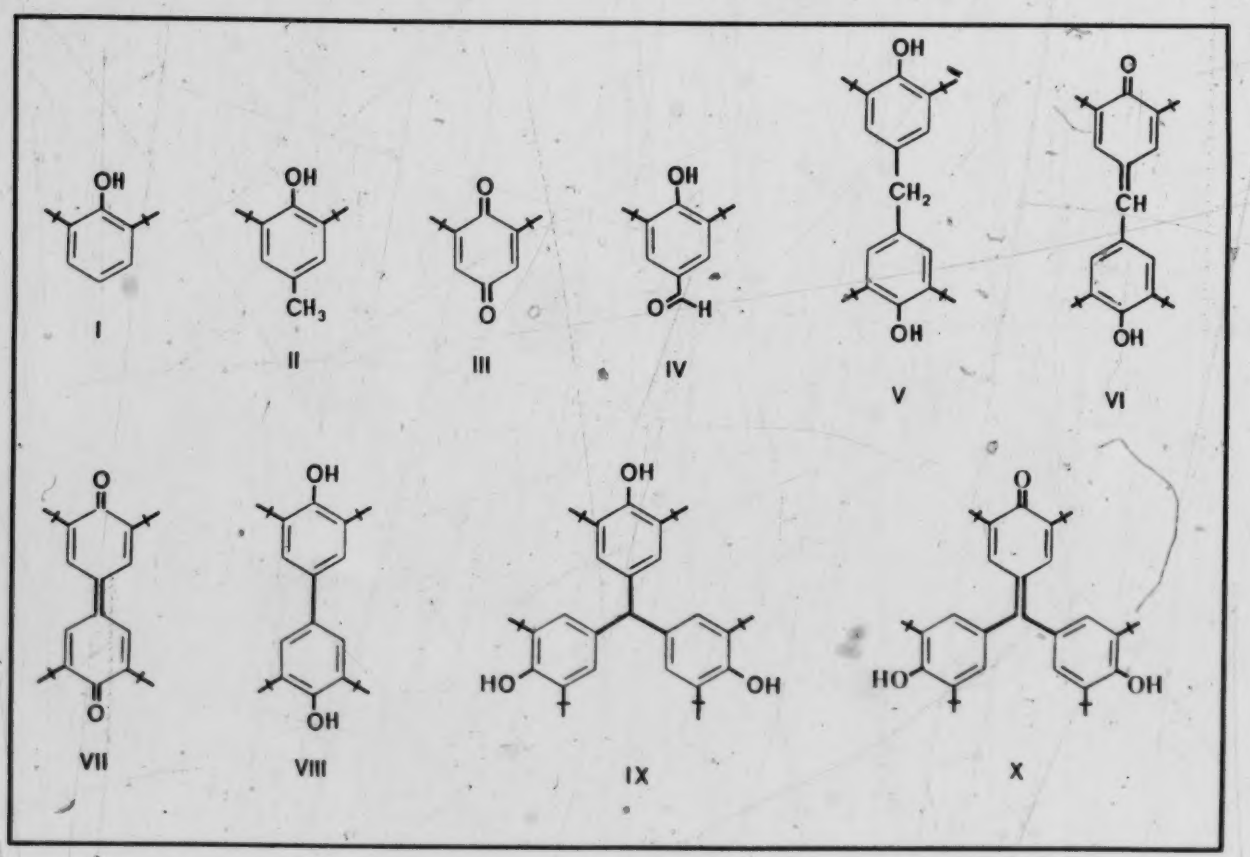

Table X. Identifiable products formed in the reaction of the $TMPD^{2+}(ClO_4^-)_2$ with 2,6-di-*tert*-butylphenol.

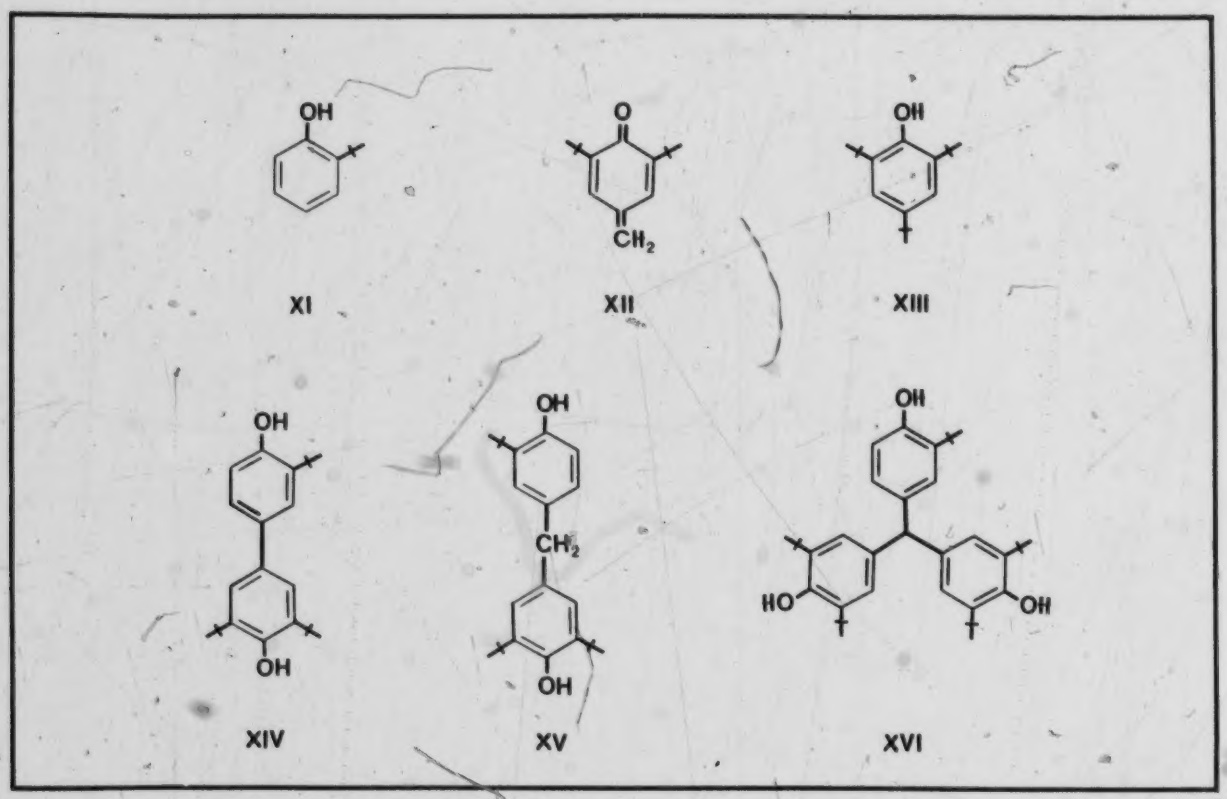

Table XI. Identifiable products formed in the reaction of the $TMPD^{2+}(ClO_4^-)_2$ with 2,6-di-*tert*-butylphenol. (The structures of XI, XII, XIV, XV, XVI are tentatively assigned since no other information was available except exact masses.)

Table XII. Exact mass measurement of products formed from the reaction of $TMPD^{2+}(ClO_4^-)_2$ and 2,6-di-*tert*-butylphenol.

Compound[a]		Calculated Mass[b]	Found Mass[a]	Deviation,[c] mmu
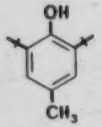	(II)	220.1827	220.1848	2.1
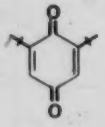	(III)	220.1463	220.1459	-0.4
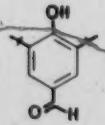	(IV)	234.1620	234.1642	2.2

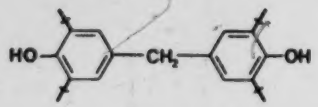 (V)	424.3341	424.3293	-4.9
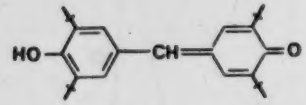 (VI)	422.3185	422.3181	-0.4
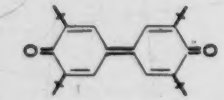 (VII)	408.3028	408.3031	0.3
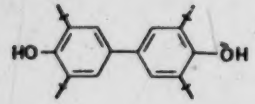 (VIII)	410.3185	410.3158	-2.7

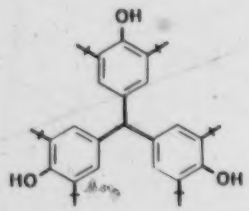	(IX)	628.4855	628.4855	0.0
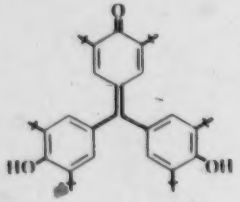	(X)	626.4699	626.4692	-0.7

a. The separation and identification was done by gc-ms using a 30 m DB-1 capillary column (see Figure 11 and 12).

b. The calculation is based on the nucliclic mass of the most abundant isotope.

c. The difference of the found mass with respect to the calculated mass is in millimass unit (acceptable range of error is ± 5 mmu).

Table XIII: Exact mass measurement of products formed from the reaction of $TMPD^{2+}(ClO_4^-)_2$ and 2,6-di-*tert*-butylphenol[d]

Compound[a]		Calculated Mass[b]	Found Mass[a]	Deviation[c], mmu
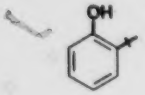	(XI)	150.1045	150.1031	-1.4
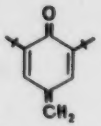	(XII)	218.1671	218.1694	2.3
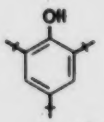	(XIII)	262.2297	262.2341	4.4

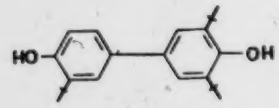 (XIV)	354.2559	354.2520	-3.9
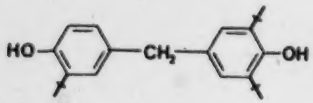 (XV)	368.2715	368.2664	-5.1
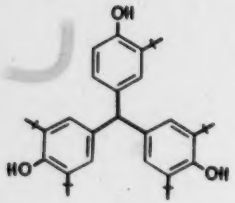 (XVI)	572.4229	572.4181	-4.8

a. The separation and identification was done by gc-ms using a 30 m DB-1 capillary column.

b. The calculation is based on the nuclidic mass of the most abundant isotope.

c. The difference of the found mass with respect to the calculated mass in millimass unit (acceptable range of error is ± 5 mmu).

d. These products are identified solely by exact mass measurement (compound XIII identity was additionally established by spiking.) Their existence was barely visible on gc-fid chromatogram.

Table XIV. Reactions of $TMPD^{2+}(ClO_4^-)_2$ with 2,6-di-*tert*-butylphenol in different solvent systems.

Entry No.	Solvent	Mole $TMPD^{2+}$/ Substrate	Reaction Period	Temp.	Product Yield,[a] % I	II	III	IV	V	VI	VII[b]	VIII[b]	IX	X	Material[d] Balance
1	Acetonitrile	2:1	54 h	60°	0.2	0	1.0	1.2	6.1	2	7.1		0	32	49.6
2	Acetonitrile	2:1	4 h	90°	17.2	5.7	1.4	0.7	22.5	3.7	2.8		3.4	33.7	89.3
3	Propionitrile	1.5:1	18 h	90°	40	3	5	3	30	0.5	4		3	4	87.5
4	Benzene[c,e]	2:1	122 h	90°	60		<1				25			0	62

a. The product analysis was carried out on a 20' glass column (2.5% XE60 ChromW AW-DMCS).

b. The separation of VII and VIII is poor and the quantitation is done based on the total area of these two.

c. The solubility of the salt in benzene is poor and longer reaction time was employed. The dealkylated products were established solely on gc-ms (exact mass measurement).

d. The material balance is based on the reacted 2,6-di-*tert*-butylphenol.

e. Other dealkylated and realkylated products of the substrate 2,6-di-*tert*-butylphenol were also identified by exact mass measurement: Compounds XI, XIII, XIV (Table XI and XIII).

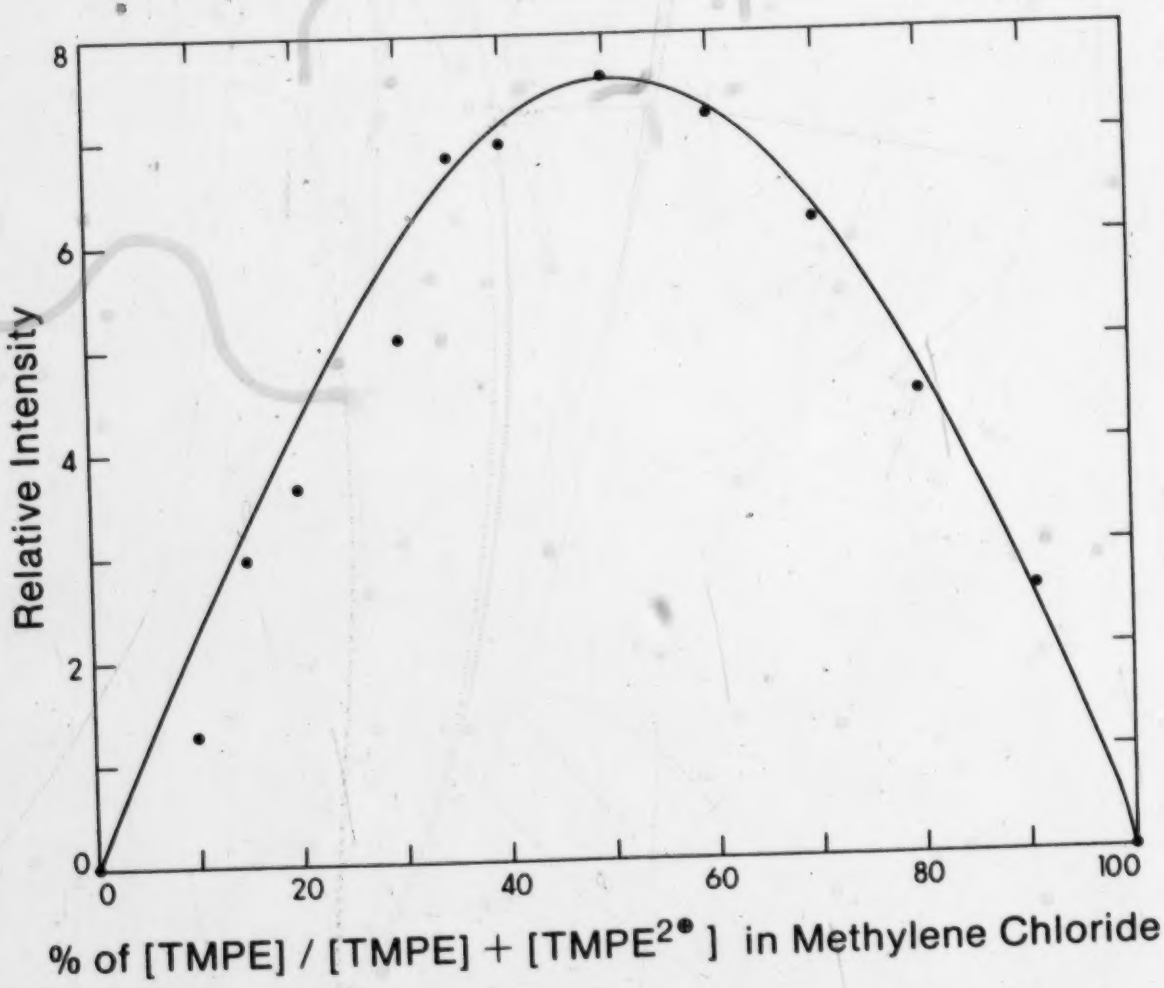

Figure 1. Plot of Relative Intensity of epr signal of $TMPE^{+\bullet}$ versus % of [TMPE]/[TMPE]+[$TMPE^{2+}$] in Methylene Chloride.

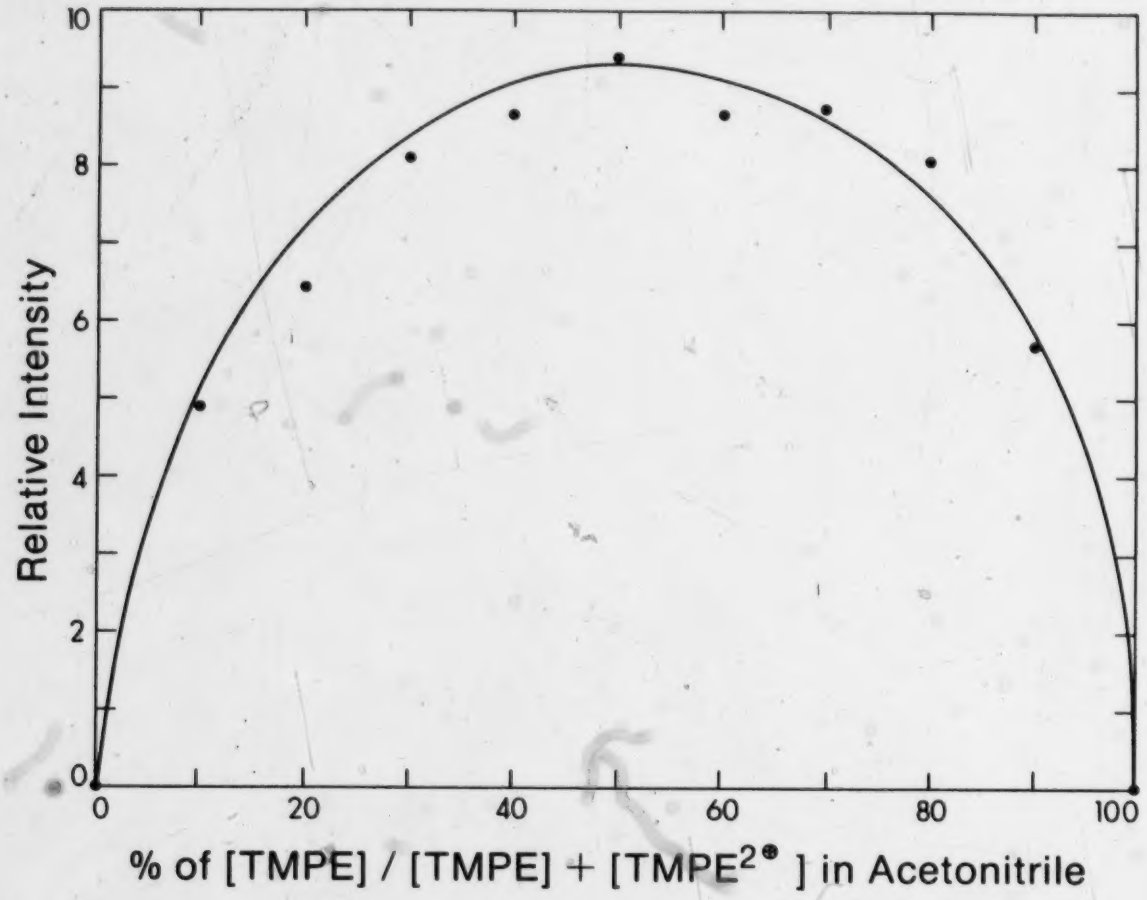

Figure 2. Plot of Relative Intensity of epr Signal of $TMPE^{+\bullet}$ versus % [TMPE]/[TMPE]+[$TMPE^{2+}$] in Acetonitrile.

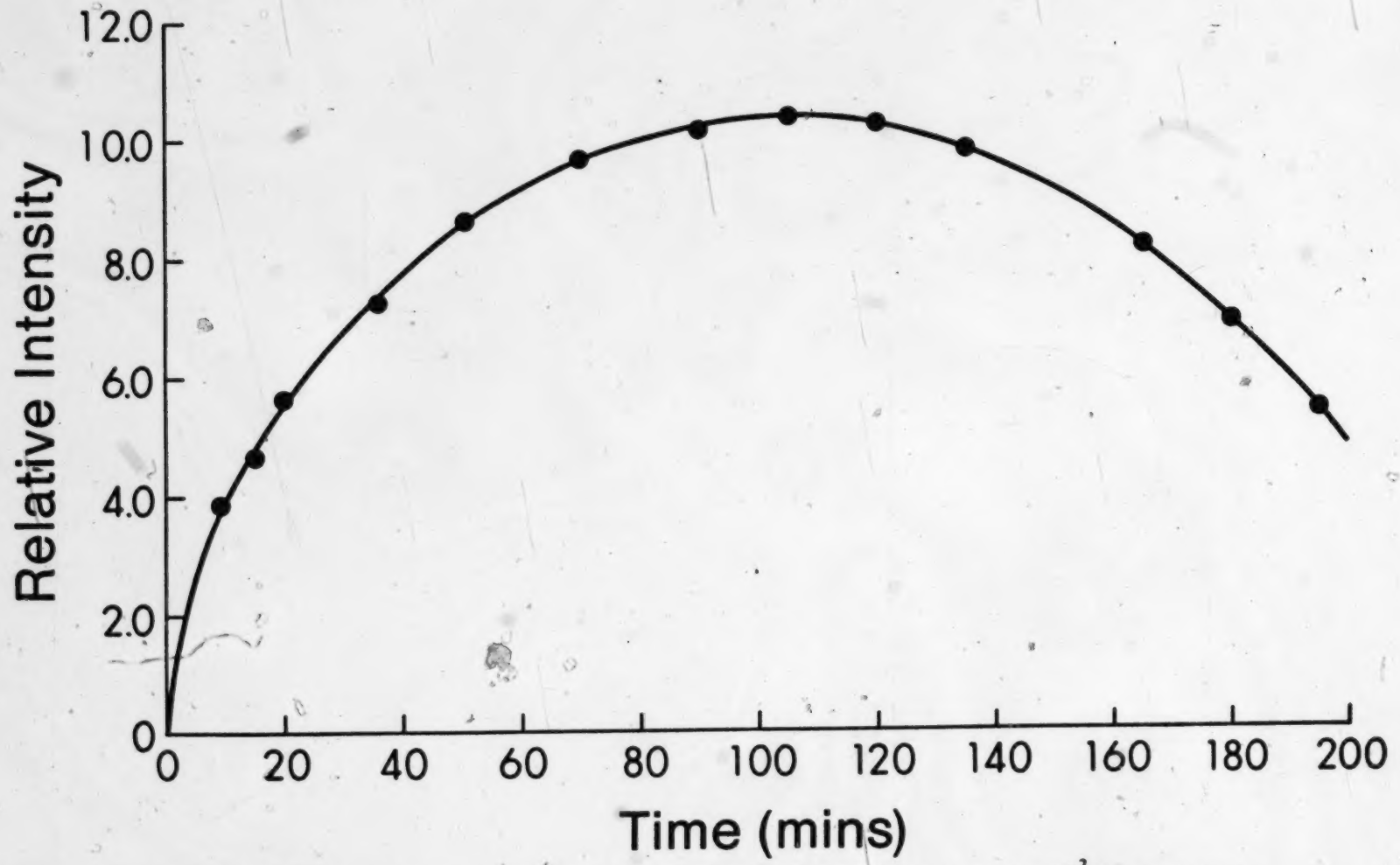

Figure 3. Plot of Relative Intensity of epr Signal of the Electrolyzed Methylene Chloride Solution of TMPE (10^{-3} *M*) versus time.

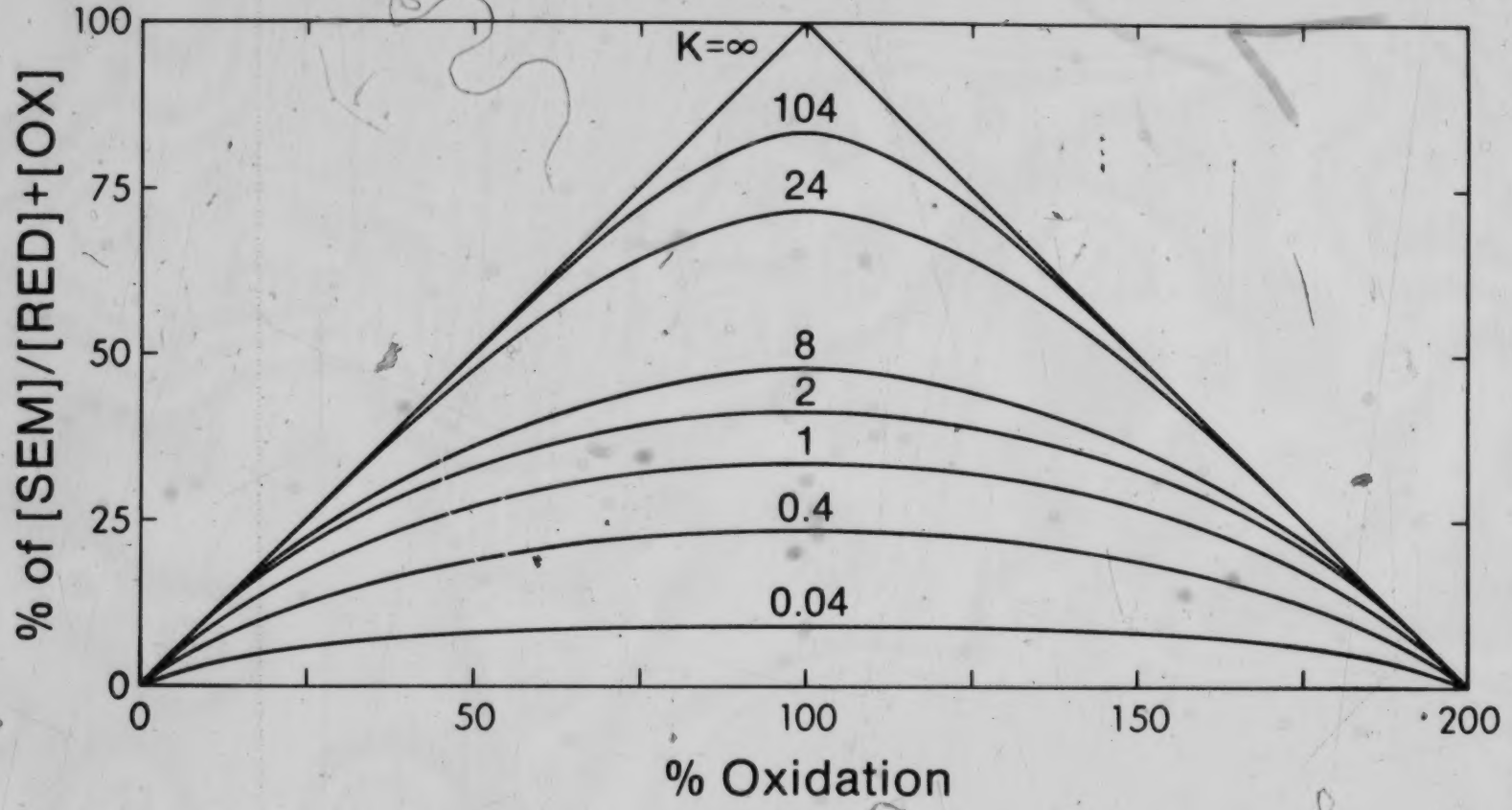

Figure 4. Plot of the percent of [SEM]/[RED]+[OX] versus percent of oxidation. The corresponding formation constant (K_{SEM} for the semiquinoid form is indicated by numerical value on top of each curve (ref. 6).

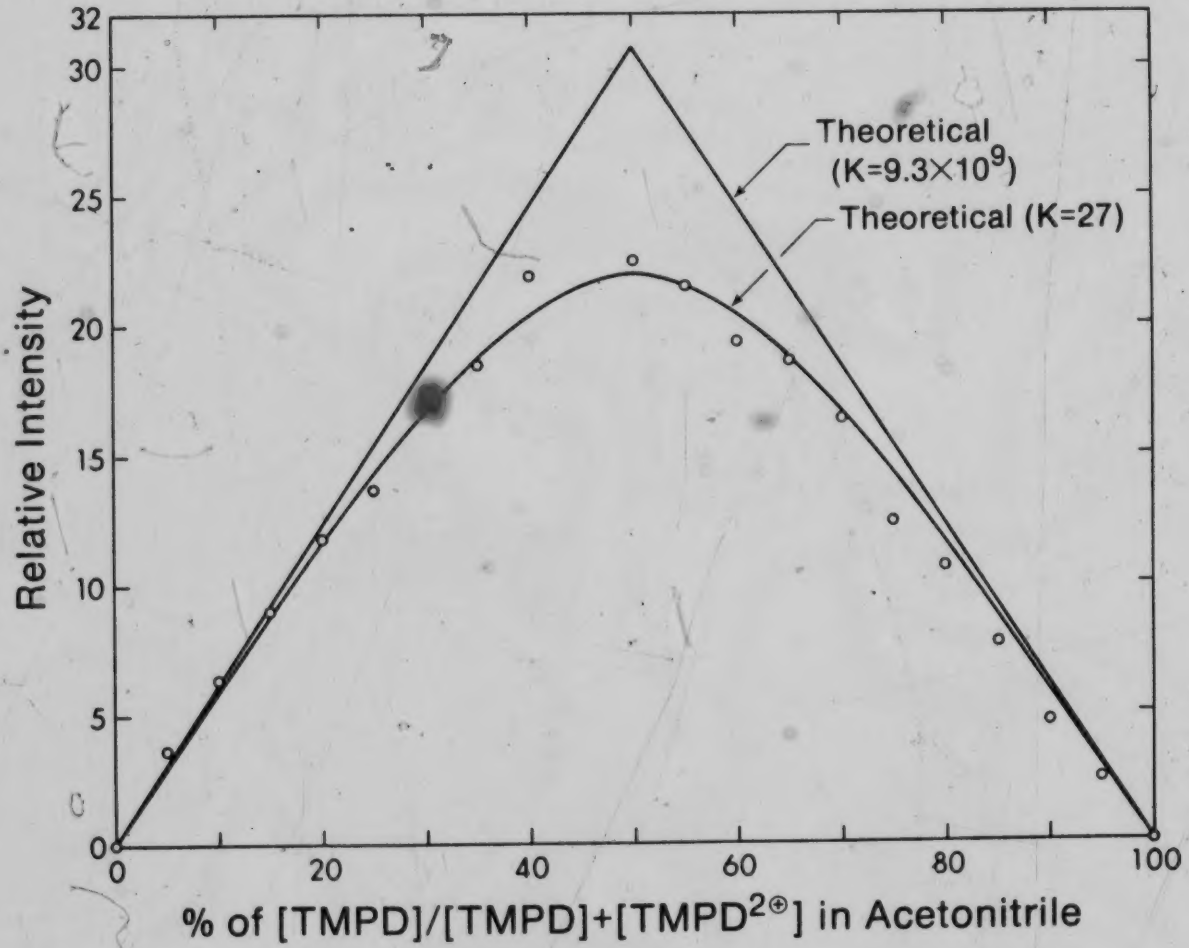

Figure 5. Plot of Relative Intensity of Epr Signal of $TMPD^{+\bullet}$ versus % of [TMPD]/[TMPD]+[$TMPD^{2+}$] in Acetonitrile (total concentration = 10^{-3} *M*)

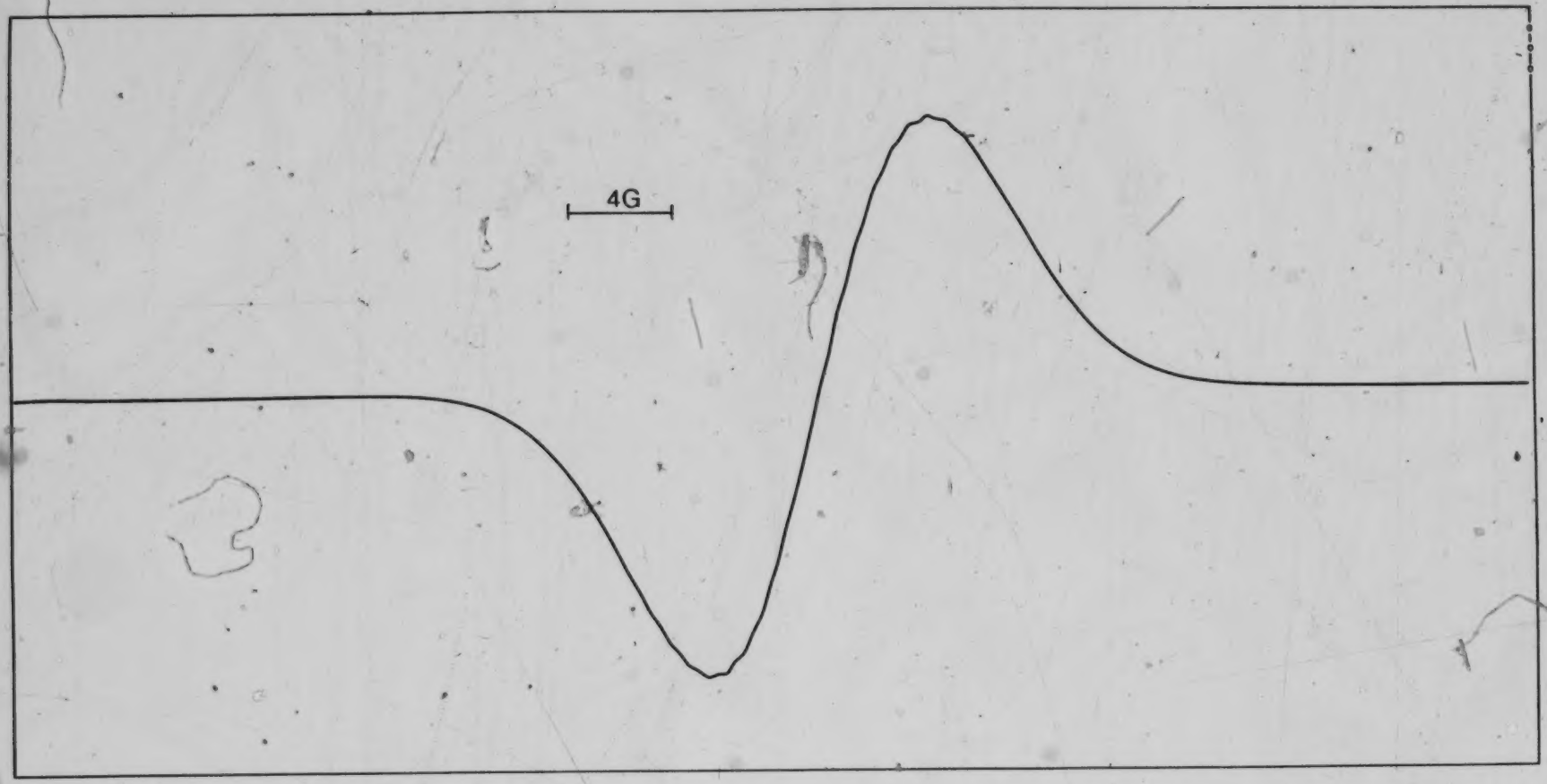

Figure 6. Overmodulated epr Signal of the Mixture of 50:50 TMPE/$TMPE^{2+}(Cl^{-})_2$ in Methylene Chloride

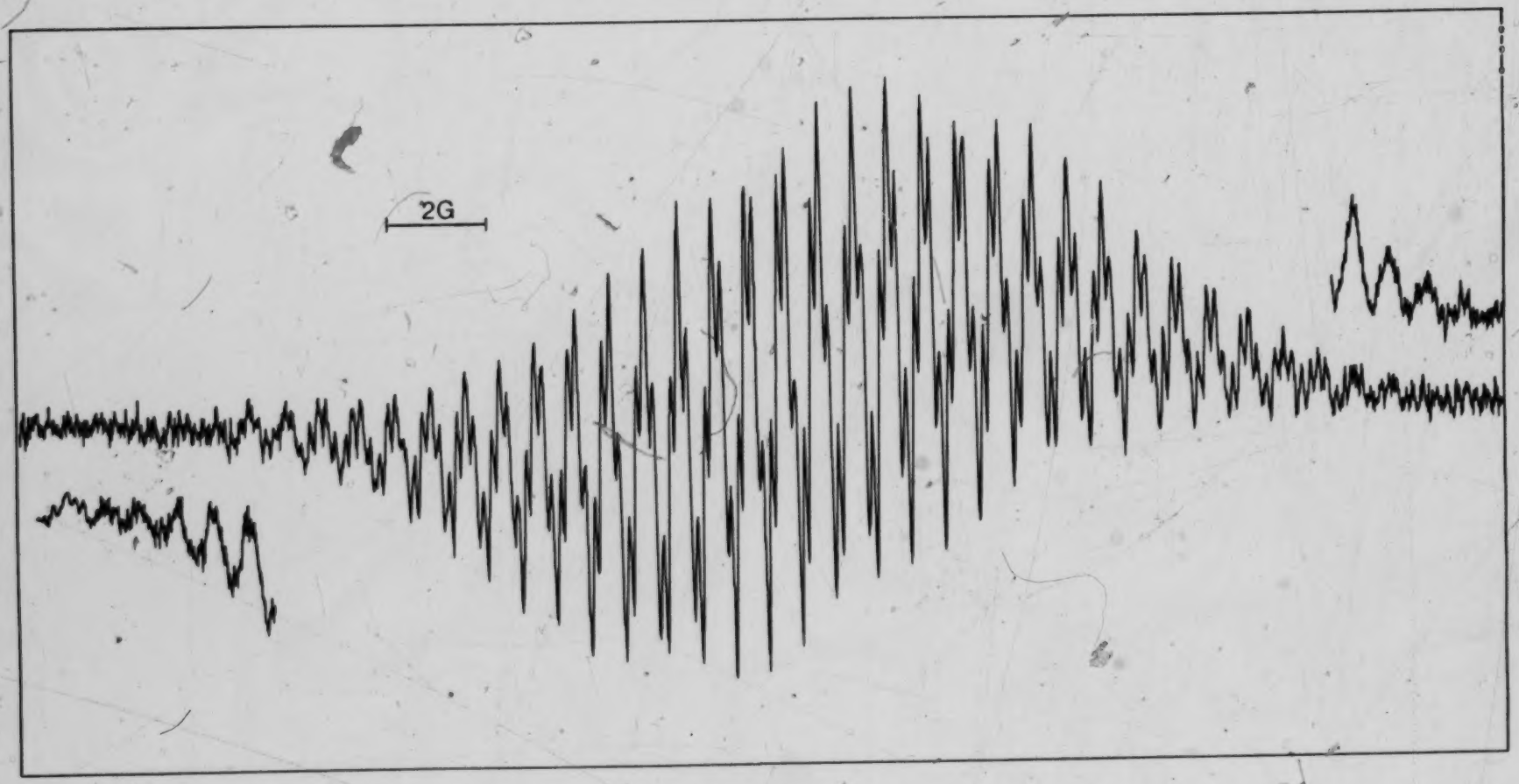

Figure 7. Resolved epr Spectrum of the 50:50 Mixture of TMPE/$TMPE^{2+}(Cl^{-})_2$ in Methylene Chloride

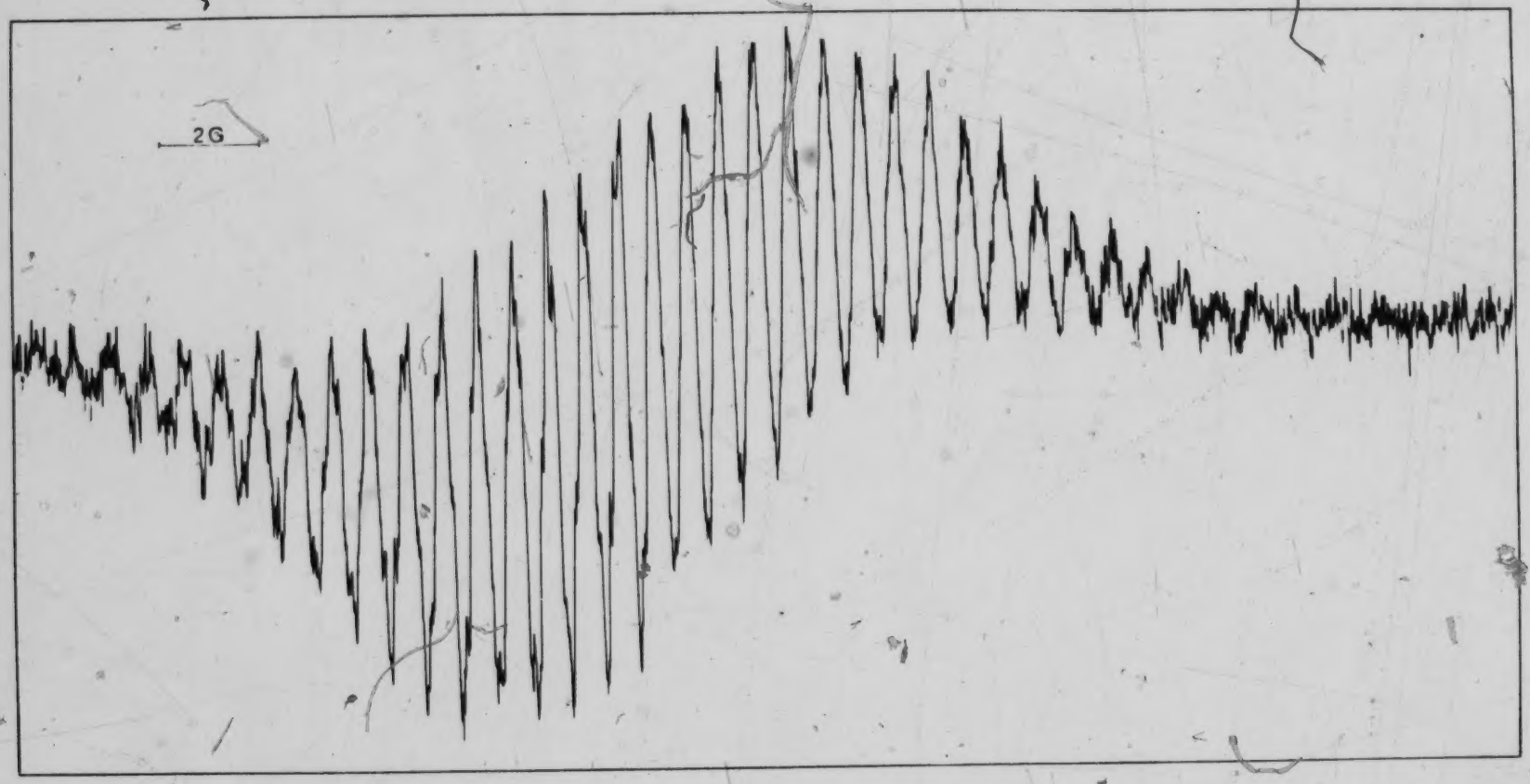

Figure 8. Resolved epr Spectrum of the 50:50 Mixture of TMPE/$TMPE^{2+}(BF_4^-)_2$ in Methylene Chloride

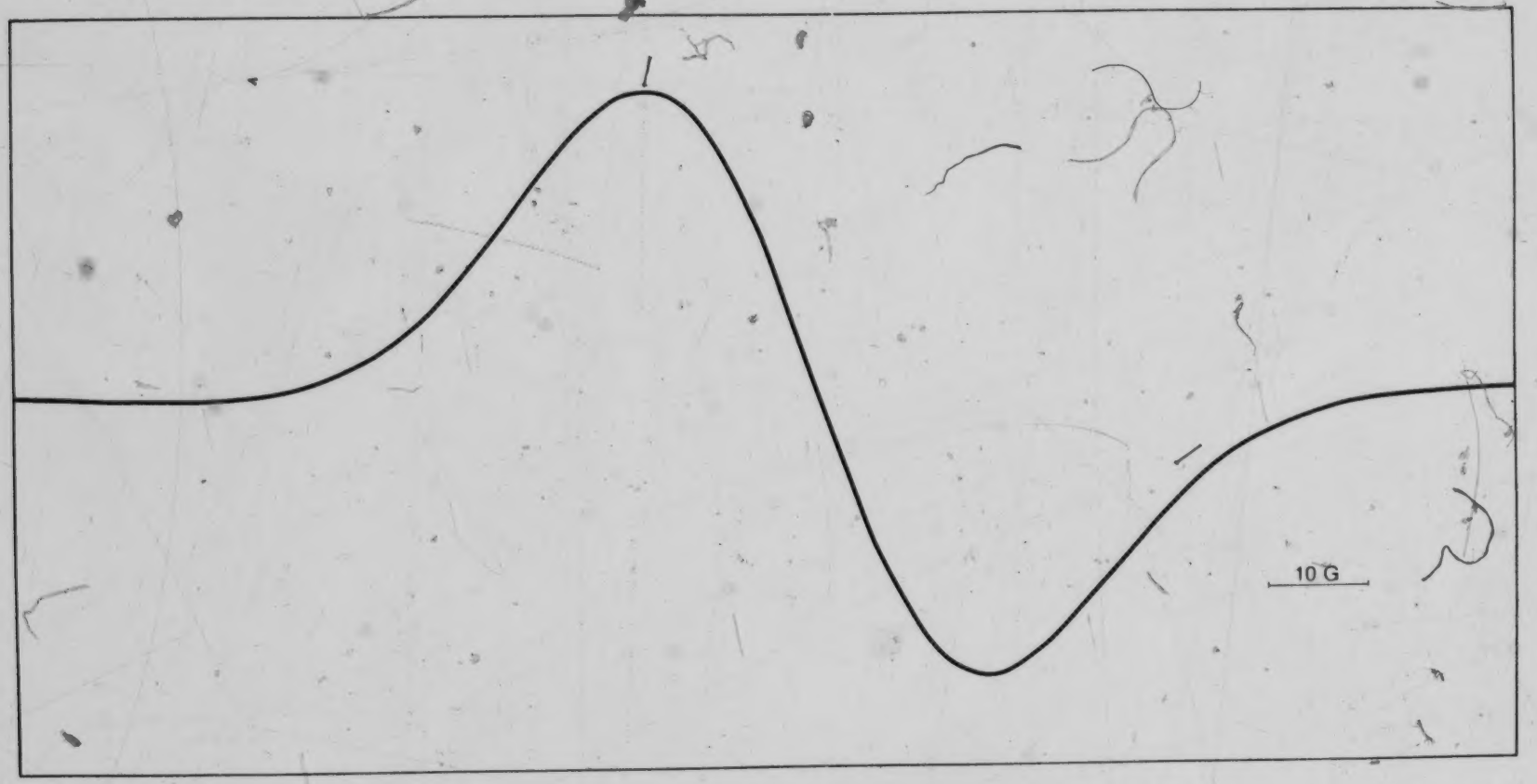

Figure 9. Overmodulated epr Signal of the Mixture of 50:50 TMPD/TMPD^{2+}(ClO_4^-)$_2$ in Acetonitrile

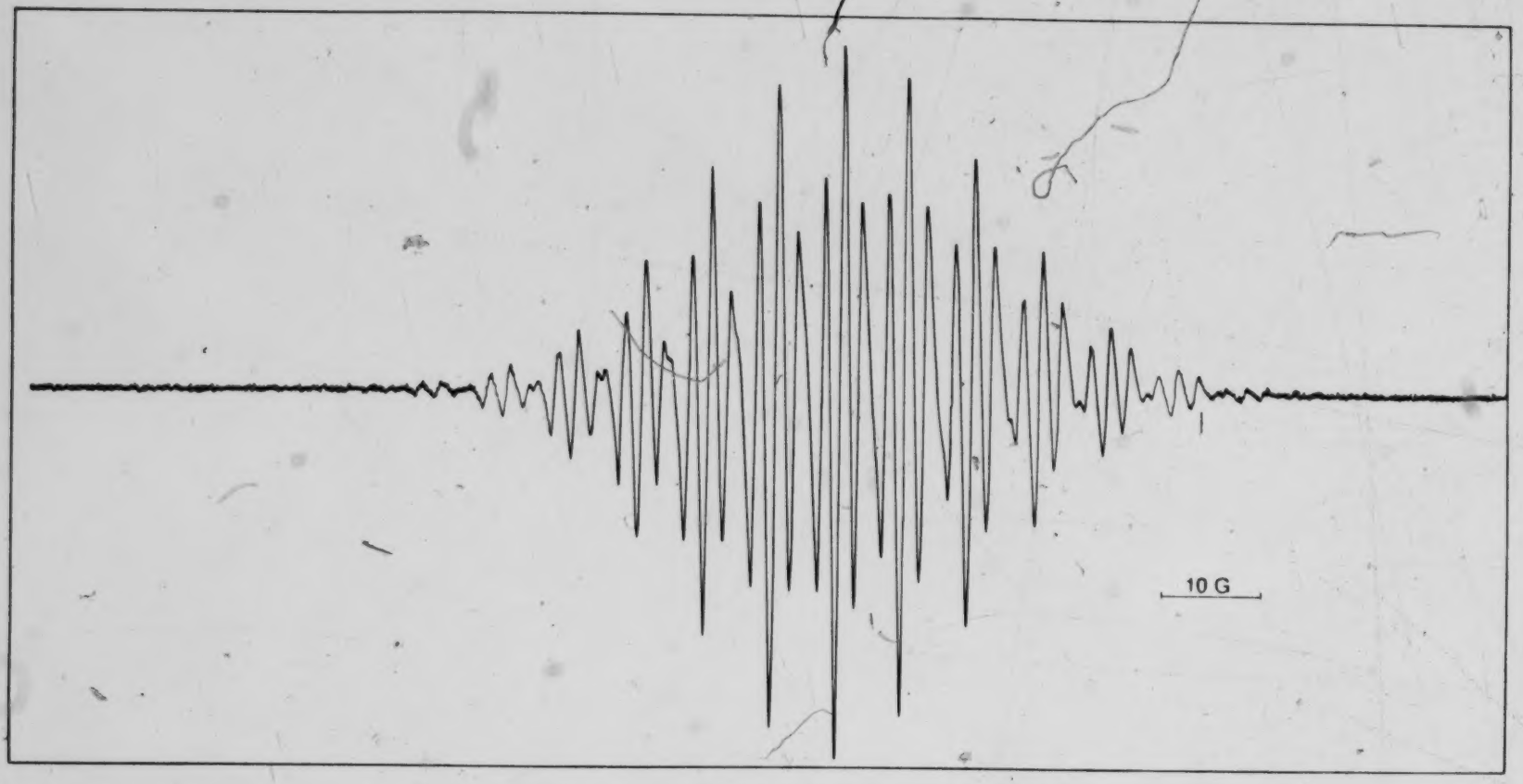

Figure 10. Resolved epr Spectrum of the 50:50 Mixture of TMPD/$TMPD^{2+}(ClO_4^-)_2$ in Acetonitrile.

Figure 11. GC-MS Chromatogram of the Reaction Mixture of $TMPD^{2+}(ClO_4^-)_2$ and 2,6-di-*tert*-butylphenol in Acetonitrile After Being Treated with Silica Gel (capillary column DB-1, 30 m). (Part I)

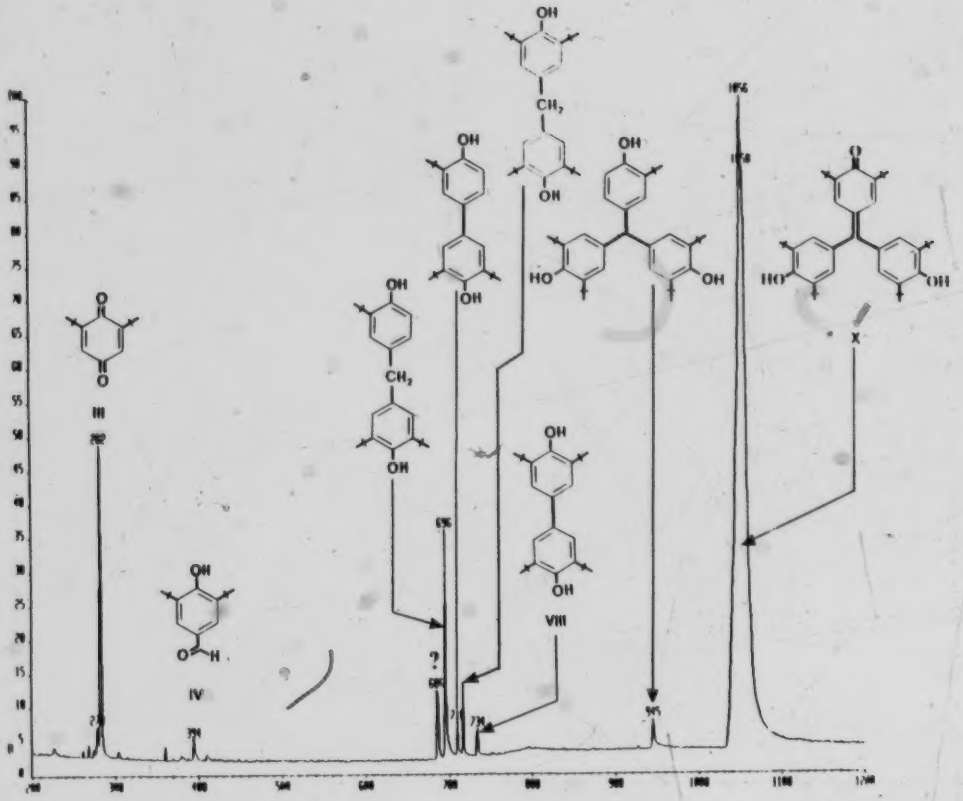

Figure 12. GC-MS Chromatogram of the Reaction Mixture of $TMPD^{2+}(ClO_4^-)_2$ and 2,6-di-*tert*-butylphenol in Acetonitrile After Being Treated with Silica Gel (capillary column DB-1, 30 m). (Part II).

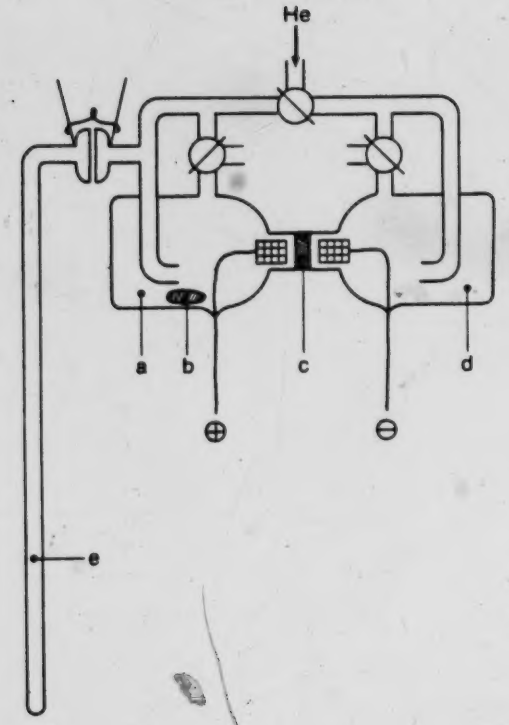

Figure 13. Electrolytic Cell Employed for the Epr Study (a) Compartment for TMPE/CH_2Cl_2 Solution, (b) Stirring Bar, (c)Sintered Membrane, (d) Compartment for $Et_4N^+Cl^-/CH_2Cl_2$ Solution, (e) 3mm OD Quartz Sidearm.

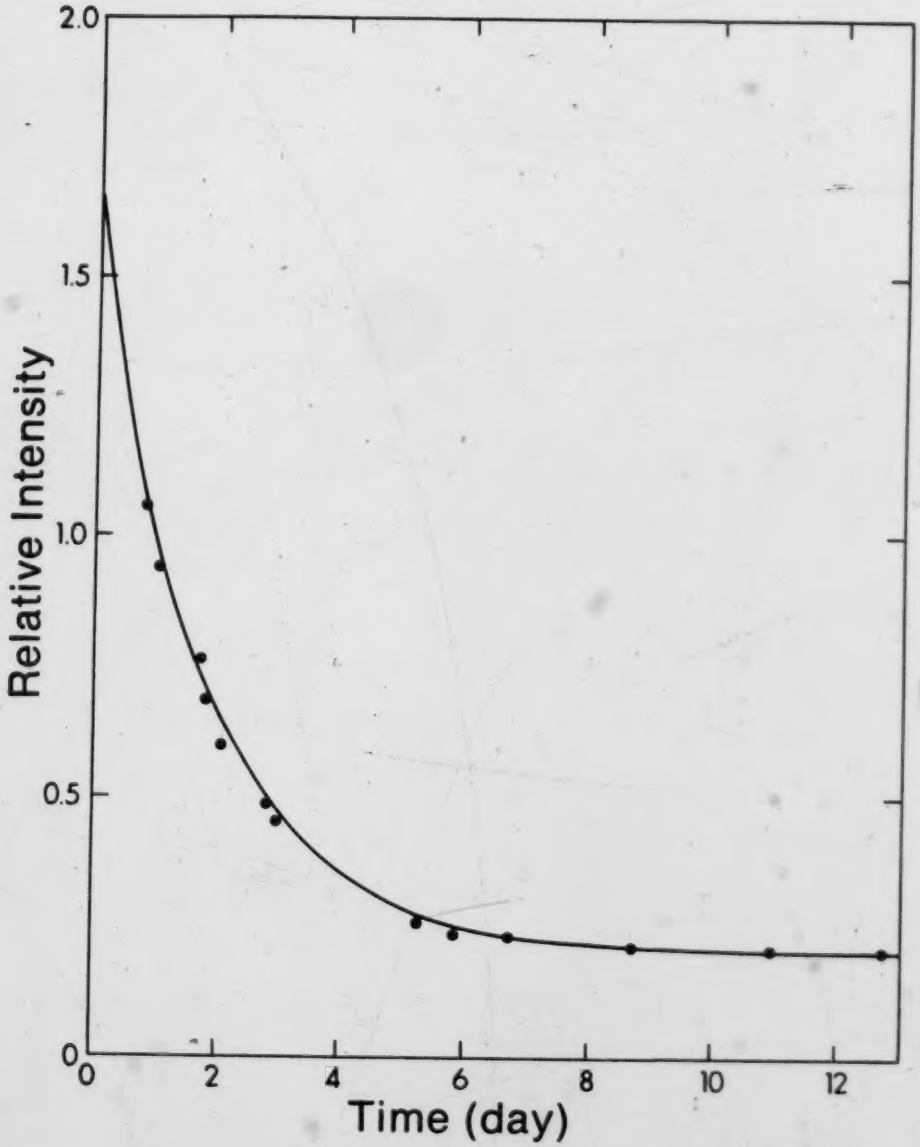

Figure 14. Plot of Relative Intensity of Epr Signal versus Time of the 50:50 Mixture of TMPD/$TMPD^{2+}(ClO_4^-)_2$ in Acetonitrile (total concentration 2×10^{-3} *M*).

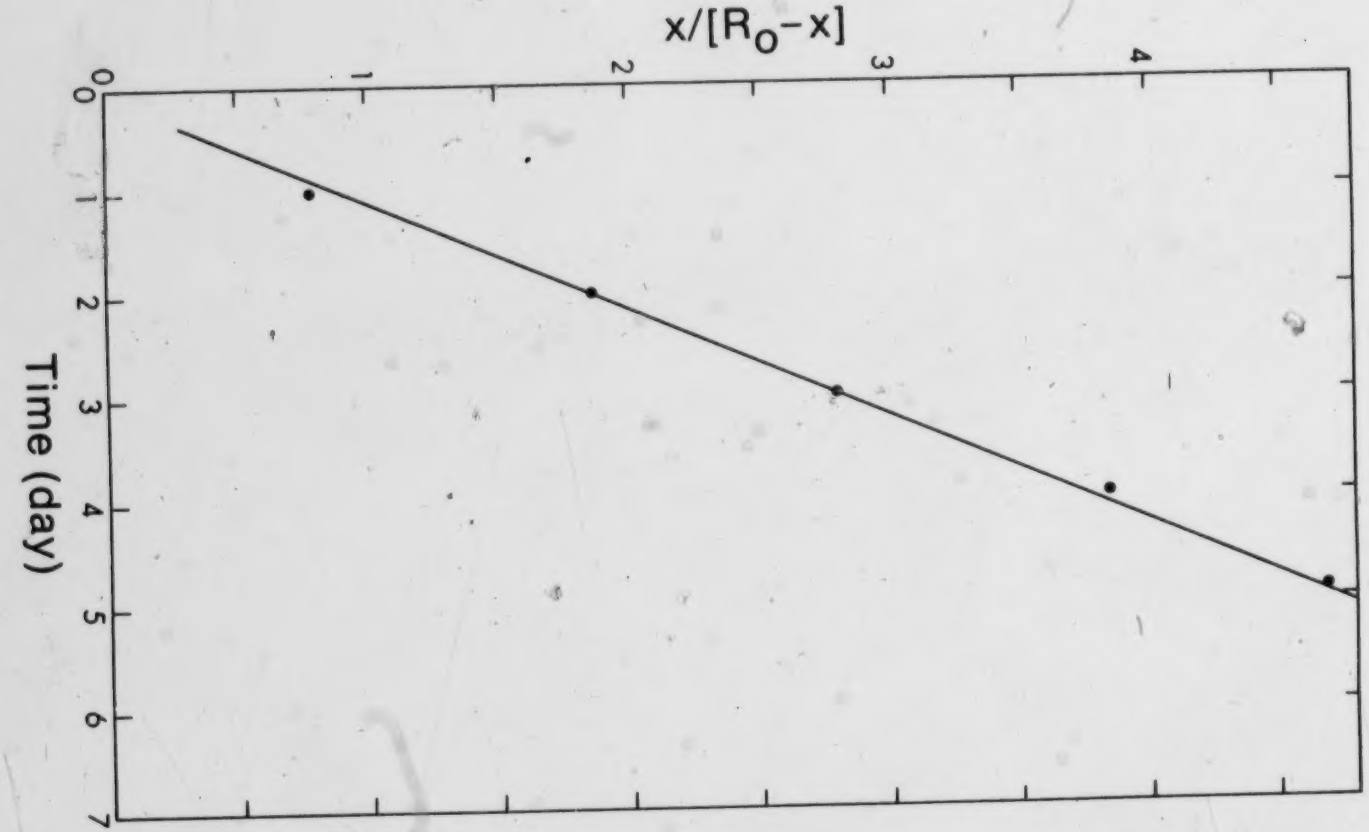

Figure 15. Plot of the Dimeric Product Concentration versus Time of the 50:50 Mixture of TMPD/$TMPD^{2+}(ClO_4^-)_2$ (total concentration $= 2 \times 10^{-3}$ *M*).

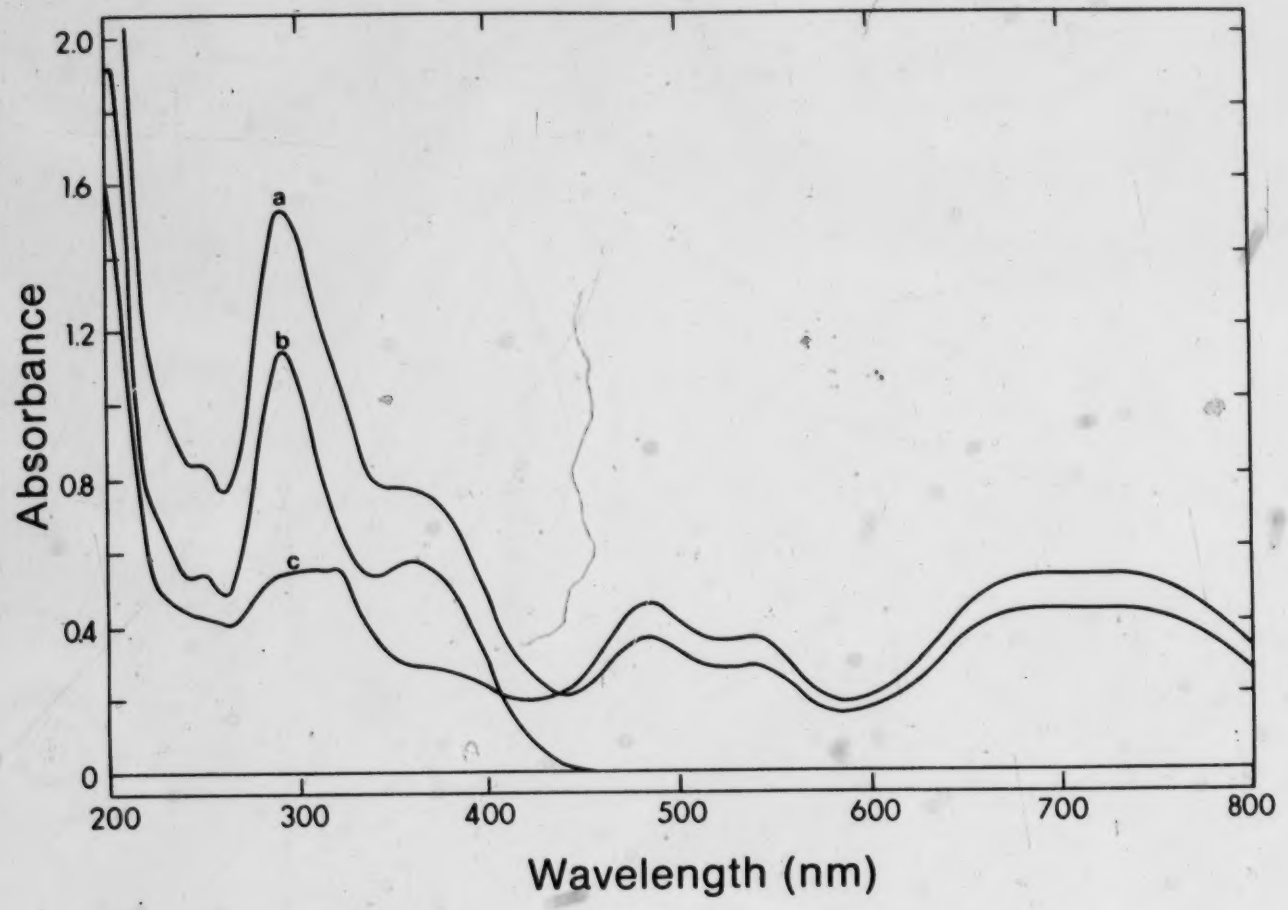

Figure 16. UV-absorption Spectra of:

(a) 50:50 Mixture Solution of TMPE/$TMPE^{2+}(Cl^-)_2$ (total concentration = 5×10^{-4} *M*).

(b) Equilibrium Concentration Solution of TMPE (2.59×10^{-4} *M*). and

(c) Equilibrium Concentration Solution of $TMPE^{2+}(Cl^-)_2$ (2.68×10^{-4} *M*).

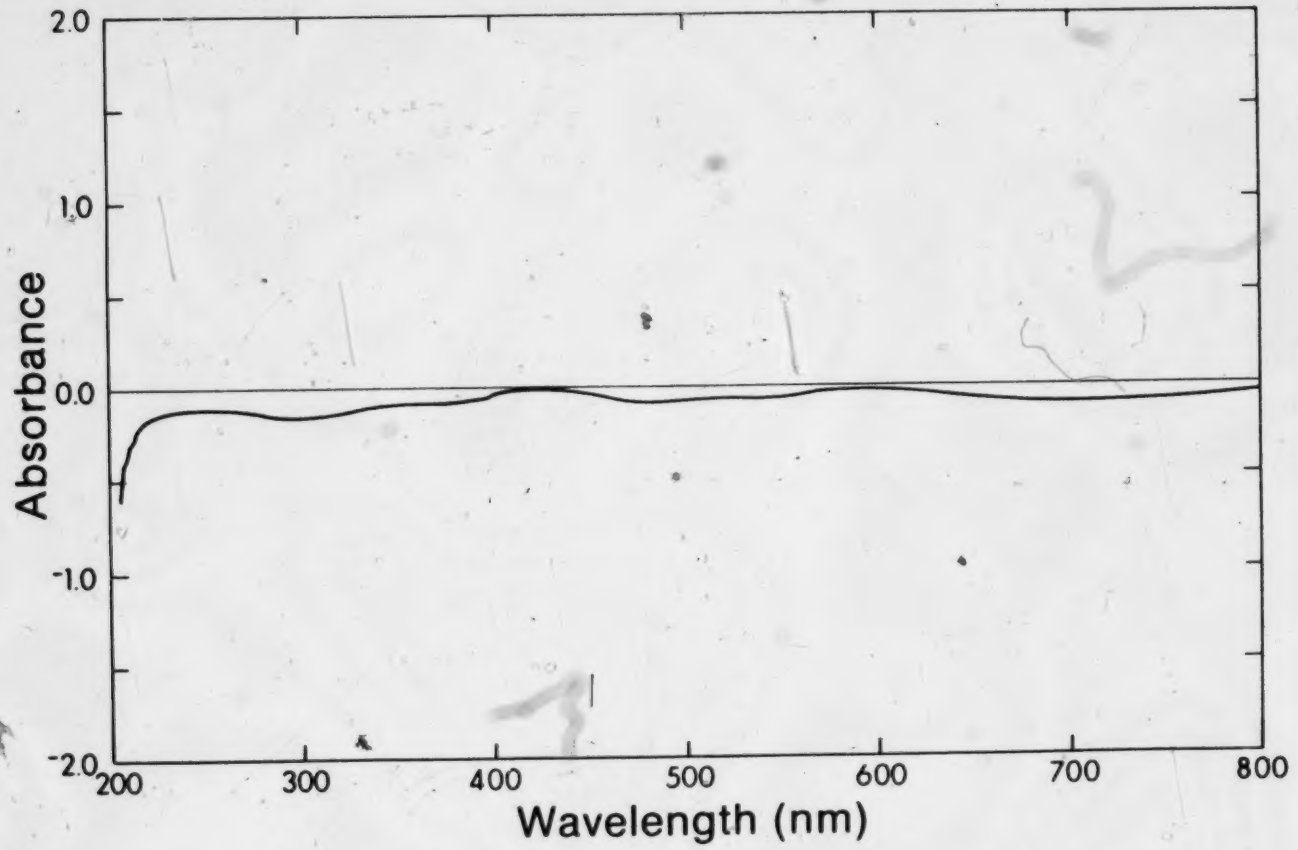

Figure 17. UV-Spectrum of the $TMPE^{+\bullet}$ Radical Cation After the Subtraction of Spectrum (b) and (c) from Spectrum (a) (See Figure 16).

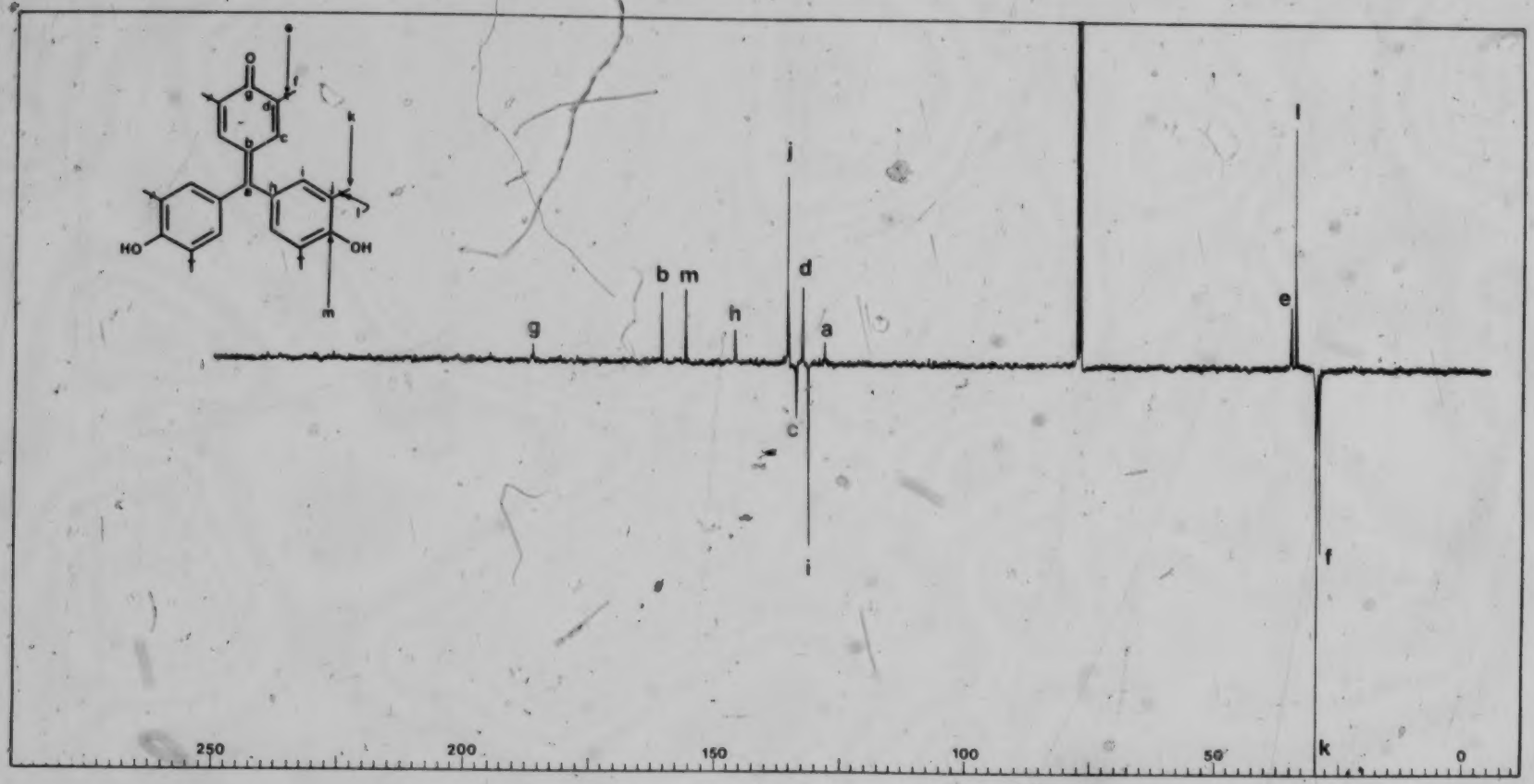

Figure 18. Tentative 100.62 MHz ^{13}C-nmr Chemical Shift Assignment for Compound (X) (in CD_2Cl_2); Singlet or Triplet (↑), Doublet or Quartet (↓).

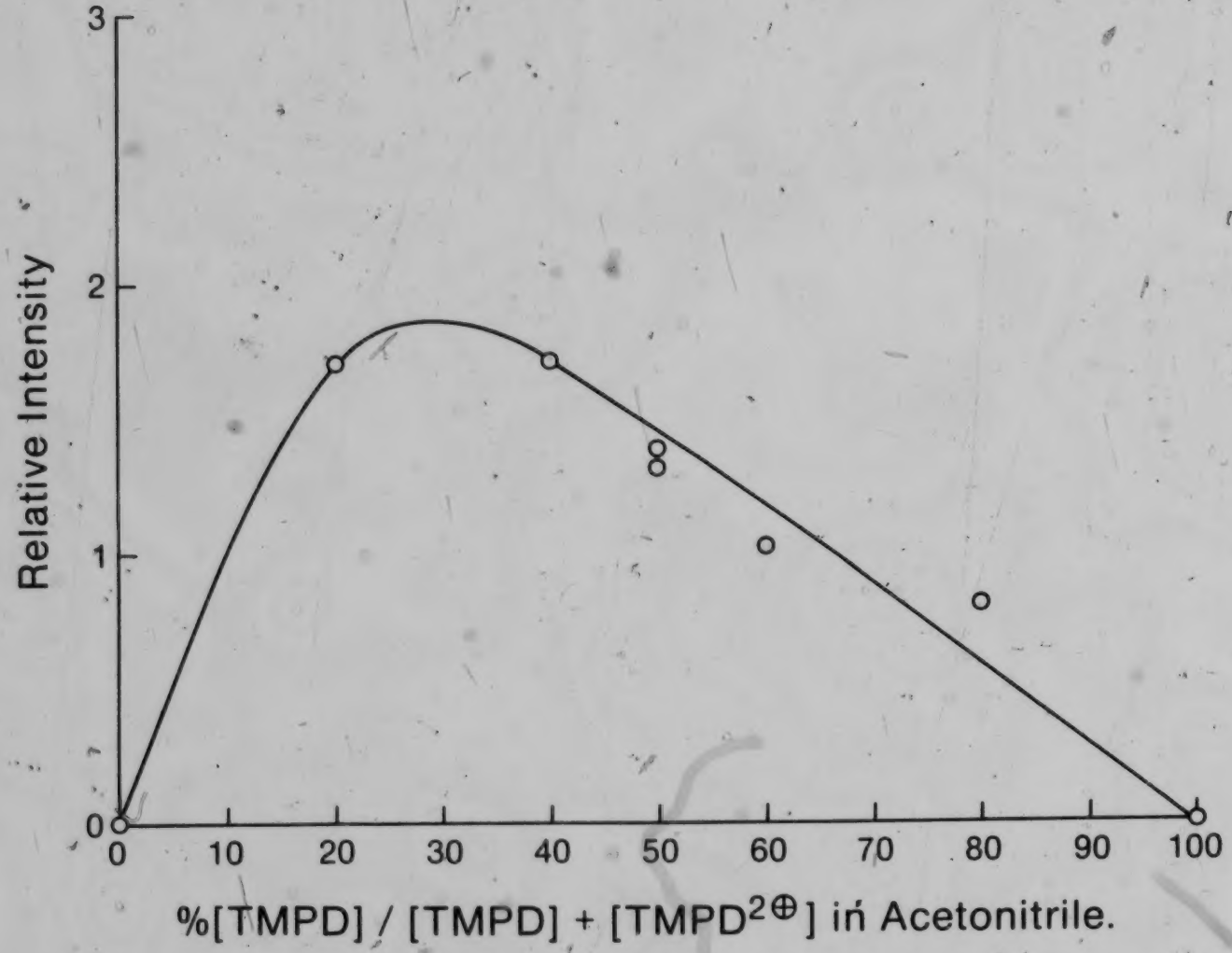

Figure 19, Plot of Relative Intensity of epr Signal of $TMPD^{+\bullet}$ versus % of [TMPD]/[TMPD]+[$TMPD^{2+}$] in Acetonitrile (total concentration $= 10^{-4}$ *M*.)

DISCUSSION

III.1 ON THE BEHAVIOUR OF THE TMPE/TMPE^{2+} SYSTEM

Subsequent to the reported preparations of the octomethyltetraaminophenylethylene by Gattermann[85] and by Willstätter and Goldman,[86] the dichloride, ditribromide, ditriiodide and diperchlorate adducts were synthesized by Wizinger.[87] The preparation of the dibromide, diiodide, dinitrate and disulfate adducts were also reported by Madelung and Oberwegner.[88] The ionic character of these adducts was firmly established by electroconductivity studies carried out by Buckles and Meinhardt.[89] Sandin and coworkers subsequently described the epr activity of the diiodo salt of the parent molecule in solution.[2,49-51] The observation of a featureless epr spectrum was rationalized by the assumption that in ethylene chloride solution the diiodide salt is reversibly converted back to the parent TMPE molecule and two iodine atoms [49] (Scheme I).

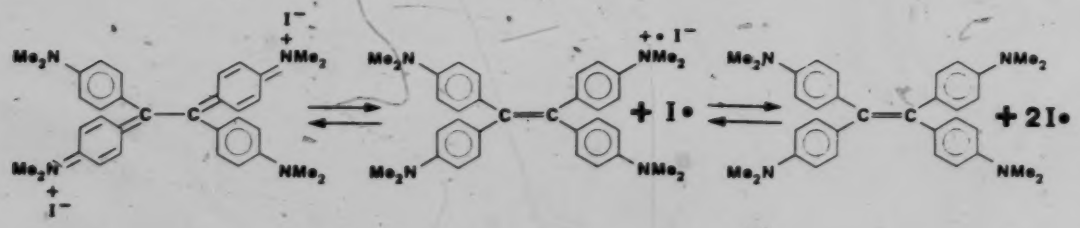

Scheme I

The suggestion was given some support by the observation that solutions of the dinitrate salt of TMPE did not exhibit any epr activity.[49] In an attempt to purify the dichloride salt of TMPE, in collaboration with Sandin, we noted that upon heating the salt to 75° under vacuum some of the salt was converted back to the parent TMPE molecule and that a methylene chloride solution of this solid is paramagnetic. When the diodide, dichloride, dinitrate and ditetrafluoroborate salts were purified by a continuous extraction method the methylene chloride solution of these salts does not exhibit paramagnetism but mixtures of the salts and the olefin gave an intense epr signal. Since the most intense signal was obtained at a

50:50 mixture of TMPE/$TMPE^{2+}$ salt it was suspected that an electron transfer equilibrium exists between the dication salt and the olefin TMPE (Scheme II).

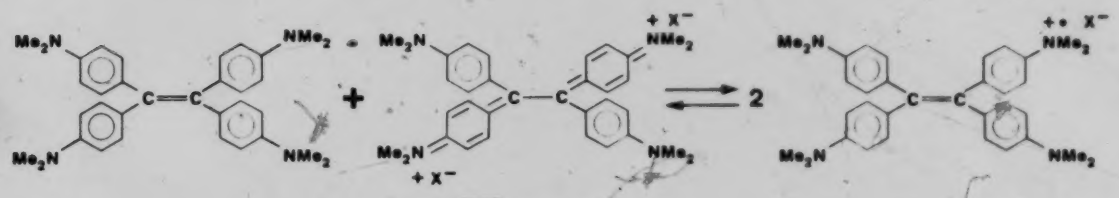

Scheme II

The concept of electron exchange between TMPE and $TMPE^{2+}$ was proposed by Bard *et al.*[56] through oxidative electrolysis studies of TMPE in acetonitrile and methylene chloride. The observation of a broad singlet was suggested as evidence for the existence of the $TMPE^{+\bullet}$ radical cation species. The measurement of the thermodynamic stability of a number of two-electron radical cation transfer systems have been previously determined electrochemically. Numerous studies of the formation constant of the radical cation (K_{SEM}) of the Wurster type and Weitz type species employing the electrochemical methods were reported by Hünig,[1,14,15,58,90] Geske and Kuwata,[24] Fritsch *et al.*,[91,92] Bard,[47,56,61] and Parker.[93,94] The key point to the successful application of the electrochemical method is governed by the magnitude of separation of the electron transfer potentials.[56] Clearly defined and well separated E_1 and E_2, $\Delta E = E_2 - E_1 > 55$-60 mV (the first and second halfwave potentials, respectively), will render K_{SEM} unambiguously determined. If, however, the second electron transfer occurs as easily or more readily than the first electron transfer the resulting first and second waves will merge and a single two-electron wave is observed, $\Delta E <$ 50 mV, the K_{SEM} will not be clearly defined. There also existed a borderline behaviour in which the differentiation between the first and second waves is still visible, ΔE = 50-60 mV. Unfortunately, the work of Bard suggested that TMPE belongs to the class of compounds showing the intermediate type of behaviour. Bard[56] attempted to put a limiting threshold for the E_2 value obtained for the reduction carried out in methylene chloride and he also predicted that K_{SEM} for the TMPE/$TMPE^{2+}$ system will have a smaller value in

acetonitrile. An accurate value of K_{SEM} was desired and an alternative approach to its determination was explored in this study.

The epr signal recorded at 0 and 100 percent of [TMPE]/[TMPE] + [$TMPE^{2+}$] indicated that both the parent olefin TMPE and the corresponding dichloride salt in acetonitrile or in methylene chloride solution exhibit negligible, if any, paramagnetism (Table I and III). It was, however, doubtful that the reversible electron transfer process has taken place between the iodide and the $TMPE^{2+}$ fragment in the case of the $TMPE^{2+}(I^-)_2$ salt in solution[49] (Scheme I). The suggestion that the paramagnetic species was formed during the disproportionation electron-transfer process of three equivalences of the $TMPE^{2+}(I^-)_2$ salt in benzene (Scheme III)[50] could not be consistent with a maximum epr intensity at the 50:50 stoichiometry.

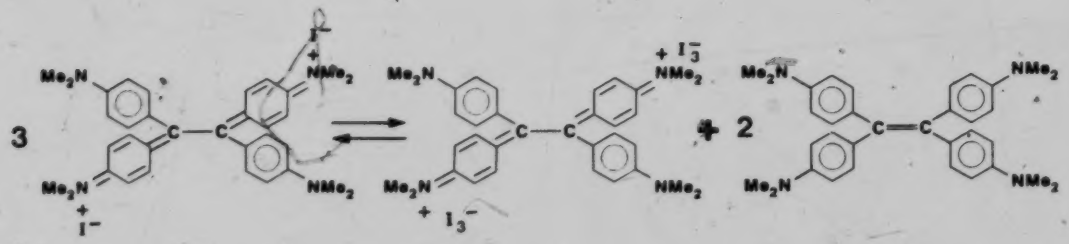

Scheme III

Subsequently, Sandin *et al.*[50] reported that the origin of the observed paramagnetic species was due to the formation of the $TMPE^{+\bullet}$ radical when an electron transfer process occurred between $TMPE^{2+}$ and its diiodide counter ions. In order to establish that the epr active $TMPE^{+\bullet}$ was actually formed by the comproportionation process the following work was done: (a) several $TMPE^{2+}$ salts with different counter anions, which would not easily undergo reversible electron transfer, were prepared, e.g., chloride, nitrate, tetrafluoroborate. These dication salts were allowed to react with a solution of TMPE. (b) oxidative electrolysis of the TMPE/CH_2Cl_2 solution was carried out under degassed condition and the epr intensity simultaneously monitored throughout the process. The oxidation was carried out to the full extent where an average of two electrons per molecule of TMPE was removed. The concept was successfully verified when the two solutions of equal concentration of TMPE and

$TMPE^{2+}(Cl^-)_2$ in methylene chloride were mixed at different relative proportions. The epr signal of the paramagnetic species formed reached its maximum intensity when the relative proportion is 50:50 (Figure 1). In other words the stoichiometry of the electron transfer interaction between TMPE and $TMPE^{2+}$ is 1:1. This indicated that one equivalent of TMPE will react with one equivalent of the $TMPE^{2+}$ to give rise to two equivalents of the $TMPE^{+\bullet}$ cation radical (Scheme II). In addition, when the TMPE/CH_2Cl_2 solution was continuously electrolyzed from zero to two equivalents, the epr signal of the observed paramagnetic species reached its maximum intensity when the oxidation reached one equivalent (an equivalent of one electron per TMPE molecule was removed). This also clearly signified that the optimum combination of TMPE and $TMPE^{2+}$ has the stoichiometry of 1:1.

The resolved hyperfine structure of the paramagnetic species could be obtained for the TMPE/$TMPE^{2+}(X^-)_2$ system (X = Cl, I, NO_3, BF_4), see Figures 7 and 8. This clearly indicated that $TMPE^+X^-$ radical is the paramagnetic species responsible for the observed epr signal previously reported. The resolved epr spectrum showed 190 lines (theoretical, 5100 lines) was obtained (see Fig. 7). The resolved epr spectrum of the 50:50 mixture of the TMPE/$TMPE^{2+}(BF_4^-)_2$ system in methylene chloride (Figure 8) is identical to that obtained from the TMPE/$TMPE^{2+}(Cl^-)_2$ system. This further supports the suggestion that the paramagnetic species observed is that of the $TMPE^{+\bullet}$ radical. The equilibrium concentration of the $TMPE^{+\bullet}$ radical obtained from the TMPE/$TMPE^{2+}(Cl^-)_2$ system in acetonitrile was calculated to be 9.78 ± 7.59 % (see Appendix Ib, 4c).

The UV absorption spectrum of the $TMPE^{+\bullet}$ radical cation, obtained after subtracting the absorption spectra of both the TMPE and $TMPE^{2+}$ at equilibrium concentration in acetonitrile from the overall absorption spectrum of the 50:50 mixture, has very low absorption which may account for the 9.8% radical existing at equilibrium (see Figures 16 and 17). These results argue for the reliability of the value $K_{eq} = 0.089$ obtained for the TMPE/$TMPE^{2+}(Cl^-)_2$ system in acetonitrile. The equilibrium constant, $K_{eq} = 6.00$ for the TMPE/$TMPE^{2+}(Cl^-)_2$ system (methylene chloride) was verified electrochemically.

When the paramagnetic species of TMPE in methylene chloride solution was generated electrochemically and a plot of relative epr intensity versus time was constructed, the K_{eq} calculated from the plot was 6.00 which corresponds to 53.3% radical at equilibrium.

Within experimental error range for the epr method of ± 10 to 20 percent, K_{eq}'s obtained by the two different methods are in satisfactory agreement. The results were also found to be consistent with those reported by Bard *et al.*[56] regarding the electrochemical behaviour of TMPE/$TMPE^{2+}(Cl^-)_2$ system in acetonitrile and methylene chloride. However, the reported K_{eq} still remained questionable since Bard utilized the suggestion of Sandin that $TMPE^{2+}(I^-)_2$ undergoes reversible electron transfer process by itself in solution and proposed the E_2 value to fall within the range between E_N ($TMPE^{2+}$/TMPE) = (E_1° + E_2°)/2 = 0.16 V and E° (I_2/I^-) = 0.20 V. This is probably not correct since the result from this work has lent strong support to the existence of an electron-transfer process occurring between $TMPE^{2+}$ and TMPE.

In conclusion, the behaviour of the TMPE/$TMPE^{2+}(Cl^-)_2$ system in acetonitrile and methylene chloride, in general, follows the trend that other similar systems do. Solvents with higher dielectric constant, e.g., acetonitrile, favor the solvation of the dication species resulting in the shift of the equilibrium towards the disproportionation direction and solvents with low dielectric constant, e.g., methylene chloride, favor the solvation of the less charged monocation species which in turn shift the equilibrium towards the comproportionation direction. The question as to when the solvation factor or the thermodynamic stability of the semiquinone monocation radical predominantly governs the direction of the equilibrium remains open for further study. One obvious fact is that in the case of the TMPD/$TMPD^{2+}$ system the stability of the cation radical is so large that even in more polar solvents such as acetonitrile the equilibrium lies far over to the comproportionation side ($K_{eq} = 10^{10.97}$).[3]

III.2 ON THE BEHAVIOUR OF THE TMPD/$TMPD^{2+}$ SYSTEM

Since the equilibrium constant (K_{SEM}) could be successfully determined for the TMPE/$TMPE^{2+}$ system in both methylene chloride and acetonitrile, a similar approach was attempted with the

TMPD/TMPD^{2+}(ClO_4^-)$_2$ system in acetonitrile. A number of electrochemical studies of the oxidation of TMPD have been reported.[3,95,96] The E_1 and E_2 values determined in these studies allow the calculation of the K_{SEM} constant. These value are compared with the result obtained from our epr studies of the TMPD/TMPD^{2+} system (see Table IX). From the epr plot (see Figure 5), the equilibrium constant for TMPD/TMPD^{2+} system in acetonitrile is calculated to be 34.28(73.30 of the material is radical at equilibrium) while that reported by Grampp and Jaenicke[3] is calculated to be 9.3×10^{10} (> 99.9% radical at equilibrium). The discrepancy may owe its explanation to the fact that TMPD$^{+\bullet}$ can undergo radical dimerization in solution.

The reversible radical dimerization of the TMPD$^{+\bullet}$ radical species in solution and in the solid state at various temperature range has previously been reported to explain the paramagnetism behaviour observed.[97-109] In our laboratory the paramagnetism was found to decay irreversibly with time (see Figure 14) and the radical half-life estimated to be three days. Our DPPH calibration (85.9% radical at equilibrium, see entry 4, Table IX) inferred the radical concentration is lower than that predicted by electrochemistry (> 99.9% radical at equilibrium) which meant some reservation after this since the method is only approximately correct within ± 20%. However, the shape of the theoretical curve (K = 27) agrees with that of the DPPH calibration (see Figure 5) and suggested that a rationale is needed as to why the epr method gives a correct answer but does not agree with that which came from electrochemical studies. In addition, if the presupposition that an irreversible bimolecular process occurs subsequent to the reversible formation of the TMPD$^{+\bullet}$ cation radical holds true (Scheme IV), then the radical decay would follow second-order kinetics.

The straight line plot of the ratio $[X]/[R_0 - X]$[110] versus time (see Figure 15) is consistent with this proposal. Chemical Ionization - Mass Spectral examination of the solid material recovered after several half-lives shows the existence of the monomeric TMPD (MH^+, 165) while Fast Atom Bombardment - Mass Spectrometry indicated the existence of both the monomeric TMPD (MH^+, 165) and the dimeric product of TMPD ($M'H^+$, 327) (M' is the molecular weight of the dimeric product). A thin layer chromatographic examination of the solid material (silicagel/ethyl acetate: pentane [2:8]) shows the existence

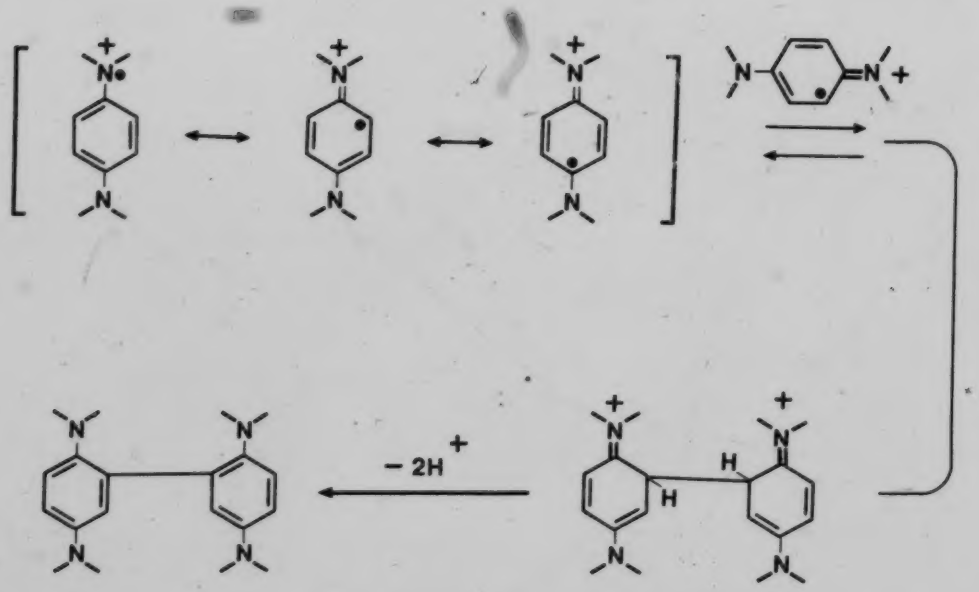

Scheme IV

of at least three components, one of which is the monomeric TMPD (by a comparison with the R_f of TMPD). A UV absorption examination of the solid material dissolved in acetonitrile solution showed an absorption spectrum identical to that of the monomeric TMPD ($\lambda_{max}^{CH_3CN}$ 260, log ϵ 3.44). All of these data lead to the conclusion that a dimeric product is at least one of the conceivable pathways to rationalize the irreversible disappearance of the paramagnetic $TMPD^{+\bullet}$ species. However, another possible rationale for the observed irreversible decay of the epr signal, which cannot be completely ruled out, is that the TMPD + $TMPD^{2+} \rightleftarrows 2$ $TMPD^{+\bullet}$ equilibrium is shifted towards the disproportionation direction by reaction of one of the reactants. This behavior could be accounted for since solutions of the dication, $TMPD^{2+}(ClO_4^-)_2$ in acetonitrile solution has been reported by Michaelis[111,112] and Kommandeur[113] to decay upon standing in aprotic solvents which are not absolutely dry. If the dication was depleted the equilibrium shifts towards the disproportionation direction. As a consequence lower concentrations of the paramagnetic $TMPD^{+\bullet}$ and lower equilibrium

constants would be observed.

An attempt to reduce the possibility of $TMPD^{+\bullet}$ radical dimerization by lowering the total concentration yielded a peculiar epr concentration plot (see Figure 19). The skewed plot which has its maxima at 25-30% may be indicative of complex formation between TMPD with its own species and/or the $TMPD^{2+}$ with its own species. The UV absorbance vs concentration plot of both TMPD and of $TMPD^{2+}(ClO_4^-)_2$ in acetonitrile solutions over the concentration range studied (5×10^{-5} - 10^{-3} *M*) indicated that the Beer-Lambert Law is strictly followed and gave no indication of complex formation. The behaviour of the epr plot at lower concentrations remains unexplained.

III.3 OXIDATION OF PHENOLS USING THE DICATION SALTS

The capacity of the $TMPD^{2+}$ and the $TMPE^{2+}$ dication fragments to gain one or two electrons to give a stable radical cation or the neutral species, respectively, is an attractive feature of the salts should they be used as potential oxidants. The substrate under investigation in this study is 2,6-di-*tert*-butyl phenol.

One of the characteristic chemical properties of the phenol family is their facile oxidative conversion to compounds of different structural types.[114-117] The diversity of phenol oxidation products offers interesting synthetic possibilities for the preparation of simple and polymeric molecules containing phenolic and/or quinonoid structural elements, particularly of those resulting from oxidative coupling of both like and unlike intermediate radical species.[118-125] In addition, mechanistic studies of oxidation reactions of phenols[118-125] have lent strong support to the interpretation that a number of biosynthetic processes actually proceed by biogenetic pathways, involving the oxidative utilization of phenolic substrates.[114,118,121-123,125]

The long-known fact that substituted phenols and the corresponding phenoxy radicals are efficient inhibitors in autoxidation processes of organic substances[126-128] has stimulated the development of chemical and physical methods, particularly esr spectroscopy, for the study of the detailed structure of phenoxy radicals and their role as intermediates in free radical reactions.[129-131] The first step in the oxidation of monohydric phenols, by oxidizing agents capable of one-electron abstraction,[114,123,125,129,132] such as lead dioxide, silver oxide, manganese dioxide, ferric and cerric ions, electrochemical methods,[133] alkaline potassium ferricyanide,[119] etc., consists in the generation of a free aryloxy radical either by homolytic hydrogen atom abstraction of the O-H bond of the phenol (Scheme V) or by the loss of one electron from the corresponding phenol or phenoxide (Scheme II). The latter pathway shown in Scheme VI is the major one in neutral or alkaline aqueous solution whereas the former is more important in strongly acidic solutions or in non-polar solvents. The formation of the transient phenoxyl radicals in the oxidation of a variety of phenols under different conditions has been amply confirmed by epr techniques.[124,134,135]

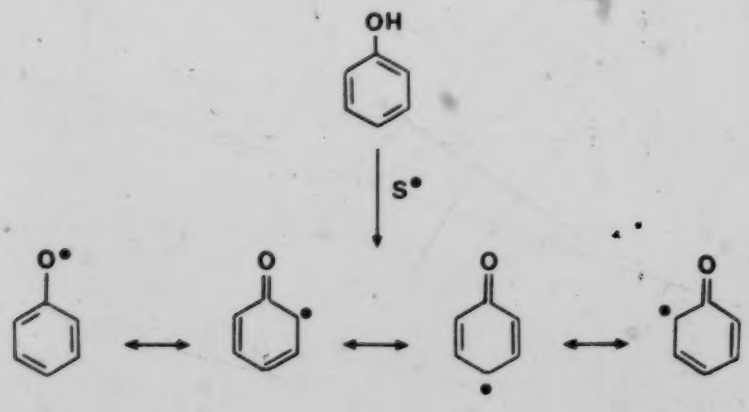

Scheme V

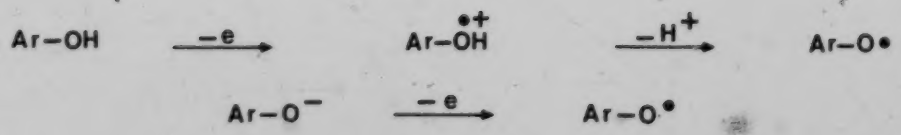

Scheme VI

The aryloxy radicals, formed in the first step of the oxidation of phenols by one electron transfer oxidants, may undergo a variety of reactions, depending on the reactivity and substitution pattern of the radicals, on experimental conditions, on the amount of oxidizing agent and on the presence of other substrates in the reaction mixture.[129-131] When the coupling positions are blocked by substituents such as alkyl, halogen, or methoxyl, the dimeric *o,o* or *o,p* products can be isolated in high yields.[136,137] With strong oxidizing agents, diphenoquinones (2) are the final products,[138] resulting from further oxidation of the dimer (1) (Scheme VII). The de-*tert*-butylation of the substituted phenols during the process of

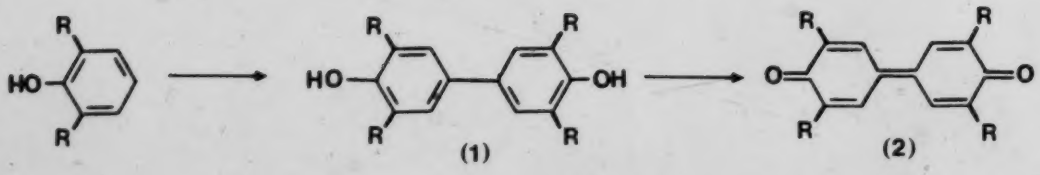

Scheme VII

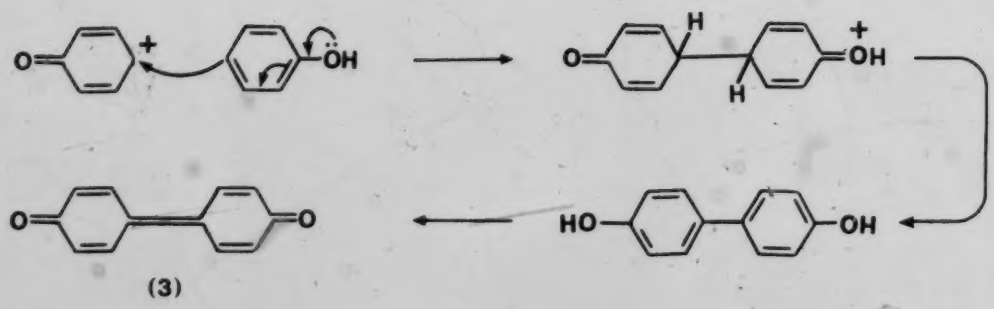

Scheme VIII

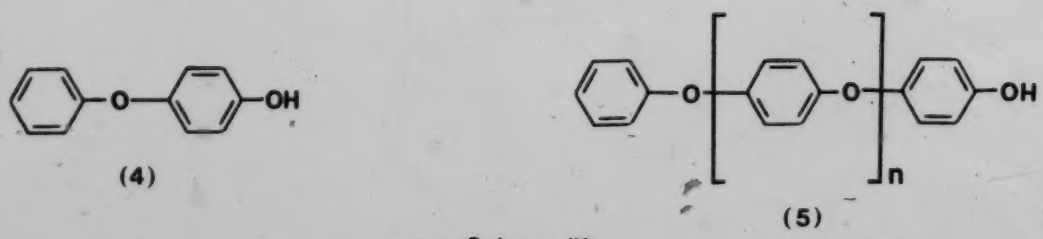

Scheme IX

oxidation has also been reported with 2,4,6-tri-*tert*-butylphenol.[139-141] With two-electron oxidants such as lead tetra-acetate, benzoyl peroxide, and possibly alkaline persulphate[142] the dominant reaction is electrophilic attack on the aromatic ring which may also consequently yield the oxidative coupling products.[143] (Scheme VIII). In regard to the discrimination between oxidants, published evidence indicates that quinones and diphenoquinones (3) but not dimers (4) or polymers (5) result from oxidations effected in acidic solution or with reagents

of high oxidation potential,[144] while with reagents such as alkaline ferricyanide an increase in alkalinity favours polymer formation[145] (Scheme IX). Catalytic oxidative coupling of 2,6-dialkylphenols, employing a variety of metal and transition metal complexes as catalysts, has also been attracting more attention from many workers during the last few years,[141,146-151]

In general, depending on the electron accepting ability of the oxidant towards the 2,6-di-*tert*-butylphenol substrate, the reactive intermediates involved in the product formation process can either be a phenoxy radical and/or a phenoxonium ion (Scheme X). The involvement of the phenoxonium ion as a reactive intermediate increases if the participating oxidant is comparatively strong. Numerous studies carried out on 2,6-di-methylphenol employing strong oxidant such as Cerium(IV), hexachloroiridate (IV)[152] and by electrochemical anodic oxidation[153] have indicated that the phenoxonium intermediate is responsible for the formation of 2,6-dimethylbenzoquinone. In the case of hexachloroiridate (IV)-catalyzed oxidation of 2,6-dimethylphenol at least 20% was found to involve this intermediate (Scheme XI).

In our laboratory the reaction of the salt $TMPD^{2+}(ClO_4^-)_2$ with 2,6-di-*tert*-butylphenol in acetonitrile at 90°C under degassed condition yielded predominantly a series of coupling products together with the di- and tri-phenolic compounds which had incorporated one or more carbon atoms (see Table X). The existence of the latter compounds led to the assumption that the solvent may be participant in their formation. Experiments were thus carried out in labelled acetonitrile, acetonitrile-1-^{13}C, acetonitrile-2-^{13}C, and in propionitrile and in benzene.

The experiments carried out in labelled acetonitrile solutions all failed to reveal any ^{13}C enrichment in these compounds, while those carried out in propionitrile yielded exactly the same pattern of products that were observed when the reaction was run in acetonitrile. The reaction carried out in benzene yielded mainly the coupling product, compound VIII (Table XIV) (2% yield after 121 hours). Prolonging the reaction period in benzene (the $TMPD^{2+}(ClO_4^-)_2$ salt was only slightly soluble in benzene) gave more de-*tert*-butylated product together with tlc-non eluted material, which is suspected to be polymeric materials.

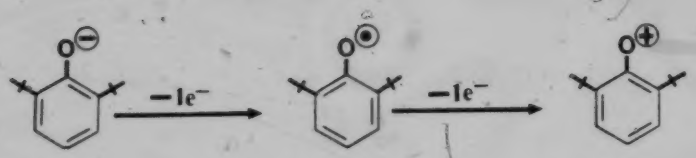

Scheme X

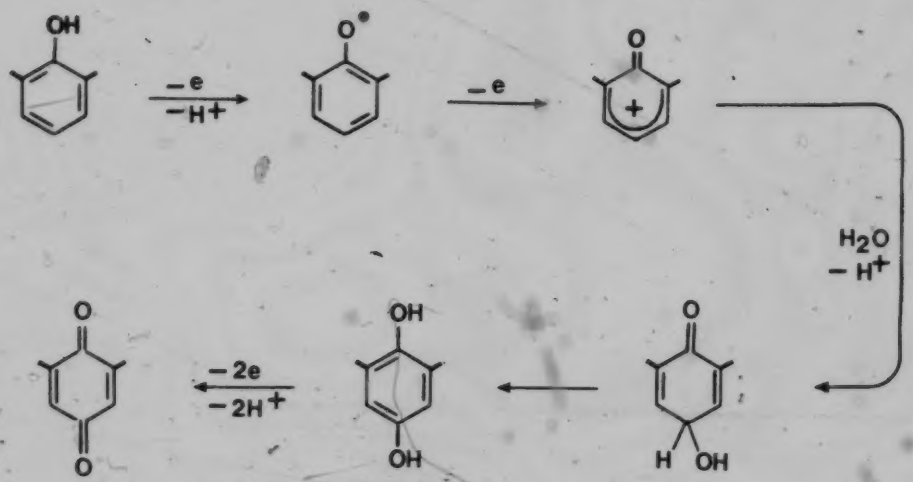

Scheme XI

The yield of the products of the reaction of the salt $TMPD^{2+}(ClO_4^-)_4$ with 2,6-di-*tert*-butylphenol in different solvent systems are listed in Table XIV.

Attempts to react the next higher homologue of $TMPE^{2+}$: compound tetraethyl-1,4-diiminoquinone diperchlorate with 2,6-di-*tert*-butylphenol in acetonitrile after 48 hours at 90°C under degassed condition failed to provide any of the oxidative products and the starting phenolic substrate was recovered quantitatively. These observations led to the conclusion that the newly incorporated carbons in compounds II, III, V, VI, IX and X (Table IX) came from the $TMPD^{2+}(ClO_4^-)_2$ salt. The demethylation of the dication salt and its homologue TMPE to give formaldehyde was previously reported by Michaelis,[111,112] and by Sandin.[51]

The formation process of compounds (VII) and (VIII) (Table X) can be depicted as either a homolytic (Scheme XII) or ionic process (Scheme XIII). Since the $TMPD^{2+}(ClO_4^-)_2$ salt is comparatively strong oxidant, i.e., being capable of undergoing

two-electron oxidation, the possible involvement of the 2,6-di-*tert*-butyl phenoxonium ion as a reactive intermediate could not be ruled out. The observation of several de-*tert*-butylated products (compounds XI, XIV, XV and XVI) and *tert*-butylated product (compound XII) (see Tables XI and XII) lent strong support to the existence of the *tert*-butyl carbonium ion. The formation pathway of (XI) is given in Scheme XIV.

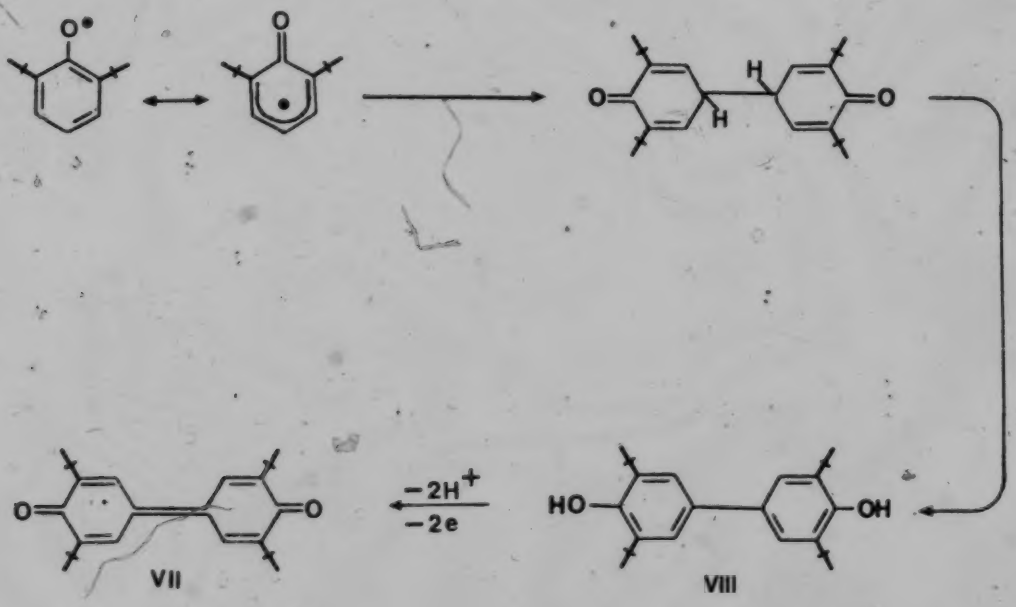

Scheme XII

Compound XIII (Table XI) is generated through the realkylation of the phenolate ion of the reactive *tert*-butyl carbonium ion formed in Scheme XIV. The formation of compound III (Table I) may actually occur during the reaction process since the reaction between $TMPD^{2+}(ClO_4^-)_2$ and 2,6-di-*tert*-butylphenol in all cases were carried out under degassed condition. The mechanism of this process is depicted in Scheme XV. The existence of compound II (Table X) and compound XII (Table XI) are no doubt related to one another. It is likely that XII was first formed and then reduced to give compound II (Scheme XVI). The reductants responsible for this process are likely TMPD and $TMPD^{+\bullet}$ radical cation.

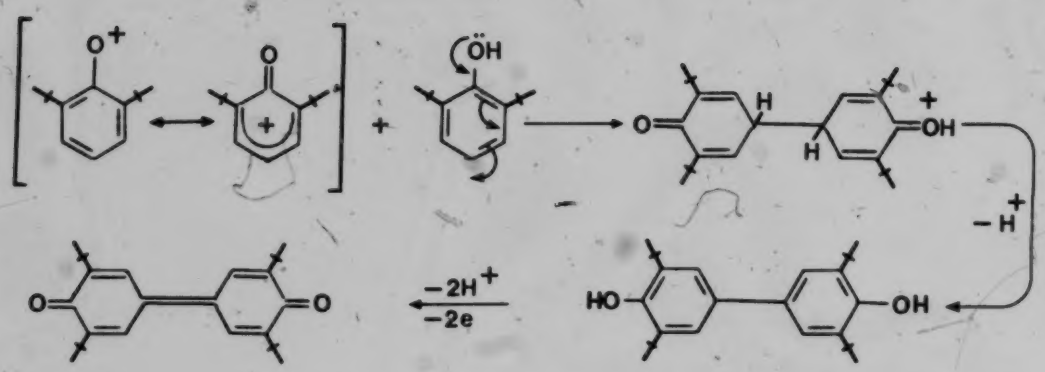

Scheme XIII

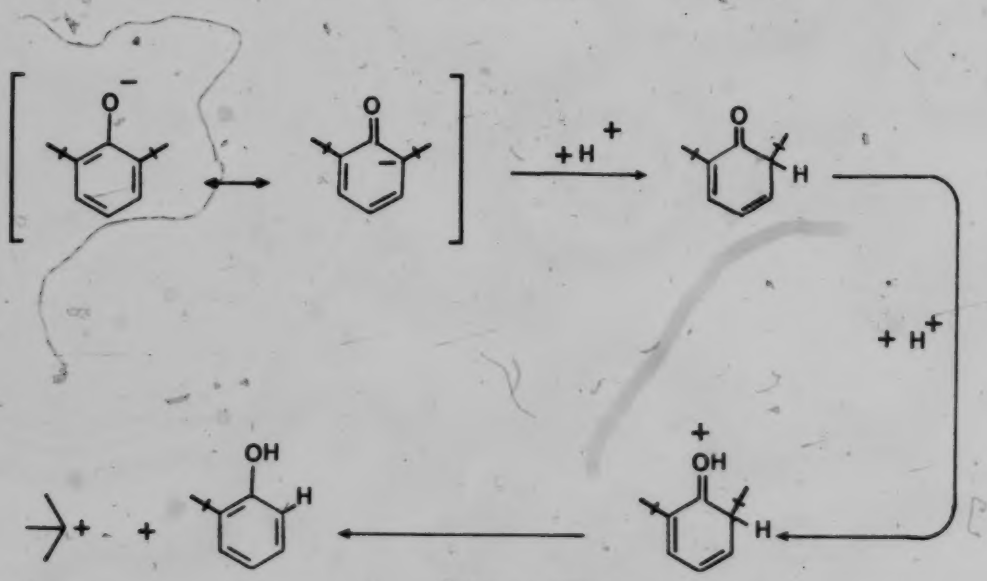

Scheme XIV

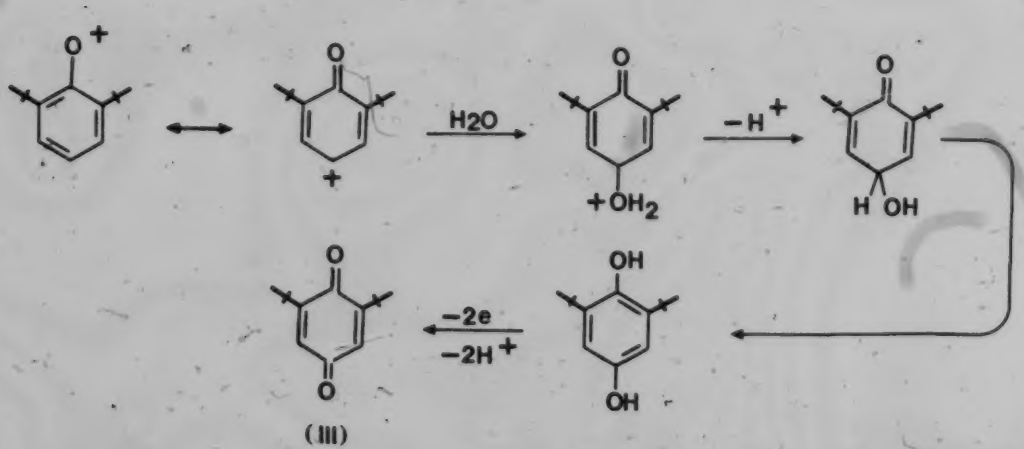

Scheme XV

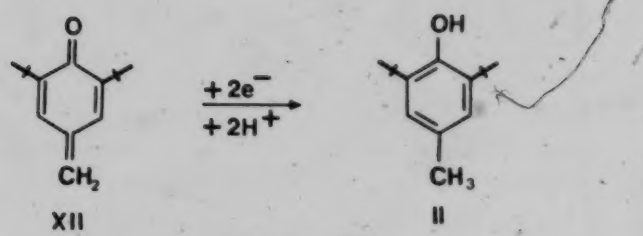

XII II

Scheme XVI

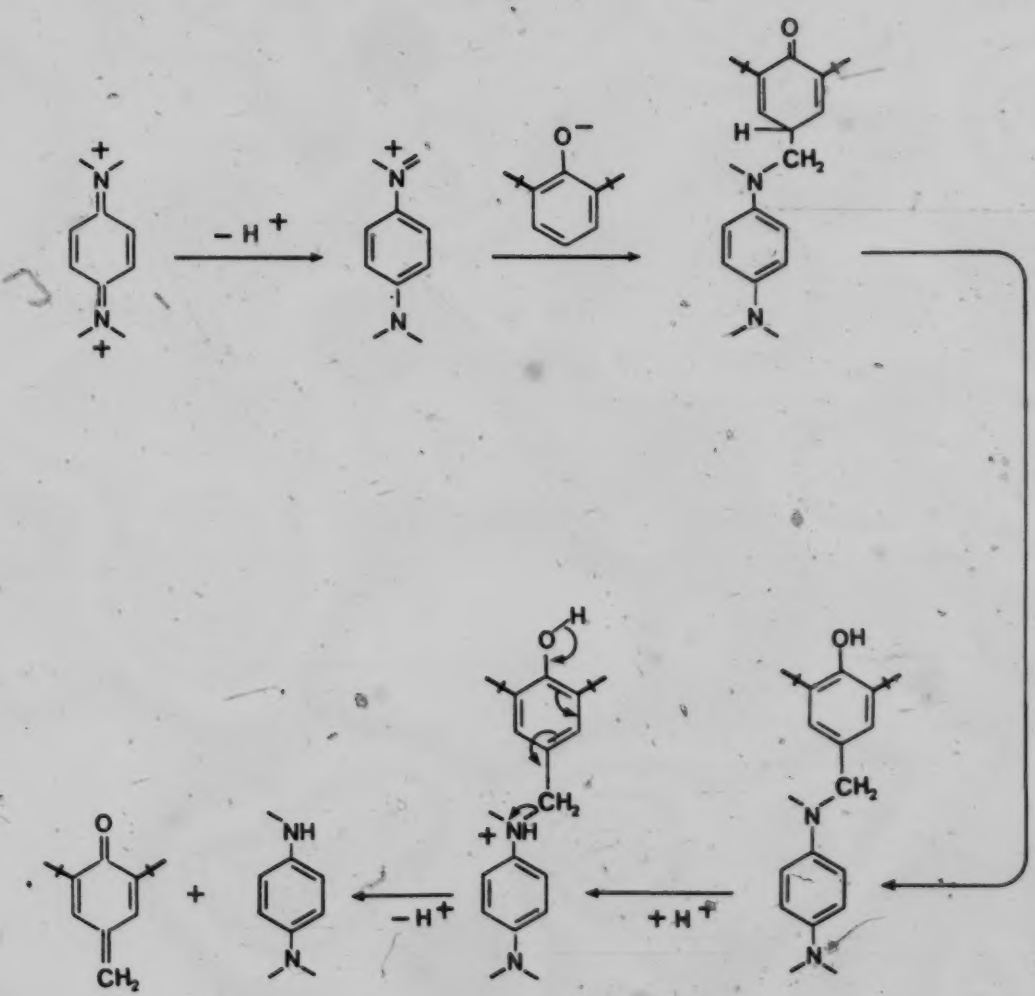

Scheme XVII

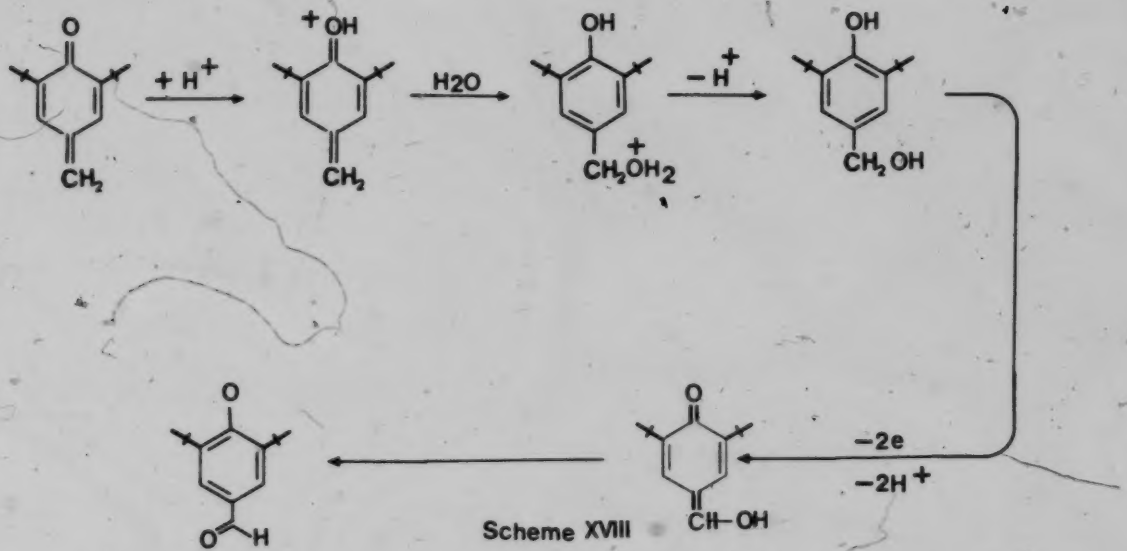

Scheme XVIII

IV

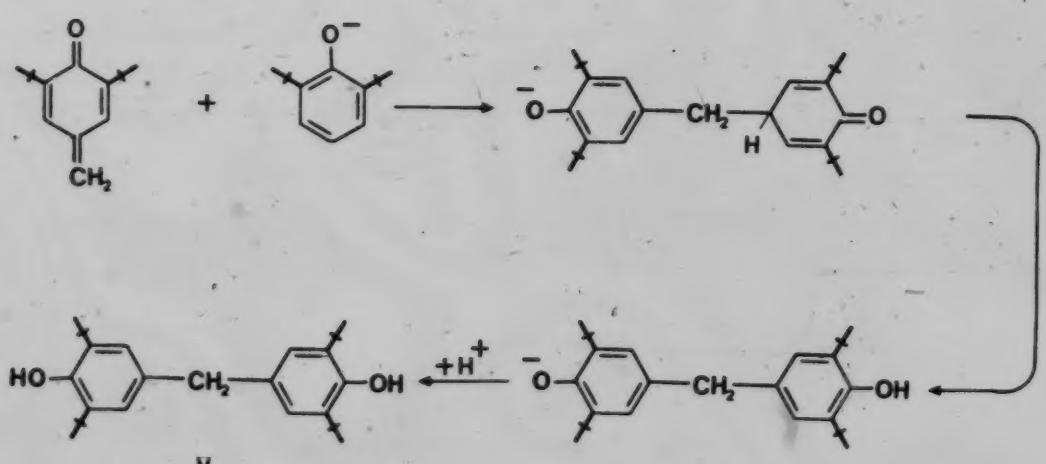

V

Scheme XIX

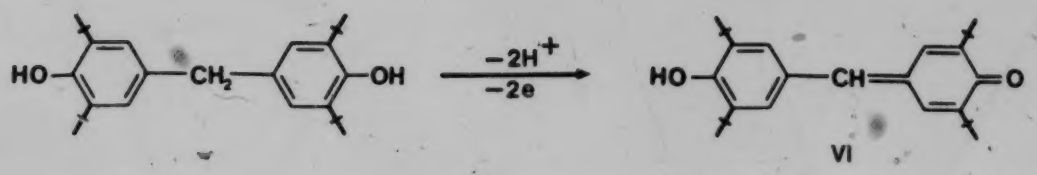

VI

Scheme XX

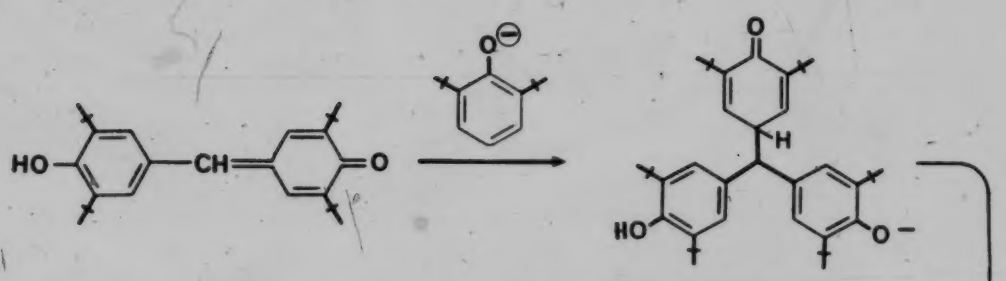

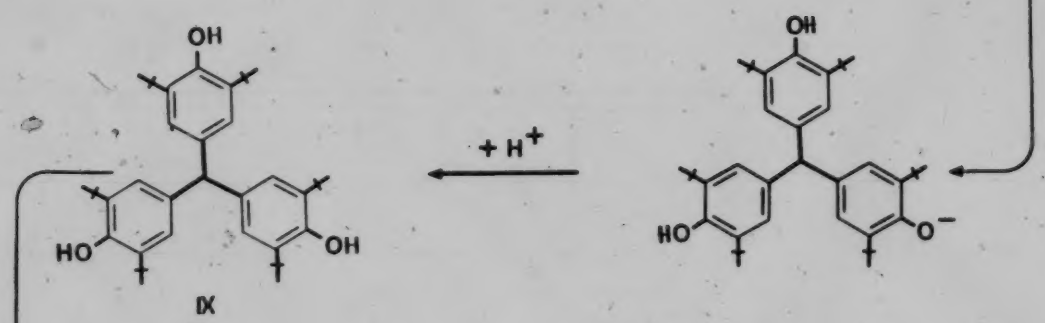

IX

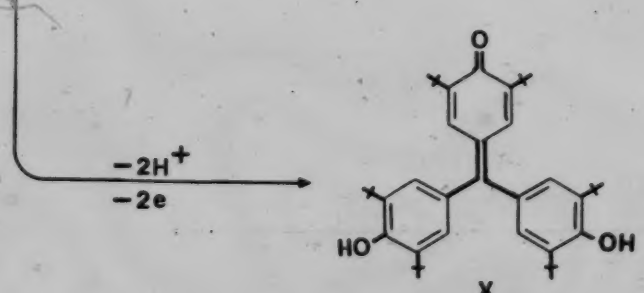

X

Scheme XXI

Compound XII (Table XI) is likely to be formed through the mechanism depicted in Scheme XVII. Attack of the phenolate anion on the $TMPD^{2+}$ fragment is highly possible since in polar solvents such as acetonitrile ionization of the 2,6-di-*tert*-butylphenol to give the phenolate anion is favorable. The formation of compound IV, in the presence of adventitious water is depicted in Scheme XVIII. The formation of compounds V, VI,IX, and X are interrelated to each other and may have originated from the active intermediate XII. The mechanism for the formation of compound V is shown in Scheme XIX. The pathway through which compound VI can be formed is depicted in Scheme XX.[155] Compound IX is formed from further condensation of compound VI with the phenolate anion, the mechanism of which is given in Scheme XXI and was previously reported by Yang[154] who synthesized IX in this manner. Compound X is the product of the oxidation of compound IX and the mechanism of its formation is depicted in Scheme XXI.

III.4 CONCLUSIONS

The nature of the paramagnetic species generated from the 50:50 mixture of TMPE/$TMPE^{2+}$ was identified as the $TMPE^{+\bullet}$ radical cation. The plot of relative epr intensity versus the variation in absolute percentage of TMPE (i.e., % [TMPE]/[TMPE] + [$TMPE^{2+}$]) was employed to obtain the semiquinone radical cation formation constant (K_{SEM}). The method was proven to be an excellent alternative substitute for the well-known electrochemical method which, because of the nature of the electron transfer process, rendered ambiguous K_{SEM} values for the TMPE/$TMPE^{2+}$ system in different solvents. The K_{SEM} values of 8.64 and 0.036 obtained for the TMPE/$TMPE^{2+}(Cl^-)_2$ system in methylene chloride and acetonitrile demonstrated that solvents of higher polarity, e.g., acetonitrile, favoured the equilibrium over the disproportionation direction, while solvents with lower polarity, e.g., methylene chloride, favored the comproportionation. Application of the same epr method to the TMPD/$TMPD^{2+}$ system resulted in K_{SEM} which was significantly in disagreement with reported results obtained electrochemically. The discrepancy was found to originate from the failure of the electrochemical method to detect further possible chemical processes occurring after the radical formation stage. The $TMPD^{+\bullet}$ paramagnetic species was found to disappear irreversibly with time and mass spectrometric evidence indicated that the dimeric product of TMPD was formed. The epr method was thus only applicable in the measurement of K_{SEM} for RED/OX systems where radical dimerization or other interfering chemical proceses did not occur.

Results obtained from the reaction between 2,6-di-*tert*-butylphenol and $TMPD^{2+}(ClO_4^-)_2$ pointed out that the salt can be employed as a strong oxidant and as an effective methylating agent in the phenol oxidation reactions.

EXPERIMENTAL

IV.1 MATERIALS

Glacial Acetic Acid (Fischer Scientific Co.) was purified according to the method of Orton and Bradfield[156] but instead of CrO_3, 2-5% (w/w) of $KMnO_4$ was used. The mixture was heated to reflux for 2-5 h before it was distilled.

Acetonitrile (Caledon Lab.Ltd.) HPLC grade solvent was heated to reflux over calcium hydride (Terochem Ltd.) and distilled prior to use.

Dichloromethane (Caledon Lab.Ltd.) solvent was heated to reflux over phosphorus pentoxide and fractionally distilled prior to use. Column glpc analysis showed it to be > 99.8% pure.

Acetonitrile-1-^{13}C (99.7%) and Acetonitrile-2-^{13}C (92.3%) (D. Merck Sharp and Dohme Canada Ltd.) were used without further purification.

2,6-Di-*tert*-butylphenol (99% Aldrich Chemical Company, Inc.) was recrystallized from Skelly B and dried *in vacuo* over paraffin wax and P_2O_5 at room temperature: mp. 37-38°C (lit.[167] mp 38°C).

Propionitrile (99% Aldrich Chemical Company, Inc.) was checked for purity by glpc and no further purification was carried out.

Benzene (Thiophene free - McArthur Chemical Co. Ltd.) (column glpc analysis showed it to be > 99.8% pure) was used without further purification.

N,N,N',N'-Tetramethyl-1,4-phenylenediamine (Aldrich Chemical Co.) was dissolved in petroleum ether and passed through a short column of basic activated alumina (Al_2O_3, Aluminum Oxide 90 Active, E. Merck). Evaporation of the solvent, followed by one additional vacuum sublimation at 49°-50° afforded colorless crystals. Drying over P_2O_5 *in vacuo* at room temperature gave loose colorless flakes: mp 51-52°C[157] (lit.[158] mp 51-52°C).

Anal. Cald for $C_{10}H_{16}N_2$: C, 73.13; H, 9.82; N, 17.06. Found: C, 73.31; H, 9.80; N, 16.87.

N,N,N',N'-Tetramethyl-1,4-benzoquinone diiminium perchlorate was prepared from N,N,N',N'-tetramethyl-1,4-phenylenediamine by oxidation using perchloric acid 70%, glacial acetic acid and sodium dichromate[159,160]. The product was isolated by filtration and the resulting white solid was washed several times with dried acetic acid until the greenish color disappears, washed with dichloromethane and dried over P_2O_5 *in vacuo* at 56°C.

Anal. Cald for $C_{10}H_{16}N_2O_8Cl_2$: C, 33.08; H, 4.44; N, 7.72; Cl, 19.53. Found: C, 33.09; H, 4.44; N, 7.64; Cl, 19.35.

Benzeneiodo Dichloride was prepared from iodobenzene and chlorine in chloroform according to the method suggested by Lucas and Kennedy.[161]

Tetrakis(*p*-N,N-dimethylaminophenyl)ethylene (TMPE) was repared from Michler's ketone, 4,4'-bis(dimethylamino)benzophenone, (Eastman Kodak) and mossy tin in concentrated HCl.[85,86] The resultant salt of the olefin is dissolved in water and made alkaline with 10% NaOH. The crystalline olefin was collected and washed with water until it is free of NaOH. After two recrystallizations from benzene the product was dried *in vacuo* and gave light yellow-green powdery material: mp. 294-296°C. (lit.[87] mp 295-300°C); $\lambda_{max}^{CH,CN}$ 290, 360 nm, log ϵ 4.64, 4.36 repectively;mass spectrum *m/e* (rel. intensity) 504 (100), 488 (1.96), 252 (10.8); 80 MHz ^1H nmr data (benzene-d6) δ 2.45 (s, 24H), 6.90 (m,

16H).

Anal. Cald. for $C_{34}H_{40}N_4$: C, 80.91; H, 7.99; N, 11.10. Found: C, 81.16; H, 7.90; N, 10.91.

Tetrakis(*p*-N,N-dimethylaminophenyl)ethylene dichloride was prepared from tetrakis(*p*-N,N-dimethylaminophenyl)ethylene and benzeneiodo dichloride.[2] To a stirred solution of 2 g of TMPE in 50 mL of chloroform was added dropwise 1.2 g of freshly prepared benzeneiodo dichloride in 50 mL of chloroform and the mixture was left to stand for 3 hours. Carbon tetrachloride (300 mL) was added and the mixture was left to stand overnight. The precipitate was then collected by filtration. The crude dication salt (91.5 g) was dissolved in 10 mL of chloroform, filtered and reprecipitated with carbon tetrachloride (200 mL), left to stand overnight and filtered. The salt was then dried *in vacuo* over P_2O_5 at 75°C: UV spectrum $\lambda_{max}^{CH_3CN}$ 325, 485 nm, log ϵ 4.34, 4.22 respectively.

Anal. Cald. for $C_{34}H_{40}N_4Cl_2$: C, 70.95; H, 7.00; N, 9.73. $C_{34}H_{40}N_4Cl_2 \cdot H_2O$: C, 68.79; H, 7.13; N, 9.44. Found: C, 71.46; H, 7.10; N, 9.44.

Tetrakis(*p*-N,N-dimethylaminophenyl)ethylene ditetrafluoroborate was prepared from tetrakis(*p*-N,N-dimethyl aminophenyl)ethylene dichloride and silver tetrafluoroborate. To a stirring solution of 1 g of the dichloride salt in 50 mL of distilled water was added dropwise 372 mg of silver tetrafluoroborate in 50 mL water for a period of 10 h. The precipitate was filtered with a 10-20 μ sintered funnel and dried *in vacuo* over P_2O_5 at 75°C: UV spectrum $\lambda_{max}^{CH_3CN}$ 325, 480, 535 nm, log ϵ 4.30, 4.60, 4.51 respectively.

Anal. Cald. for $C_{34}H_{40}N_4F_8B_2$: C, 60.20; H, 5.94; N, 8.26. $C_{34}H_{40}N_4F_8B_2$ [illegible]: C, 58.65; H, 6.08; N, 8.05. $C_{34}H_{40}N_4F_8B_2 \cdot 2H_2O$: C, 57.17; H, 6.21; N, 7.84. Found: C, 58.03; H, 5.72; N, 8.05.

Tetrakis(*p*-N,N-dimethylaminophenyl)ethylene dinitrate was prepared from TMPE and silver nitrate. To 2.7 g of silver nitrate dissolved in 150 mL distilled water was added with

stirring 4 g of TMPE. Stirring was left overnight and the precipitate was collected and dried *in vacuo* over P_2O_5 at 75°C: UV spectrum $\lambda_{max}^{CH_3CN}$ 325, 480, 535 nm, log ϵ 4.31, 4.44, 4.35 respectively.

Anal. Cald for $C_{34}H_{40}N_6O_6$: C, 64.96; H, 6.44; N, 13.37. $C_{34}H_{40}N_6O_6 \cdot H_2O$: C, 63.15; H, 6.54; N, 12.99. Found: C, 63.84; H, 6.39; N, 12.36.

Tetrakis(*p*-N,N-dimethylaminophenyl)ethylene diiodide was prepared from the TMPE dinitrate and potassium iodide. To 2.275 g (3.6 mmole) of the dinitrate salt in 100 mL of water was added 1.3 g (10% excess) potassium iodide. Stirring was left overnight and the precipitate was filtered by suction. The crude crystalline mass was redissolved in water and purified by liquid-liquid extraction using diethyl ether as the other liquid phase. The extraction was carried out for six days and the water layer was reduced. The water volume was reduced by rotary evaporation (~ 40°C). The resulting crystals were dried *in vacuo* over P_2O_5 at 75°C: UV spectrum $\lambda_{max}^{CH_3CN}$ 325, 480, 535 nm; log ϵ 4.40, 4.56, 4.44 respectively.

Anal. cald. for $C_{34}H_{40}N_4I_2$: C, 53.84; H, 5.32; N, 7.39. $C_{34}H_{40}N_4I_2 \cdot H_2O$: C, 52.59; H, 5.45; N, 7.21. Found: C, 54.29; H, 5.42; N, 7.83.

N,N,N',N'-Tetraethyl-1,4-phenylenediamine was prepared from *p*-phenylenediamine and diethyl sulfate[162] in a water solution of sodium bicarbonate which was maintained at 18-22°C. The final crystalline slurry was steam distilled at higher temperature to give oily product which solidifies at about 20°. The crude crystal was dried *in vacuo* over P_2O_5 and chromatographed (Al_2O_3/diethyl ether) to give pure white crystal: mp 45-47°C; 80 MHz ^1H nmr data ($CDCl_3$) δ 1.10 (t, 12 H), 3.25 (m, 8H), 6.80 (s, 4H); exact mass measurement: cald. 220.1939. Found 220.1940, mass spectrum *m/e* (rel. intensity) 220(68.6), 205 (100), 191 (25.2), 176 (21.4), 161 (32.9).

Anal. cald for $C_{14}H_{24}N_2$: C, 76.3; H, 11.0; N, 12.7. Found: C, 76.24; H, 10.9; N, 12.67.

N,N,N',N'-Tetraethyl-1,4-benzoquinone diiminium perchlorate was prepared from N,N,N'-N'-tetraethyl-*p*-phenylenediamine and perchloric acid 70% [159] at room temperature in glacial acetic acid and sodium dichromate. The solvent was removed by vacuum filtration and the resulting white solid was washed several times with dried acetic acid until the greenish color disappeared, washed with methylene chloride and dried over P_2O_5 *in vacuo* at 56°C.

Anal. cald for $C_{14}H_{24}N_2Cl_2O_8$: C, 40.11; H, 5.77; N, 6.68. Found: C, 39.81; H, 6.23; N, 6.60.

3,5,3',5'-Tetra-*tert*-butyl-4,4'-diphenoquinone (VII) was prepared from 2,6-di-*tert*-butyl phenol and potassium ferricyanide in benzene and alkalinized water at room temperature under dried nitrogen.[163] The solution was poured on to crushed ice and the benzene layer was removed and washed with water, dried over Na_2SO_4. The solvent was removed by rotary evaporation and the resulting red crystals were recrystallized from absolute ethanol and dried under vacuum over P_2O_5. mp 242-244°C (lit. mp 246°[164]); mass spectrum *m/e* (rel. intensity) 408 (93.5), 393 (29.7), 366 (26.6), 351 (37.6), 57 (100). Exact mass measurement: cald 408.3028, found 408.3031; 80 MHz ^{1}H nmr data ($CDCl_3$) δ 1.35 (s, 36H), 7.7 (s, 4H); ir ($CHCl_3$) 2970, 1604, 1470, 1370 cm^{-1}.

Anal. cald for $C_{28}H_{40}O_2$: C, 82.31; H, 9.87. Found: C, 82.15; H, 9.92.

4,4'-Dihydroxy-3,5,3',5'-Tetra-*tert*-butyl diphenyl (VIII) was prepared from the corresponding diphenoquinone and sodium hydrosulfite in ethanol.[164] The resulting pale yellow crystals were recrystallized twice from ethanol to give pale yellow needles: mp 183-185°C (lit. mp 185°[164]); 80 MHz ^{1}H nmr data (DMSO-d6) δ 1.45 (s, 36H), 6.9 (s, 2H), 7.2 (s, 4H); exact mass measurement: cald 410.3185, found 410.3187, *m/e* (rel. intensity) 410 (100), 395 (15.3), 190(10.8), 57 (42.1); ir ($CHCl_3$) 3631, 2988, 1429, 1228 cm^{-1}.

Anal. cald for $C_{28}H_{42}O_2$: C, 81.90; H, 10.31; Found: C, 82.09; H, 10.84.

4,4',Dihydroxy-3,5,3'-5'-Tetra-*tert*-butyldiphenyl methane (V) was prepared from

2,6-Di-*tert*-butyl phenol, 36% formaldehyde and sodium hydroxide in absolute ethanol under dried nitrogen.[165] The white crystals were recrystallized twice from ethanol: mp 153-154°C (lit.[165] mp 154°C); 200 MHz ^{1}H nmr data ($CDCl_3$) δ 1.4 (s, 36H), 3.85 (s, 2H), 5.05 (s, 2H), 7.1 (s, 4H); exact mass measurement: cald 424.3341, found 424.3343, mass spectrum *m/e* (rel intensity) 424 (100), 409 (69.5), 393 (2.0), 367 (16.2), 219 (18.4), 57 (30); ir ($CHCl_3$) 3642, 2958, 1494, 1292 cm^{-1}.

Anal. cald for $C_{29}H_{44}O_2$: C, 82.08; H, 10.44; O, 7.53. Found: C, 81.95; H, 10.40; O, 7.65.

4,4'-Dihydroxy-3,5,3',5'-tetra-*tert*-butyldiphenylbromomethane was prepared from the corresponding diphenylmethane and bromine in glacial acetic acid at room temperature.[165] The resulting precipitate was washed with acetic acid and dried under vacuum in a desiccator: mp 158-159°C (lit.[165] mp 159-160°).

Anal. cald for $C_{29}H_{43}O_2Br$: C, 69.17; H, 8.61; Found: C, 69.25; H, 8.36.

2,6,3',5'-Tetra-*tert*-butyl-4'-hydroxyphenyl-4-methylene-2,5-cyclohexadiene-1-one (VI) was prepared from the parent diaryl bromomethane and 5% sodium hydroxide in ethanol under dried nitrogen.[165] The reaction mixture was poured onto crushed ice, neutralized with acetic acid and extracted with ether. The solvent was removed under vacuum by rotary evaporation. Two recrystallizations from aqueous ethanol give yellow crystals: mp 156-157°C (lit.[157] 158-159°); mass spectrum *m/e* 422 (100), 407 (92.6), 391 (7.4), 379 (16.1), 365 (96.7), 57 (62.2); exact mass measurement: cald 422.3184, found 422.3183; ir (CH_2Cl_2) 3630, 2957, 1611, 1360 cm^{-1}.

Anal. cald for $C_{29}H_{42}O_2$: C, 82.42; H, 10.02. Found: C, 82.32; H, H, 9.97

Bis(3,5-di-tert-butyl-4-hydroxyphenyl)(3,5-di-*tert*-butyl-4-oxo-cyclohexa-2,5-dienylidene) methane (X) was prepared from 2,6-di-*tert*-butylphenol and N,N,N',N'-tetramethyl-p-benzoquinone diiminium perchlorate in acetonitrile at 90°C. To a stirring solution of 1.63 g of the perchlorate salt in 10 mL acetonitrile (under dry nitrogen) was added dropwise

0.63 g of the phenol in 10 mL acetonitrile. The reaction mixture was stirred at 90°C for 19 h after which the product was isolated by adding a large amount of water saturated with NaCl. The resulting precipitate was extracted several times with methylene chloride. The solvent methylene chloride was reduced in volume by rotary evaporation, under reduced pressure, and the residue was subjected to chromatography using eluent toluene on silica gel (Merck, grade 60, 230-400 mesh, 60 Å, Aldrich Chemical Company, Inc.). Evaporation of toluene followed by one recrystallization from n-decane and drying under vacuum over P_2O_5 and parafin wax gave bright orange-red grainy crystal: mp 282-283°C (lit.[154] mp 278-279°C); λ_{max}^{MeOH} 450 nm, log ϵ 4.402 (lit.[154] λ_{max} 449 nm, log ϵ 4.41); mass spectrum (chemical ionization - NH_3) *m/e* (rel. intensity) 627 (100), 597 (12.5), 566 (4.5); mass spectrum *m/e* (rel intensity) 626 (100), 611 (53.5), 595 (5.0), 584 (16.1), 569 (67.4), 57 (40.8); 400 MHz ^1H nmr data ($CDCl_3$) δ 1.25 (s, 18H), 1.35 (s, 36H), 5.5 (s, 2H), 7.05 (s, 4H), 7.2 (s, 2H); 100.62 MHz ^{13}C nmr data ($CDCl_3$) δ 30.0 (q, 18C), 31.0 (q, 36C), 34.0 (s, 2C), 35.0 (s, 4C), 127.5 (s, 1C), 131 (d, 4C), 132 (s, 2C), 135 (d, 2C), 135 (s, 4C), 146 (s, 2C), 156 (s, 2C), 160 (s, 1C), 186 (s, 1C); exact mass measurement: cald 626.4699, found 626.4692; ir (vapour) 3660, 2970, 1620, 1440 cm^{-1}.

Anal. cald for $C_{43}H_{62}O_3$: C, 82.38; H, 9.97; O, 7.65. Found: C, 82.45; H, 10.01; O, 7.54.

IV.2 INSTRUMENTATION

All melting point values were measured with a Mel-Temp melting point apparatus and were uncorrected.

Nmr spectra, 400 MHz ^1H and 200 MHz ^1H, were obtained using a Bruker WH-400 nmr and a Bruker WH-200 nmr respectively. The 80 MHz ^1H nmr spectra were obtained using a Bruker WP-80 nmr spectrometer. The 100.62 MHz ^{13}C nmr spectra were obtained using a Bruker WH-400 nmr spectrometer.

Exact mass measurements were carried out using a Kratos MS-50 mass spectrometer coupled to a Data General Nova 3 DS-55. Medium resolution mass spectra were carried out using an AEU NS-12 mass spectrometer coupled to a Data General Nova 3 DS-55. Low resolution gas chromatography - mass spectral (glpc-ms) data were obtained using a Varian Aerograph 1400 gas chromatograph coupled to an AEI MS-12 mass spectrometer with a Data General Nova 3 DS-55. High resolution glpc-ms data were obtained using a Vista 600 (30 m capillary DB-1) gas chromatograph coupled to a VG-70E magnetic mass spectrometer.

Gas chromatography-infrared spectral (glpc-ir) data were obtained using a Nicolet 7199 FT-IR spectrometer interfaced to a Varian 370 gas chromatograph. The column for glpc-ms (low resolution) and glpc-ir analyses was the same as for glpc analyses (1/8" x 20' glass column containing 2.5% Silicone GE XE-60 on Chromosorb W/AW/DMCS 100-120 mesh ASTM).

Glpc analyses with packed columns were carried out using a Hewlett Packard HP-5840A gas chromatograph equipped with a flame ionization detector. The detector was calibrated using a mixture of synthetic materials and an internal standard.

Infrared spectra were recorded on a Nicolet 7199 FT-IR spectrophotometer. Ultraviolet spectra were obtained with a Hewlett Packard HP8450 A diode array spectrophotometer using a 1-mm quartz cell.

ESR spectral data were obtained with a Bruker ER-420 console instrument equipped with a Varian V3600 12-in. magnet and a field dial controller. The ESR cavity is a Bruker B-ER400X-UR TE_{102} Resonator. Oxidative electrolysis was carried out using an electrolytic cell (shown in Figure 13) coupled to a Hewlett Packard Harrison 6525A DC Power Supply and a Hewlett Packard DC Multi-Function Unit connected to a Hewlett Packard 3440 A Digital Voltmeter.

IV.3 ANALYTICAL PROCEDURES

Generation of the radical cation of tetrakis (*p*-dimethyl aminophenyl) ethylene at different percentage concentration of the tetraamine in methylene chloride and in acetonitrile. Two

50-mL stock solutions of the tetraamine and the corresponding dication salt were prepared ($1.99 \times 10^{-3} - 2 \times 10^{-3}$ *M*). Known volumes of each of the stock solutions were pipetted into each limb of an H-shaped pyrex ampoule which had connected to it a 5 mm-OD quartz epr sidearm. The total volume of the two aliquots was always kept constant at 4 mL while the volume of each of the two aliquots varies. A series of ampoules with the percentage concentration of the tetraamine varying from 0% to 100% were prepared. The ampoules were degassed three times by the freeze-thaw technique, sealed, equilibrated to 25°C and mixed before the quartz sidearm was inserted into the epr cavity for intensity measurement. The relative intensity was plotted against percentage concentration of TMPE and the equilibrium constant was calculated as outlined in Appendix Ib. The percentage of the radical at equilibrium was calculated according to Appendix Ic.

Generation of the radical cation of tetrakis(*p*-dimethylaminophenyl) ethylene at different percentage concentration of the tetraamine in methylene chloride by electrolysis. An aliquot methylene chloride solution (10 mL) of the tetraamine (1.01×10^{-3} *M*) solution was placed in one side of the electrolysis cell while another side was placed an aliquot (10 mL) of an electrolyte solution of tetraethylammonium chloride (0.11 *M*), see Figure 13. Both sides were degassed with helium for a period of 5 minutes, after which a constant current of 136.4 μA was passed through the cell (2 hours) which is equivalent to an average removal of one electron per molecule (or one equivalence of electron) and then continued for another 2 hours which is equivalent to an average removal of two electrons per molecule.

During the 4 hours electrolysis period the cell was occasionally taken out of the epr cavity, tilted so that the solution in the epr quartz sidearm was allowed to mix with the solution in the mother cell, electrolyzed, tilted again to get part of the mother solution back into the quartz sidearm, and the epr spectrum recorded. A plot of the relative intensity of the epr signal against time was established and the equilibrium constant was calculated as outlined in Appendix Ib. The percentage of the radical at

equilibrium was calculated according to Appendix Ic.

Calibration of TMPE radical cation concentration in methylene chloride and acetonitrile at equilibrium using DPPH. A 50/50 mixture solution of TMPE and $TMPE^{2+}(Cl^-)_2$ was prepared from the two corresponding stock solutions (2.01×10^{-3} *M* and 1.99×10^{-3} *M* respectively), placed in a 1 x 20 cm epr flat cell and the overmodulated epr signal was recorded. The same epr cell was then rinsed several times with acetonitrile and an acetontirile solution of 2,2-diphenyl-1-picrylhydrazylhydrate (DPPH) free radical (95%) (1.19×10^{-3} *M*) was transferred into the cell. The overmodulated signal recorded at exactly the same instrumental settings. The TMPE radical cation concentration at equilibrium was calculated as outlined in Appendix Ia.

Verification of concentration of TMPE radical cation of the TMPE/$TMPE^{2+}$ system at equilibrium in acetonitrile. Two 50-mL stock solutions of the tetraamine and the corresponding dichloride salt were prepared (5.01×10^{-4} *M*, 4.97×10^{-4} *M* respectively). Equal volumes (4×10^{-3}L) of the stock solutions were mixed well together before being transferred into a 1-mm quartz cell and the UV spectrum (see spectrum **a**, Figure 16) recorded. From the K_{eq} found by the epr method the equilbirium concentration of the reactants and product were calculated. The two solutions one of the olefin and another of the dication whose concentrations (2.59×10^{-4} *M* and 2.68×10^{-4} *M* respectively) corresponded to the equilibrium concentration were prepared. The UV spectra were recorded (see spectrum **b** and **c**, Figure 16).

Spectra **b** and **c** were subtracted (computer subtraction) from spectrum **a** to obtain the spectrum of radical cation species at equilibrium (see Figures 16 and 17).

Generation of the radical cation of tetramethyl-*p*-phenylene diamine at different percentage concentration of the diamine in acetonitrile. Two 100-mL stock solutions of the diamine and the corresponding diiminium perchlorate salt were prepared (0.99×10^{-3} and 1.008×10^{-3} *M* respectively). Known volumes of each of the stock solutions were pipette into

each limb of the H-shaped pyrex ampoule which is connected to a 3mm-OD quartz epr sidearm. The total volume of the two aliquots is always kept constant at 10 mL, while the volume of each of the two aliquots varies. A series of ampoules with the varying percentage concentration of the diamine were prepared. The ampoules were degassed three times by the freeze-thaw technique, sealed, equilibrated to 25°C and mixed. The quartz sidearm was inserted into the epr cavity for the intensity measurement. The plot of relative intensity versus percentage concentration was constructed and the equilibrium constant was calculated as outlined in Appendix Ib. The percentage of the radical cation at equilibrium was calculated according to Appendix Ic.

Calibration of TMPD radical cation concentration at equilibrium in acetonitrile by using DPPH. The 50/50 mixture of TMPD and $TMPD^{2+}(ClO_4^-)_2$ solutions was prepared from the two corresponding stock solutions (1.98×10^{-3} *M* and 1.99×10^{-3} *M* respectively), pipetted in equal volumes into a 1 x 20 cm epr flat cell and the overmodulated signal recorded in a B-ER 400X-UR TE_{102} Bruker Resonator. The same epr cell was then rinsed several times with acetonitrile, the 2,2-diphenyl-1-picryl hydrazyl hydrate free radical (95%) in acetonitrile (1.19×10^{-3} *M*) was transferred into the cell and the overmodulated signal recorded under exactly the same instrumental conditions. The radical cation concentration at equilibrium was calculated according to Appendix Ia.

The reaction of 2,6-di-*tert*-butylphenol with N,N,N',N'-tetramethyl-*p*-benzoquionone diiminium perchlorate salt in acetonitrile. An aliquot (3×10^{-3} L) of a solution of 2,6-di-*tert*-butylphenol (0.133 *M*) was pipetted into one limb of an H-shaped pyrex ampoule, weighed amount of the perchlorate salt (0.813 mmol) was placed in the other arm of the reaction vessel. The ampoule was degassed three times, by the freeze-thaw method, sealed, equilibrated to 90° for 10 minutes and the materials were mixed. After the ampoule was thermostated for the required time length the tube was opened, a known amount of triphenylmethane standard added, a cooled aqueous solution of water saturated with sodium chloride was added and the reaction mixture was extracted two

times with dichloromethane. The organic layer was dried over magnesium sulfate and analyzed by glpc. Glpc analysis was carried out using a 1/8" x 20' glass column of 2.5% silicone GE XE-60 on Chromosorb W/AW/DMCS (100-120 mesh) (120-270°C).

The products were identified by a comparison of their retention times, ir, mass spectra, with those of authentic materials; by a comparison of their glpc-ir, glpc-ms spectra with those of authentic materials; the products formed are listed in Tables X, XI, XII and XIII:

Compound (I): ir (vapour) 3650, 2960, 1430, 750 cm^{-1}; mass spectrum *m/e* (rel. intensity) 206 (M^+, 17.6), 191 (100.0), 131 (26.3), 57, 89.5); exact mass measurement 206.1663.

Compound (II): ir (vapour) not available; mass spectrum *m/e* (rel. intensity) 220 (M^+, 22.6), 205 (100.0), 145 (12.1), 135 (35.1); exact mass measurement 220.1848.

Compound (III): ir (vapour) 2960, 1670, 1300 cm^{-1}; mass spectrum *m/e* (rel. intensity), 220 ($M^{+\cdot}$, 72.7), 205 (43.2), 192 (13.9), 177 (100.0); exact mass measurement 220.1459.

Compound (IV): ir (vapour) 3650, 2970, 1700, 1200 cm^{-1}; mass spectrum *m/e* (rel. intensity) 234 ($M^{+\cdot}$, 23.7), 219 (100.0), 191 (17.1), 57 (17.4); exact mass measurement 234.1642.

Compound (V): ir (vapour) 3650, 2960, 1430, 1230 cm^{-1}; mass spectrum *m/e* (rel. intensity), 424 ($M^{+\cdot}$, 100.0), 409 (69.5), 367 (16.2), 219 (18.4); exact mass measurement 424.3293.

Compound (VI): ir (vapour) 3650, 2970, 1635, 1250 cm^{-1}; mass spectrum *m/e* (relative intensity) 422 ($M^{+\cdot}$, 49.0), 407 (100.0), 379 (16.5), 365 (81.3); exact mass measurement 422.3181.

Compound (VII) and compound (VIII): The separation of these two compounds is poor on pack column; ir (vapour) 3650, 2960, 1630, 1430 cm^{-1}; mass spectrum *m/e* (relative intensity) for compound (VII) 408 ($M^{+\cdot}$, 58.0), 393 (22.0), 366 (14.0), 352 (24.0), for compound (VIII) 410 ($M^{+\cdot}$, 100.0), 395 (15.3), 190(10.8), 57 (42.1); exact mass measurement for (VII) 408.3031; exact mass measurement for (VIII) 410.3158.

Compound (IX): ir (vapour) 3660, 2960,1430, 1230 cm^{-1}; mass spectrum *m/e* (relative intensity) 628 ($M^{+\cdot}$, 64.0), 613 (12.1), 571 (100.0), 423 (19.7); exact mass measurement 628.4855.

Compound (X): ir (vapour) 3660, 2960, 1620, 1430 cm^{-1}; mass spectrum *m/e* (relative intensity) 626 ($M^{+\cdot}$, 100.0), 611 (53.5), 584 (16.3), 569 (67.4); exact mass measurement 626.4692.

Compound (XI) - (XVI): ir data are not available due to poor separation and low yields.

Compound (XI): mass spectrum: *m/e* relative intensity 150 ($M^{+\cdot}$, 27.1), 135 (99.1), 107 (100.0), 91 (38.9); exact mass measurement 150.1031.

Compound (XII): mass spectrum *m/e* (relative intensity) 218 ($M^{+\cdot}$, 31.2), 203 (43.1), 163 (36.5), 147 (100.0); exact mass measurement 218.1694.

Compound (XIII): mass spectrum *m/e* (relative intensity) 262 ($M^{+\cdot}$, 0.8), 247 (66.2), 80 (12.0), 57 (100.0); exact mass measurement 262.2341.

Compound (XIV): mass spectrum *m/e* (relative intensity) 354 ($M^{+\cdot}$, 100.0),339 (43.1), 134 (6.3),57 (8.3); exact mass measurement 354.2520.

Compound (XV): mass spectrum *m/e* (relative intensity) 68 ($M^{+\cdot}$, 84.2), 353 (100.0),

311 (22.2), 163 (32.0); exact mass measurement 368.2664.

Compound (XVI): mass spectrum *m/e* (relative intensity) 572 ($M^{+\cdot}$, 72.8), 557 (21.9), 515 (100.0), 57 (38.8); exact mass measurement 572.4181.

The yields were determined using standard calibration mixture. The yield was calculated by using the following equation:

$$\text{Concentration X} = \frac{\text{Area X}}{\text{Area Std}} \times \text{CF} \times \text{Concentration STD}$$

Where CF is the calibration factor determined from the analysis of a standard calibration mixture prepared from known amounts of authentic materials.

$$\text{CF} = \frac{\text{Concentration of X / Concentration of Std}}{\text{Area integration X / Area integration Std}}$$

Test for incorporation of ^{13}C in compound Bis(3,5-di-*tert*-butyl-4-hydroxyphenyl) (3,5-di-*tert*-butyl-4-oxocyclohex-2,5-dienylidene) methane. Since the galvinol analogue is formed in good yield and easily separated by flash chromatography it is chosen as a target molecule for the test of ^{13}C incorporation. The two labelled acetonitrile-2-^{13}C (92.3%) and acetonitrile-1-^{3}C (99.7%) were diluted with dried acetonitrile to 5.8% and 6.3% respectively. An aliquot (4×10^{-3} L) of the solution of 2,6-di-*tert*-butylphenol (0.30 *M*) was pipetted into one limb of an H-shaped pyrex ampoule which has already contained weighed amount (2.41 mmol) of the perchlorate salt in the other limb. The ampoule was cooled in dry ice, degassed three times by the freeze-thaw method, sealed, and thermostated at 90°C for 10 minutes. The materials were mixed and allowed to stand at 90°C for 40 to 49 hours. The tube was opened, a chilled aqueous solution of the saturated sodium chloride solution was added and the mixture was extracted three times with methylene chloride, and the solution was dried over anhydrous magnesium sulfate. The solvent was removed under vacuum by rotary evaporation and the residue was subjected to flash chromatography with silicagel (Merck, grade 60, 230-400 mesh). Benzene was

used as the eluent. One fraction yielded the galvinol analogue when the benzene was removed by rotary evaporation. The compound was recrystallized twice from *n*-decane, dried (55°) over P_2O_5 and paraffin wax. ^{13}C Nmr analyses of the recovered material showed that no isotopic carbon had been incorporated in either cases..

Reaction of 2,6-di-*tert*-butylphenol with N,N,N',N'-tetramethyl-*p*-benzoquinone diiminium perchlorate salt in propionitrile and benzene. The general procedure was exactly the same as that carried out in acetonitrile except that propionitrile or benzene was used. The products obtained in propionitrile solvent were exactly identical to that obtained in acetonitrile solvent (see Tables X, XII and XIV). The products obtained in benzene solvent were compounds III and VIII (see entry 4, Table XIV).

REFERENCES

1. Deuchert, K.; Hünig, S. *Angew. Chem. Int. Ed. Engl.* **1978,**, *17*, 875-886 and references cited therein.
2. LePage, G.A.; Elofson, R.M.; Schulz, K.F.; Laidler, J.; Kowalewski, K.P.; Hay, A.S.; Crawford, R.J.; Tanner, D.D.; Sandin, R.B. *J. Med. Chem.* **1983**, *26*, 1645.
3. Grampp, T.; Jaenicke, W. *Ber. Bunseriges. Phys. Chem.* **1984**, *88*, 325-334 and references cited therein.
4. Hünig, S.; Geuder, W.; Suchy, A. *Angew. Chem. Int. Ed. Engl.* **1983**, *22*, 489.
5. Gompper, R.; Gessner, T. *Angew. Chem. Int. Ed. Engl.* **1985**,*24*, 982.
6. Michaelis, L. *Chem. Rev.* **1935**, *16*, 243.
7. Wurster, C.; Schobig, E. *Ber. Dtsch. Chem. Ges.* **1879**, *12*, 1807.
8. Wurster, C.; *Ber. Dtsch. Chem. Ges.* **1879**, *12*, 528.
9. Wurster, C.; Sendtner, R. *Ber. Dtsch. Chem. Ges.* **1879**, *12*, 1803.
10. Weitz, E. *Angew. Chem.* **1954**,*66*, 658.
11. Weitz, E.; Fischer, K. *Angew. Chem.* **1925**, *38*, 1110.
12. Weitz, E.; Fischer, K. *Ber. Dtsch. Chem. Ges.* **1926**, *59*, 436.
13. Hünig, S. *Liebigs Ann. Chem.*,**1964**, *676*, 32.
14. Hünig, S. *Pure Appl. Chem.*, **1967**, *15*, 109.
15. Hünig, S. *Angew. Chem. Int. Ed. Engl.* **1969**, *8*, 286-287.
16. For the chemistry behaviour of TCNE see Cairns, T.L.; McKusick, B.C. *Angew. Chem.* **1961**, *73*, 520.
17. The designation "electron-rich olefins" is not quite accurate. These compounds should strictly speaking be described as olefins whose π-electron density on the carbon is distinctly greater than 1.0 (for example, a value of 1.16 has been calculated for (1)[32]).
18. Wiberg, N. *Angew. Chem. Int. Ed. Engl.* **1968**, *7*, 766-779.
19. Wanzlick, H.W. *Angew. Chem.* **1962**, *74*, 129.

20. Wanzlick, H.W. *Angew. Chem. Int. Ed. Engl.* **1962**, *1*, 129.

21. Briegleb, G. In "Elektronen-Donator-Acceptor-Komplexe," Springer, Berlin, **1961**.

22. Hoffman, R.W. *Angew. Chem. Int. Ed.*, **1968**, *7*, 754.

23. Lemal, D.M. in "The Chemistry of the Amino Group," S. Patai, Interscience, New York-London, pp 701-748, **1968**.

24. Kuwata, K.; Geske, D.H. *J. Am. Chem. Soc.* **1964**, *86*, 2101.

25. Hünig, S., private communication with Hoffmann, R.W.

26. Wiberg, N. and Buchler, J.W., unpublished.

27. Wiberg, N.; Buchler, J.W. *Chem. Ber.* **1963**, *96*, 3223.

28. Electron donor-acceptor complexes in which substantial transfer of the electrons from the donor to the acceptor has occurred are paramagnetic or diamagnetic, according to the spins of the unpaired electrons of the donor and acceptor molecules are parallel or antiparallel. The question of whether the complex is paramagnetic or diamagnetic may depend on the state (pure substances, solution), the nature of the solvent, the concentration in a solvent, and the temperature [36, 37].

29. Liptay, W.; Briegleb, G.; Schindler, K. *Z. Elektrochem., Ber. Bunsenges. physik. Chem.* **1962**, *66*, 331.

30. In solution. In the solid state, the complex exhibits weak electron spin resonance at g = 2.00.

31. Wiberg, N.; Buchler, J.W. *Chem. Ber.* **1964**, *97*, 618.

32. Kainer, H.; Wherle, A. *Ber.* **1955**, *88*, 1147.

33. Isenberg, I.; Baird, S.L. *J. Am. Chem. Soc.* **1962**, *84*, 3803.

34. Eastman, J.W.; Engelsma, G.; Calvin, M. *J. Am. Chem. Soc.* **1962**, *84*, 1339.

35. Webster, O.W.; Mahler, W.; Benson, R.E. *J. Am. Chem. Soc.* **1962**, *84*, 3678.

36. Schneider, F.; Möbius, K.; Plato, M. *Angew. Chem.* **1965**, *77*, 888.

37. Schneider, F.; Möbius, K.; Plato, M. *Angew. Chem. Int. Ed. Engl.* **1965**, *4*, 865.

38. Foster, R.; Thomson, T.J. *Trans. Faraday Soc.* **1962**, *58*, 860.

39. Foster, R.; Thomson, T.J. *Trans. Faraday Soc.* **1963**, *59*, 1059.

40. Mulliken, R.S. *J. Am. Chem. Soc.* **1950**, *72*, 605.

41. Mulliken, R.S. *J. Am. Chem. Soc.* **1952**, *74*, 811.

42. Mulliken, R.S. *J. Phys. Chem.* **1952**, *56*, 801.

43. Briegleb, G.; Czekalla, *Z. Elektrochem.***1954**, *58*, 249.

44. Foster, R.; Hammick, D.L.; Placito, P.J. *J. Chem. Soc.* **1956**, 3881.

45. Foster, R. *Tetrahedron* **1960**, *10*, 96.

46. The equilibrium (1) cannot be established unless TDAE and $TDAE^{2+}$ are soluble in the reaction medium.

47. Wiberg, N., unpublished.

48. Bard, A.J. *Pure Appl. Che.* **1971**, *25*, 379.

49. Anderson, D.H.; Elofson, R.M.; Gutowsky, H.S.; Levine, S. and Sandin, R.B. *J. Am. Chem. Soc.* **1961**, *83*, 3157.

50. Elofson, R.M.; Anderson, D.H.; Gutowsky, H.S.; Sandin, R.B.; Schulz, K.F. *J. Am. Chem. Soc.* **1963**, *85*, 2622.

51. Elofson, R.M.; Schulz, K.F.; Sandin, R.B. *Can. J. Chem.* **1969**, *47(23)*, 4447-54.

52. Schlenk, W.; Bergmann, E. *Liebigs Ann. Chem.*, **1928**, *463*, 40.

53. Nagai, T.; Shingaki, T.; Yamada, H. *Bull. Chem. Soc. Jpn.* **1977**, *50(1)*, 248-253.

54. Kawano, K.I.; Lemal, D.M. *J. Am. Chem. Soc.* **1962**, *84*, 1761.

55. The optical spectrum of [TMPD][TCNE] solutions, unlike that of $TDAE[TCNE]_2$ solutions, changes with time, since the TCNE formed in accordance with [TMPD][TCNE] $\rightleftarrows$ TMPD + TCNE is consumed by side reactions.

56. Bard, A.J.; Phelps, J. *J. Electroanal. Chem.* **1976**, *68*, 313-335.

57. Bard, A.J.; Ledwith, A.; Shine, H.J. *Adv. Phys. Org. Chem.* **1976**, *13*, 155-278.

58. Hünig, S.; Grob, J. *Tetrahedron Lett.* **1968**, *21*, 2599-2604.

59. Bernasconi, C.F.; Bergstrom, R.G.; Hünig, S. *Chem. Comm.* **1971**, 1485.

60. Bennion, B.C.; Auborn, J.J.; Eyring, E.M. *J. Phys. Chem.* **1972**, *76*, 701.

61. Bard, A.J.; Phelps, J. *J. Electroanal. Chem.* **1970**, App. 2-5.

62. Hünig, S.; Scheutzow, D.; Schlaf, H. *Justus Liebigs Ann.* **1972**, *765*, 126.

63. Hünig, S.; Groβ, J.; Schlenk, W. *Justus Liebigs. Ann.* **1973**, *1*, 324.

64. Hünig, S.; Kiesslich, G.; Quast, H.; Scheutzow, D. *Justus Liebigs Ann.* **1973**, *1*, 310.

65. Gruver, G.A.; Kuwana, T. *J. Electroanal. Chem.* **1972**, *36*, 85.

66. Niizuma, S.; Nakamaru, K.; Koizumi, M. *Chem. Lett.* **1972**, 59-64.

67. Dorfman, L.M. *Acc. Chem. Res.* **1970**, *3*, 224.

68. Diebler, H.; Eigen, H.; Matthies, P. *Z. Naturforsch* **1961**, *B16*, 629.

69. Hartmann, G.; Hünig, S. in "Chemische Grundlagen der Biologie pratikum für Studenten der Medizin und Biologie," Würburg, **1975**.

70. Boon, W.R. *Endeavour*, **1967**,*26*, 27.

71. Dodge, A.D. *Endeavour*, **1971**, *30*, 130.

72. Bellin, J.S.; Alexander, R.; Mahoney, R.D. *Photochem. Photobiol.* **1973**, *17*, 17.

73. Qitt, H.T. *Quart. Rev. Biophys.* **1971**, *4*, 365.

74. Fanchiang, Y.T.; Gould, E.S. *J. Am. Chem. Soc.* **1977**, *99*, 5226.

75. Land, E.J.; Swallow, A.J. *Ber. Bunsenges Phys. Chem.* **1975**, *79*, 436.

76. Jeffreys, R.A.; Williams, L.A. (Kodak), *Res. Disclosure*, **1971**, 61.

77. Goffe, C.A. *Res. Disclosure* **1974**, *40*.

78. Naarmann, H. *Naturwissenschaften* **1967**, *56*, 308.

79. Ganto, A.F.; Heeger, A.J. *Acc. Chem. Res.* **1974**, *7*, 232.

80. Amberger, E.; Fuchs, H.; Polborn, K. *Angew. Chem. Int. Ed. Engl.* **1985**, *24*, 968.

81. Reynolds, G.A.; Van Allan, J.A. Fr. Pat. **1971** (7127768).

82. See Ref. 1, pp 884.

83. Perlstein, J.H. *Angew. Chem.* **1977**, *89*, 534.

84. Perlstein, J.H. *Angew. Chem. Int. Ed. Engl.* **1977**, *16*, 519.

85. Gatterman, L. *Ber.*, **1895**, *28(3)*, 2869.

86. Willstätter, R.; Goldman, M. *Chem. Ber.* **1906**, *39*, 3765-3776.

87. Wizinger, R. *Berichte* **1927**, *60*, 1377.

88. Madelung, W.; Oberwegner, M.*Berichte* **1927**, *60*, 2469.

89. Buckles, R.E.; Meinhardt, N.A. *J. Am. Chem. Soc.* **1952**, *74*, 1171.

90. Hünig, S.; Schlaf, H.; Kieblich, G.; Scheutzow, D. *Tetrahedron Lett.* **1969**, *27*, 2271-2274.

91. Fritsch, J.M.; Weingarten, H.; Wilson, J.D. *J. A. Chem. Soc.* **1970**, *92*, 4038-4046.

92. Fritsch, J.M.; Weingarten, H.; Wilson, J.D. *J. Am. Chem. Soc.* **1968**, *90*, 793.

93. Parker, V.D.; Nyberg, K.; Eberson, L. *J. Electroanalyt. Chem.* **1969**, *22*, 150.

94. Svanholm, U.; Jensen, B.S.; Parker, V.D. *J. Chem. Soc. Perk. Trans. II* **1974**, 907.

95. Yao, T.; Musha, S.; Munemori, M. *Chem. Lett.* **1974**, 939-944.

96. Dvorak, V.; Nemec, I.; Zyka, J. *Microchem. J.* **1967**, *12*, 324-349.

97. Kimura, K.; Yamada, H.; Tsubomura, H. *J. Chem. Phys.* **1967**, *48*, 440-444.

98. Uemura, K.; Nakayama, S.; Seo, Y.; Suzuki, K.; Ooshika, Y. *Bull. Chem. Soc. Japan.* **1966**, *39*, 1348.

99. Kawamori, A.; Honda, A.; Joo, N.; Suzuki, K.; Ooshika, Y. *J. Chem. Phys.* **1966**, *44*, 4363.

100. Hausser, K.H., *Z. Naturforsh.* **1956**, *11(a)*, 20.

101. Hausser, K.H.; Murrell, J.N. *J. Chem. Phys.* **1957**, *27*, 500.

102. Edelstein, A.S.; Mandel, M. *J. Chem. Phys.* **1961**, *35*, 1130.

103. Duffy, Jr. W. *J. Chem. Phys.* **1962**, *36*, 490.

104. McConnell, H.M.; Pooley, D.; Bradbury, A. *Proc. Natl. Acad. Sci. (US)* **1962**, *48*, 1480.

105. Okumura, K. *J. Phys. Soc. Japan*, **1963**, *18*, 69.

106. Thomas, D.D.; Keller, H.;McConnell, H.M. *J. Chem. Phys.* **1963**, *39*, 2321.

107. Rhodes, R.S.; Burgess, J.H.; Edelstein, A.S. *Phys. Rev. Letters*, **1961**, *6*, 462.

108. Sakata, T.; Nagakura, S. *Bull. Chem. Soc. Japan*, **1969**, *42*, 1497-1503.

109. Sakata, T.; Nagakura, S. *Mol. Phys.* **1970**, *19*, 321-328.

110. The dimer concentration is equivalent to 1/2 concentration of the disappeared radical species.

[x] is the dimer concentration

$[R_0]$ is the initial concentration of the $TMPD^{+\cdot}$ radical which is $\sim 10^{-3}$ *M*.

111. Michaelis, L.; Schubert, M.P.; Granick, S. *J. Am. Chem. Soc.* **1939**, *61*, 1981.

112. Michaelis, L.; Granick, S. *J. Am. Chem. Soc.* **1943**, *65*, 1747.

113. Pott, G.T.; Kommandeur, J. *J. Chem. Phys.* **1967**, *47*, 395.

114. Musso, H. *Angew. Chem. Int. Ed. Engl.* **1963**, *2*, 723.

115. Mihailovic, M.L.J.; Cekovic, Z. "Oxidation and Reduction of Phenols" in "The Chemistry of the Hydroxyl Group", S. Patai, Interscience, Vol. I, **1971**, pp 505.

116. Whiting, D.A. "The Oxidation of Phenols" in "Comprehensive Organic Chemistry," J.F. Stoddart, Pergamon, London, Vol. I, **1979**, pp 739.

117. Sebastian, C.F. *Can. J. Chem.* **1981**, *59*, 2776, 2780.

118. Willstätter, R.; Kubli, H. *Ber.* **1909**, *42*, 4135.

119. Barton, D.H.R.; Cohen, T. in "Festschrift Arthur Stoll," Birkhäuser, Basel, **1967**, pp 144-165.

120. Waters, W.A. *Progr. Org. Chem.*, **1961**, *5*, 35-45.

121. Loudon, J.D. *Progr. Org. Chem.*, **1961**, *5*, 46.

122. Beecken, H.; Grizycki, U.V.; Gottschalk, E.M.; Krämer, H.; Maassen, D.; Matthies, H.G.; Musso, H.; Rathjen, C.; Zahorsky, U.I. *Angew. Chem.* **1961**, *73*, 665.

123. Musso, H. *Angew. Chem.* **1963**, *75*, 965.

124. Waters, W.A. in "Mechanisms of Oxidation of Organic Compounds," Methuen, London, **1964**, pp 132-149.

125. Scott, A.I. *Quart. Rev.* **1965**, *19*, 1.

126. Ingold, K.U. *Chem. Rev.* **1961**, *61*, 563.

127. Reference 120, pp 17-26.

128. Reference 124, pp 6-16 and pp 145-147.

129. Altwicker, E.R. *Chem. Rev.* **1967**, *67*, 475.

130. Strigun, L.M.; Vartantyan, L.S.; Emanuel, N.M. *Usp. Khim.* **1968**, *37*, 969.

131. Pokhodenko, V.D.; Khizhnii, V.A.; Bidzilya, V.A. *Usp. Khim.* **1968**, *37*, 998.

132. Reference 120, pp 26-45.

133. Weinberg, N.L.; Weinberg, H.R. *Chem. Rev.*, **1968**, *68*, 449.

134. Stone, T.J.; Waters, W.A. *Proc. Chem. Soc.* **1962**, 253.

135. Stone, T.J.; Waters, W.A. *J. Chem. Soc.* **1964**, *213*, 4302.

136. Kaeding, W.W. *J. Org. Chem.*, **1963**, *28*, 1063.

137. Müller, E.; Mayer, R.; Narr, B.; Rieker, A.; Scheffler, K. *Ann.*, **1961**, *645*, 25.

138. Auwers, K.V.; Markovits, T.V. *Ber.* **1905**, *38*, 226.

139. Suttie, A.B. *Tetrahedron Lett.* **1969**, *12*, 953-956.

140. Harrod, J.F.; Pathak, A. *Can. J. Chem.* **1980**, *58(7)*, 686-93.

141. Rio, M.F.; Pujol, D.; Charreton, C.B.; Fauvet, M.P.; Gaudemer, A.; *J. Chem. Soc. Perkin Trans. I*, **1984**, 1971.

142. Reference 124, Chapter 9.

143. Waters, W.A. *J. Chem. Soc. (B)* **1971**, 2026.

144. Cecil, R.; Littler, J.S. *J. Chem. Soc. (B)* **1968**, 1420.

145. Haynes, C.G.; Turner, A.H.; Waters, W.A. *J. Chem. Soc.* **1956**, 2823.

146. Capdevielle, P.; Maumy, M. *Tetrahedron Lett.* **1983**, *24*, 5611-5614.

147. Verlaan, J.P.J.; Zwiers, R.; Challa, G. *J. Mol. Catal.* **1983**, *19*, 223-232.

148. Tsuruya, S.; Kinumi, K.; Hagi, K.; Masai, M. *J. Mol. Catal.* **1983**, *22*, 47-60.

149. Jallabert, C.; Lapinte, C.; Riviere, H. *J. Mol. Catal.* **1982**, *14*, 75-86.

150. Oudejans, J.C.; Bekkum, H.V. *J. Mol. Catal.* **1981**, *12*, 149-157.

151. Tsuruya, S.; Kuse, T.; Masai, M.; Iimamura, S.I. *J. Mol. Catal.* **1981**, *10*, 285-303.

152. Cecil, R.; Littler, J.S. *J. Chem. Soc. B.* **1968**, 1420.

153. Ronlán, V. *Chem. Comm.* **1971**, 1643.

154. Yang, N.C.; Castro, A.J. *J. Am. Chem. Soc.* **1960**, *82*, 6208.

155. Coppinger, G. M. *J. Am. Chem. Soc.*, **1957**, *79*, 501.

156. Orton, K.J.P.; Bradfield, E. *J. Chem. Soc.* **1924**, 960; **1927**, 983.

157. Cox, J.R.; Smith, S.D. *J. Org. Chem.* **1964**, *29*, 489.

158. Dippy, J.F.J.; Evans, R.M.. *J. Org. Chem.* **1950**, *15*, 451.

159. Hünig, S.; Daum, W. *Chem. Ber.* **1955**, *88*, 1238.

160. Hünig, S.; Richters, P. *Chem. Ber.* **1958**, *91*, 442.

161. Lucas, H.J.; Kennedy, E.R. *Org. Synth.* **1955**, *3*, 482.

162. Hünig, S.; Quast, H. *Org. Synth.* **1973**, *5*, 1018.

163. Nonhebel, D.C.; Dagleish, D.T.; Pauson, P.L. *J. Chem. Res. (M)* **1977**, *Part II*, 0228-0236.

164. Kharasch, M.S.; Joshi, B.S. *J. Org. Chem.* **1957**, *22*, 1439.

165. Kharasch, M.S.; Joshi, B.S.; *J. Org. Chem.* **1957**, *22*, 1435.

166. Wertz, J.E.; Bolton, J.R. in "Electron Spin Resonance - Elementary Theory and Practical Applications," McGraw-Hill Inc., **1972**, pp 450-467.

167. Gersmann, H.R. *Berichte* **1927**, *60*, 1377.

Appendix Ia. Calibration of radical concentration at equilibrium by standard 2,2-diphenyl-1-picryl hydrazyl free radical

Assuming that the relative intensity of overmodulated epr signal does reflect the radical concentration, the relationship between the concentration of standard ([STD]) and the concentration of the radical species under investigation ([X]) can be established as follow:[166]

$$\frac{[X]}{[STD]} = \frac{A_x R_x (scan_x)^2 G\ std\ M\ std\ (g_{std})^2 [S(S+1)]_{std}}{A_{std} R_{std} (scan_{std})^2 G_x M_x (g_x)^2 [S(S+1)]_x} \qquad \text{(eqn. 1)}$$

A is the measured area under the absorption curve (this may be in arbitrary units as long as they are the same for unknown and standard).

Scan is the horizontal scale in Gauss per unit length on the chart paper.

G is the relative gain of the signal amplifier.

M is the modulation amplitude in gauss.

R is defined as $\sum_j D_j/D_k$ (D_k is the degeneracy of the most intense line and $\sum_j D_j$ is the sumof the degeneracies of all the lines in the spectrum) (for detail see ref. 166).

Appendix Ib. Calculation of Equilibrium Constant (Keq.) from Plot of Relative Intensity vs % Concentration

The relationship between radical concentration and observed overmodulated epr signal is established as follows:

$$R = C \times I \qquad \text{(eqn. 2)}$$

R is the radical concentration (mol. l^{-1})

C is the proportionality constant (L. mol^{-1})

I is the relative intensity (non-dimensional).

I is equal to the ratio of peak-to-peak height (h) to peak-to-peak width (w) over signal gain (g).

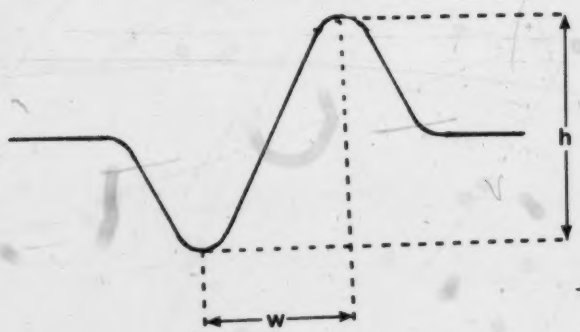

$$I = \frac{h}{w.g}$$

assuming that the relative intensity reflects the true number of radical concentration. This assumption requires the microwave power (P_0) is such that it does not oversaturate ground state population. In this experiment the microwave power is normally set at 17 - 20 dB.

The equilibrium involves a 1:1 molar ratio of TMPD and $TMPD^{2+}$ which gives rise to two equivalents of the reversibly formed radical cation $TMPD^{+}$.

$$TMPD + TMPD^{2+} \rightleftharpoons 2TMPD^{\bullet +}$$

Concentration	Concentration	Concentration	Time
A_0	B_0	0	0
$A_0 - R/2$	$B_0 - R/2$	R	t

By definition then:

$$K_{eq} = \frac{[R]^2}{[A_0 - R/2][B_0 - R/2]} = \frac{[CI]^2}{[A_0 - CI/2][B_0 - CI/2]}$$

(eqn. 3a) (eqn. 3b)

R is radical concentration at equilibrium and is related to relative intensity by equation 2. For each two adjacent positions (e.g. point 1 and point 2) on the plot of relative intensity versus % concentration one can establish the following equations:

$$K_{eq} = \frac{[CI_1]^2}{[A_0 - CI_1/2][B_0 - CI_1/2]} \quad \text{(eqn. 4)}$$

$$K_{eq} = \frac{[CI_2]^2}{[A_0 - CI_2/2][B_0 - CI_2/2]} \quad \text{(eqn. 5)}$$

Combination of eqn. 4 and eqn. 5 gives:

$$\frac{[CI_1]^2}{[A_0 - CI_1/2][B_0 - CI_1/2]} = \frac{[CI_2]^2}{[A_0 - CI_2/2][B_0 - CI_2/2]} \quad \text{(eqn. 6)}$$

Equation 6 can be solved for C_{12} (subscript 12 denotes the two pairs in use).

In a similar way the next two consecutive points will give a corresponding proportionality constant C and so on. These C values are then averaged and the average C is

fed back to equation (3b) (where I is in the relative intensity of the epr signal at 50/50 mixture of the two species) to solve for the K_{eq} constant (see Tables I - IV and Ia - IVa).

Appendix Ic. Calculation of Radical Concentration at Equilibrium

Equation (3a), at 50:50 of the two starting materials, can be expanded as follow:

$$(K_{eq} - 4)\, R^2 - 2(A_0 + B_0)\, K_{eq}\, R + 4\, K_{eq}\, A_0 B_0 = 0 \qquad \text{(eqn. 7)}$$

The above quadratic equation is solved for R under the condition that $R \leq (A_0 + B_0)$.